COMMISSURAL AXON KINETICS AND THE ROLE OF NETRIN IN EARLY BRAIN CIRCUITRY DEVELOPMENT

Thesis by

Magdalena Bak-Maier

In Partial Fulfillment of the Requirements

for the Degree of

Doctor of Philosophy

CALTECH

California Institute of Technology

Pasadena, California

2004

(Defended September 9th)

Acknowledgements

With much gratitude I would like to thank the many individuals that have supported me during my thesis research at Caltech.

Most of all, I would like to thank my present research mentor and advisor Scott Fraser for his continuous support of this project and for the independence he has given me. I cannot recall a single time when he did not cheer me on with his enthusiasm and positive attitude. His ability to free his busy schedule for useful discussions was truly exemplary. I would also like to thank my thesis committee: John Allman, Andres Collazo and Kai Zinn for taking great interest in my research project and their invaluable comments and advice during the past four years.

The Fraserland, as the Fraser lab is commonly known, is a huge family of folks and I would like to thank all of them for the supportive lab atmosphere. In particular I would like to thank Helen McBride, David Koos, Cyrus Papan and Rusty Lansford for their support, intellectual discussions and assistance. I have learned a lot from each of you and your scientific excellence has inspired as well as challenged me to strive for further perfection. I also thank Raj Kulkarni whose intuitive knowledge of optics and mathematics allowed us to undertake a fun set of experiments together. Many great thanks to Tania Demyanenko and Aura Keeter for their excellent technical assistance and help as well Gary Belford and Mary Flowers. Finally, I would like to thank the members of Bronner-Fraser lab for being very kind and helpful with reagents and equipment. In particular I would like to thank Lisa Ziemer for her help and support.

Many special thanks to my highly enthusiastic collaborator from UK, Ivor Mason, for putting up with me during the summer of 2003 when he came to visit our lab and for

his support and help in choosing my postdoctoral position. It is not very often that a student gets a chance to work side by side with a professor and I will always cherish that summer as the best time I had at Caltech.

My Caltech experience would not have been complete without few other individuals who have made a large difference in my graduate career. I would especially like to thank Marianne Bronner-Fraser for her insights and support, Jerry Pine for being a great teacher and mentor and David Anderson for a great course in developmental neurobiology as well as Elaine Bearer for good discussions during the later part of my last year. I would also like to thank Candace Rypisi from the Women Center for help and support.

None of this would have happened of course had it not been for my undergraduate research advisors especially the professors from the NYU Neuroscience department in particular Chiya Aoki as well as Costa Dobrenis from the Albert Einstein Medical School. They both were my first research mentors and have most directly contributed to my desire to undertake graduate training.

Lastly, I would like to thank Stefan for his love and support, which has made all the difference.

Abstract

As neurons begin to differentiate, they send out processes called axons to initiate the formation of functional nerve connections. A specialized structure at the end of an axon called the growth cone is believed to possess the impressive navigational and target recognition ability crucial for this process. The goal of the research presented in this thesis was to understand the cellular and molecular mechanisms that shape axon growth and guidance *in vivo* during early brain development using a multifaceted experimental approach.

Towards this goal we employed the simple, well-characterized neuronal scaffold of the embryonic zebrafish brain in combination with cell labeling techniques and performed studies in three specific areas: (1) the dynamic behaviors of navigating growth cones to obtain information about their cellular interactions with each other and the local environment, (2) the action of specific proteins (netrin and its receptor DCC) known to be involved in axon guidance in order to determine their function *in vivo*, and (3) the mobility of GFP in growth cones as a way to gain insight into the dynamics of molecular species in these structures as they actively navigate.

Critical to our studies was a stable transgenic gata2::GFP zebrafish line in which we found high level of GFP expression in early forebrain neuronal clusters allowing *in vivo* timelapse study of the growth cones that pioneer the postoptic commissural (POC) axon tract. Following the development of the POC also allowed us to investigate how early commissural growth cones behave at the midline.

Timelapse analysis of POC axon kinetics revealed important insight into growth cone interactions with each other and their environment and showed that these have behavioral

consequences. While it was known that commissural axons slow down while crossing the midline, our data showed that this is only true for the leader axons. Follower axons do not slow down unless the leader axon is ablated. Together this analysis revealed that in addition to specific molecular cues, axon-axon interactions are important for establishing early axon tract.

This characterization of POC axon kinetics and growth cone behavior in turn, provided us with an assay for studying the specific role of netrin, primarily a midline attractant for commissural axons in the spinal cord and its receptor, deleted in colorectal cancer (DCC). Loss- and gain-of-function experiments in combination with timelapse imaging uncovered a novel function for netrin as a positional repellent cue for POC axons.

Finally, prompted by the observed differences in leader and follower POC growth cones, we developed a new experimental approach to assay GFP mobility as a reporter for the diffusion rates of other molecular species inside growth cones *in vivo*. We found that diffusion rates in actively pioneering growth cones are significantly decreased compared to follower axons suggesting that diffusion rates might be linked to growth cone pathfinding.

Collectively, the findings presented in this thesis constitute a framework that allows for an integrative approach of studying growth cone navigation *in vivo*. Basic integrative knowledge of this sort is expected to aid the development of medical therapies related to nerve injury and repair.

Table of Contents

Table of Figures

Table of Tables

Chapter 1 Introduction

1.1 Motivation for this work

To perform its function, the nervous system requires that neurons establish correct connections. This process involves the extension of an axon from the neuronal cell body, its navigation towards a specific target cell and formation of synaptic contacts. Frequently axon guidance requires that inappropriate targets are bypassed and conflicting guidance cues integrated as axons extend for long distances before reaching their final partners. Axon navigation is orchestrated by the presence of cellular and molecular clues that are interpreted by a highly motile axon tip called the growth cone. Disfunction in these clues result in axon guidance defects that can in turn lead to potentially devastating pathologies such as epilepsy or HGPPS (horizontal gaze palsy with progressive scoliosis). One of the most basic yet essential questions concerns the cellular and molecular mechanisms involved in the establishment of early brain tracts and the role of regional and cellular domains that in turn influence axon tract position and growth.

While the dissection of the mechanisms that guide axons towards the establishment of appropriate connections is difficult to tackle in adult vertebrate brains due to its high complexity, embryonic brains are much simpler containing a small number of neuronal clusters and axon tracts. This means that we can examine the behaviors of early navigating axons that are likely recapitulated as more connections develop.

Since R. G. Harrison first observed extending growth cones almost a century earlier in culture[1,2] and Spiedel followed single growth cones at the ends of sensory axons *in vivo* in the growing tail fin of the frog[3], the cell biology of axon growth and growth

cone guidance has been intensively studied using elegant in vitro assays[4-7], invertebrate [8-23] and vertebrate model organisms [24-41]. Despite the identification of numerous candidate guidance molecules and elucidation of their signaling pathways, the challenge has been to understand how growth cones integrate external guidance cues in vivo to form the stereotypical axon tracts common to early vertebrate brains. To address this we turned towards a vertebrate with a simply arranged embryonic brain scaffold[34,37,42] that readily lends itself to imaging studies to allow us to monitor the formation of early brain connections as they occur in vivo. In particular we examined the behavior of commissural axons that form the postoptic commissure (POC) and their growth cones in the zebrafish forebrain[43].

Some of the greatest insights into the behaviors of axons have been made over a century ago by Santiago Ramon y Cajal. His sample preparations impregnated by the Golgi stain allowed him to examine nerve cells and their growth cones with phenomenal detail that continues to amaze neuroscientists today. Combining sound microscopic techniques and golgi staining Ramon y Cajal was able to make specific predictions about axon guidance that are being demonstrated today. The one element missing in Cajal's work was the ability to observe how axons grow dynamically in living preparations. In this respect, the most influential studies towards our understanding of growth cone behavior were performed by Mason and Wang in which they examined growth cone behaviors along the retinal axon pathway using dynamic imaging[31,32]. Timelapse analysis revealed that axon growth was discontinuous with axons alternating between extension periods and pauses[31,32]. Further, growth cone shape was dependent on growth cone behavior so that rapidly moving growth cones were streamlined with few filopodia while

those that paused more frequently had complex shapes with many more filopodia[31,32]. This confirmed similar growth cone shape differences between leading growth cones and later axons growing along them in fixed samples[28,29] and showed that filopodia are likely the sampling antennas used to probe the local environment in order to orient the growth cone[28,29]. Looking also at the retinal axon pathway, Hutson and Chien applied timelapse imaging to examine the molecular basis of axon pathfinding at the optic chiasm using wildtype and *astray* (a Robo2 defective receptor mutant) zebrafish embryos[44]. This study revealed that lack of functional Robo2 resulted in an inability of growth cone errors to be fixed at the optic chiasm compared to wildtype embryos where similar errors were corrected[44]. Cohen-Cory and Fraser used in vivo microscopy to follow individual optic axons and the effects of the neurotrophin brain-derived neurotrophic factor (BDNF) in their development showing specific increase in axon branching and complexity[64]. By combining timelapse imaging with analysis of growth cone behaviors and axon terminals, these studies highlight the advantages of dynamic imaging towards elucidating the role of molecular candidates in axon guidance.

Most of what we know about commissural axon guidance comes from static analysis of spinal commissural neurons[24,25] and from a limited amount of dynamic studies of their behavior[30]. Thus we wished to image POC axons as they establish the commissural tract and use this system as an assay for allowing us to examine molecular and cellular mechanism(s) involved in setting up early brain tracts in vertebrate brains *in vivo*. Unlike most other timelapse studies performed in vertebrate model systems, our studies examine axon and growth cone behaviors before any other neuronal connections are formed. For example in the retinal system which have been the predominant model

system for dynamic studies of axon navigation, the early projections of the retinal axons initiate their growth towards the optic chiasm a day after the initial POC tract is formed in zebrafish[45]. Thus our studies provide insights into the formation of early commissural tracts and growth cone behaviors in vertebrate brains that might be applicable towards other vertebrate model systems.

1.2 Importance of dynamic imaging and in vivo approach for studying axon behaviors

Recent advances in cell labeling and long-term optical imaging of developmental processes are now allowing us to observe and probe the developing nervous system of vertebrates directly [46]. While many hypotheses in the field of developmental neurobiology have been generated based on inferences rooted in static analysis, direct observation of highly dynamic processes, like those taking place during nervous system development, allow us clearer understanding of what is occurring and provide clues to the mechanisms involved. A metaphor to capture the essence of the benefit that direct imaging brings to developmental biology has been elegantly captured by Lichtman and Fraser through a sport analogy[46]. If the set out objective is to deduce the rules of a game, they argue, then an observer can deduce these rules more readily from a videotaped game than from individual snapshot images of the same event [46].

Axon navigation is very much like a highly paced sport event. The main goal of axons early on in development of the nervous system is to connect with other neuronal cells or non-neuronal targets. To accomplish this, navigating axons and their growth

cones must constantly interpret various guidance cues along the way. For this reason, growth cones are highly dynamic structures that continuously probe their surrounding environment. While we could easily employ static analysis to capture the shapes of navigating growth cones, we would surely fail to notice their dynamic properties such as their interaction preferences, the duration of such interactions and their character without imaging the natural behaviors of growth cones directly. These dynamic behaviors in turn provide us with mechanistic clues that are important in axon navigation and which we can then test. For example dynamic imaging can reveal places where growth cones persist longer or where their shape changes thus giving insights into possible position of guidance points. These areas can be later compared with expression domains of specific molecules to identify candidates for axon guidance. Recent studies employing the power of live imaging have been able to reveal many new insights not readily apparent from static analysis: cell migration behaviors [47], growth cone behaviors [31,43] [9], filopodia dynamics [9,39,48]the dynamics of synapse formation and their maintenance [49-51]. Thus, dynamic imaging can help us uncover what at times appear to be seemingly imperceptible but yet critical events in neuronal circuit development.

Establishment of brain tracts is undoubtedly the result of multiple guidance cues and cell expression domains acting in concert to help guide and route early axons to correct axon tracts. However, recent work aimed at identifying additional secreted axon guidance cues, has revealed that instead a rather small set of guidance cues are often recycled or adopted for new roles depending on context and need of the system[52]. Two members of families of secreted molecules not normally associated with axon guidance have been found to affect growth cone behavior and navigation. The first is bone

morphogenetic protein 7 (BMP7). BMP7 is normally involved in cell fate specification but can also orient commissural axons [53]. Wnt5 *Drosophila* mutants also have commissural projection errors suggesting that a member of the Wnt family most known for its role in early embryonic patterning also mediates axon guidance via the derailed receptor[53,54]. It is also becoming clear that different molecular cues can and often do work in overlapping functions which might enforce, influence, interfere or even negate the same event. For example recent studies on sonic hedghog signaling suggest that sonic works as an axon guidance molecule in concert with netrin in the spinal cord in mouse[55]. These overlaps and interdependencies make testing the individual role of molecules difficult to study using static approaches especially where the phenotype can be subtle, the structure highly dynamic and the process regulative in nature. Dynamic analysis in whole embryos however offers a better chance of noticing these highly dynamic effects.

In vivo analyses are also excellent for giving us a more accurate picture of how multiple signaling events influence a common process. Reductionistic systems such as cell culture studies are excellent for understanding cell biological questions. Their simpler design allows us to tease apart and separate some of the layers of complexity of dealing with intact tissue(s) and focus on understanding the role of a single event. Today's sophisticated culture studies can also decipher entire sequences of signaling events with great accuracy and superior clarity. In the field of axon navigation for example, great insight has been obtained by studying the signal transduction mechanisms mediating axon turning decisions in response to a given guidance cue[5,56,57]. This advantage however, comes at a cost. Namely, the results obtained in *ex-vivo* studies are

only valid in the framework of that system and will reflect its design constraints. Studying dynamic processes in a living organism allows one to examine behaviors in their natural context although one should be mindful of possible imaging caveats as well[46]. With this in mind, results obtained from well-designed in vivo imaging studies are likely to most closely reveal both the function of specific genes and also the extent to which they participate and influence a given developmental process.

1.3 Choice of zebrafish (*Danio rerio)* as a model system

Zebrafish is a well-suited vertebrate model to study axon behavior during early neuronal scaffold formation *in vivo* for three main reasons. First, detailed descriptions of the early neuronal scaffold have been made[34,37,42] and the fate map of the anterior nervous system was made[58]. Second, the optical clarity of the zebrafish embryo especially in early development together with cell labeling techniques and stable GFP expressing transgenic zebrafish lines (see Chapter 2) allow us to map onto this two-dimensional picture of the early neuronal scaffold, positional information for these projections. Further, labeled cells inside the embryo and timelapse imaging studies permit us to study the behaviors of individual and whole sets of axons and neurons as they grow and build these early brain tracts in vivo. Third, a large toolbox of present and emerging molecular approaches [59,60] and mutants available from developmental screens provide great flexibility to test the role of specific genes in development. Together, these advantages make the zebrafish a good vertebrate model system to study early brain wiring and axon behavior that may be relevant to other, less accesible, vertebrate organisms.

1.4 The geography of the embryonic neuronal scaffold in the zebrafish forebrain

During one day of development the zebrafish embryo goes from a fertilized egg to a small adult[61]. As the embryo develops, the rudimentary neuronal scaffold made of specific cell clusters and connecting them axon tracts forms between 16-24hpf. Early descriptions of the arrangement of the early neuronal cells and their axons have been made possible through immunohistochemitry techniques such as horseradish peroxidase (HRP) labeling. Immunohistochemistry relies on the high binding specificity between the antibody and an antigen. In the early descriptions of the zebrafish neuronal scaffold, three specific antibodies were used: the anti-acetylated tubulin (AT), HNK-1 and anti-acetylcholine esterase (AchE) which bind to different antigens on neurons and can be later detected with standard immunohistochemistry techniques. HRP is a well established retrograde axon tracer that is readily taken up by axon terminals and transported back to the cell body. With HRP there is no need to injure cells to obtain HRP tracings. Instead a small application of HRP is made in the vicinity of axon terminals, which is sufficient to label axonal pathways. By applying these techniques to embryos at different stages, we can reconstruct the development of early axon tracts giving us information about the development of these connections[34,37,42] (Figure 1-1). To visualize the arrangement of early axon tracts and neurons on paper, camera lucida drawings were used.

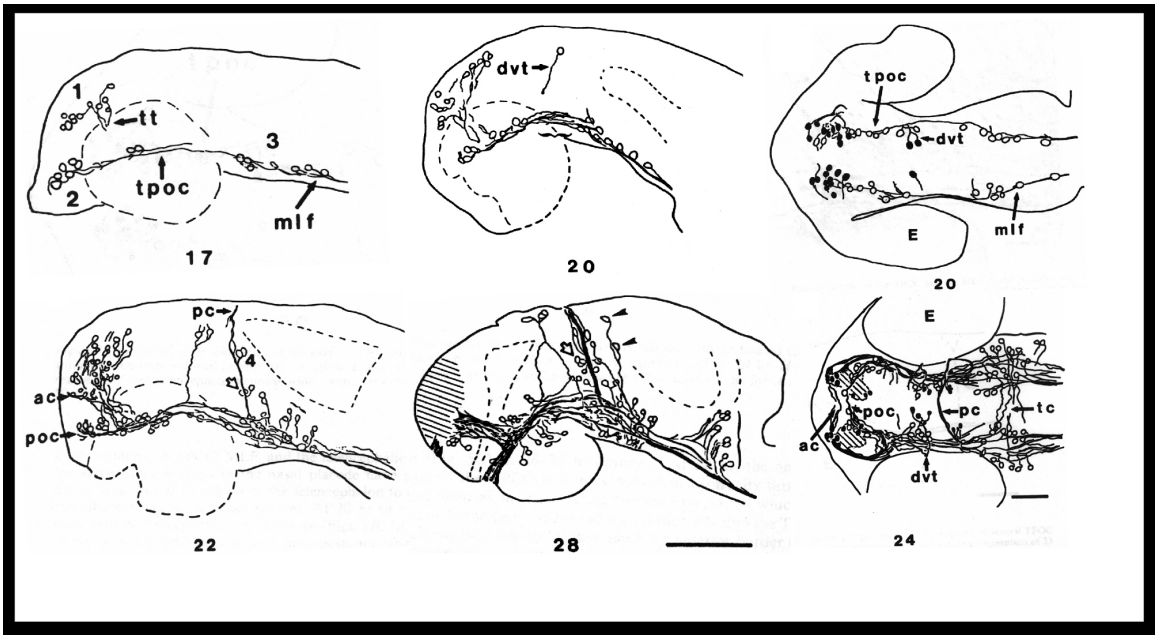

Figure 1-1: Camera lucida drawings of the development of major axonal tracts.

The neuronal scaffold was visualized with immunohistochemistry using the acetylated alpha tubulin antibody followed by HRP staining. Embryos at different developmental stages were collected and their early scaffolds traced. The drawings show a lateral view of the early scaffolds and a dorsal view. Dorso-ventral position of cell clusters has been indicated by having open and filled circles. Anterior is to the left. Scale =100 μm (Figure adapted from Chitnis et al. 1990)

Based on these early axon tracings we now know that the early forebrain zebrafish neuronal scaffold (Figure 1-2) consists of clusters of neurons named as follows: the ventrorostral cluster (vrc), the ventrocaudal cluster (vcc) and the epiphyseal cluster (ec) located in the diencephalon (except for the vcc) and the dorsorostral cluster (drc) located in the telencephalon [34,37,42,43]. The early neurons that make up these clusters send their axons to other clusters in a stereotypical manner. For example, two separate commissural tracts link the bilateral clusters of neurons (the vrc and the drc) in the forebrain: the postoptic commissure (POC) connecting the vrc clusters and the anterior commissure (AC) connecting the two drc clusters.

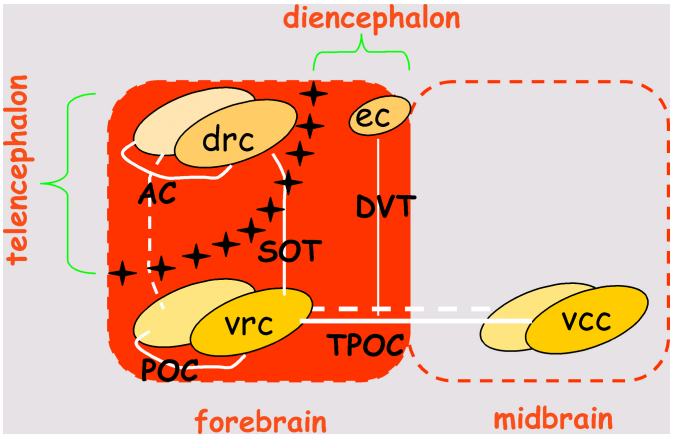

Figure 1-2 Schematic drawing depicting the arrangement of the early neuronal cell clusters and their connections in the developing zebrafish brain

The early neuronal clusters are depicted with yellow circles: (drc) dorsorostral cluster, (vrc) ventrorostral cluster, (vcc) ventrocaudal cluster, (ec) epiphysis cluster. The axon tracts are indicated in white: (AC) anterior commissure, (POC) postoptic commissure, (SOT) supraoptic tract, (DVT) dorsoventral tract, (TPOC) Track of the postoptic commissure. (Figure based on [34,37,42,43])

Axons making up the AC grow at the boundary of the telencephalon and diencephalon and those belonging to the POC tract grow along the ventral diencephalon[34,37,42]. The two commissures are separated from each other by an axon free zone[33,42,62]. The drc and vrc clusters on each side of the brain are further connected with each other by the supraoptic tract (SOT) the only axon bundle connecting the telencephalon with the diencephalon at 24hpf [34,37,42,43].

This simple arrangement of the early zebrafish primary neuronal scaffold represents a tractable starting point for understanding the influence of environmental cues on the development of this early neuronal circuitry by allowing us to examine axon behaviors as they grow from one cluster to another. The territories explored and not explored by these axons and their growth cones, their behavior and the axon kinetics

provide a direct assay to test the molecular mechanisms that guide the formation of early brain tracts in the zebrafish forebrain in vivo.

1.5 Road map through this dissertation

The main goal of this PhD thesis was to observe the behaviors of axons and their growth cones during early neuronal scaffold assembly in vivo and to deduce the molecular mechanism(s) that shape these behaviors.

This work was greatly aided by a small screen designed to identify a stable transgenic line with strong GFP expression localized to early neurons of the zebrafish forebrain (**Chapter 2)**. Using experimental data, the chapter discusses specific cell labeling methods and stable trangenic zebrafish lines for imaging studies of the developing early nervous system.

One of the basic yet important questions in developmental neurobiology is how brain circuitry is assembled. Towards this end much effort has been spent to decipher trajectories of early POC axons and how they grow. Dynamic analysis of axon behavior during early neuronal scaffold formation in a living brain was technically challenging in part due to the complicated three dimensional topology of the brain and the inaccessibility of most vertebrate embryos such as mouse or chicken either physically and/or optically. For this reason the studies done in zebrafish answered a real need in terms of providing information on the behavior of early brain axons during early neuronal scaffold development.

Chapter 3 presents results of *in vivo* time-lapse imaging experiments in zebrafish designed to study the behavior and morphology of early growing axons that make up the

postoptic commissure (POC) tract and their growth cones. This was largely due to the identification of a stable line that expresses GFP in the early neuronal cells[43]. In this line, the GFP is expressed behind a Gata2 cis regulatory domain[63]. We found that the gata2::GFP line expresses GFP at sufficiently high level to allow repeated imaging of individual POC axons and their growth cones.

The dynamic approach was instrumental in defining the behaviors of early POC growth cones and their interactions. These observations revealed that axon-axon interactions are dynamic and ongoing as axons navigate across the midline and most importantly they have behavioral consequences for axon growth rates. This new finding would not have been possible without dynamic imaging. Careful description of the axon behaviors in turn provided an in vivo assay to allow functional studies to be performed.

Building on the results of experiments in Chapter 3 we next used the POC axon assay to perturb specific candidates known to play a role in axon guidance and determine how they participate in the formation of the POC. **Chapter 4** presents experiments designed to test the role of deleted in colorectal cancer (DCC) guidance receptor and netrin a known axon guidance molecule in helping to establish the POC tract. The results of both gain- and loss-of-function experiments for both the receptor and ligand are described. These data reveal that netrin signaling via DCC receptor appears to act as a repellent cue. This keeps the POC axons in a tight bundle and functions in part to separate them from the anterior commissure axons. Thus netrin appears to be a positional cue that signals to POC growth cones to not invade more dorsally.

The experiments described in **Chapter 5** were prompted by a perceived gap between what we know in terms of specific guidance molecules and their role in axon

guidance on the one hand and what is happening inside actively pathfinding growth cones that allows external cues to be translated into growth cone movements on the other. To address this gap we decided to use the strongly expressing GFP as a natural reporter for freely diffusible molecular species and to measure GFP diffusion rates in navigating growth cones. We reasoned that knowledge about local diffusion in growth cones will be needed to understand growth cone signaling during axon guidance.

In these studies the strength of the gata2::GFP zebrafish line (Chapter 2 and 3) has been combined with the knowledge of growth cone behavior and kinetics (Chapter 3 and 4) to perform fluorescence recovery after photobleaching (FRAP) studies to find out the kinetics of local free diffusion properties of molecules based on the FRAP analysis of cytoplasmic GFP in the gata2::GFP line. These studies resulted in a number of exciting findings. We found that GFP diffusion rate decreases progressively from the cell body towards the growth cone and differences in local diffusion rates between actively pioneering growth cones and follower growth cones. By using pharmacological perturbations of the actin and microtubule networks we found that actin is the primary modulator of diffusion in growth cones.

The concluding **Chapter 6** presents a summary of the work presented in this thesis, which is then placed in the context of other zebrafish imaging studies in the field of developmental neurobiology. The chapter concludes with an outlook on possible future studies that can be undertaken in this system based on the results we obtained.

1.6 References

1. Harrison, R. G. Observations on the living developing nerve fiber. *Anat. Rec* **1**, 116-118 (1907).
2. Harrison, R. G. The outgrowth of the nerve fiber as a mode of protoplasmic movement. *Journal of Experimental Zoology* **9**, 787-846 (1910).
3. Speidel, C. C. Adjustments of nerve endings. *Harvey Lectures* **36**, 126-158 (1941).
4. Tessier-Lavigne, M. & Goodman, C. The molecular biology of axon guidance. *Science* **274**, 11231133 (1996).
5. Guan, K. & Rao, Y. Signaling mechanisms mediating neuronal responses to guidance cues. *Nature Reviews in Neuroscience* **4**, 941-956 (2003).
6. Rosentreter, S. M. et al. Response of retinal ganglion cell axons to striped linear gradients of repellent guidance molecules. *Journal of Neurobiology* **37**, 541-562 (1998).
7. Devenport, R., Thies, E. & Cohen, M. Neuronal growth cone collapse triggers lateral extensions along trailing axons. *Nature Neuroscience* **2**, 254-259 (1999).
8. Araujo, A. & G, T. Axon guidance mechanisms and molecules:lessons from invertebrates. *Nature Reviews in Neuroscience* **4**, 910-922 (2004).
9. Myers, P. & Bastiani, M. Growth cone dynamics during the migration of an identified commissural growth cone. *The Journal of Neuroscience* **13**, 127-143 (1993).

10. Bastiani, M., Raper, J. & Goodman, C. Pathfinding by neuronal growth cones in grasshopper embryos III. Selective affinity of the G growth cone for the P cells within the A/P fascicle. *The Journal of Neuroscience* **4**, 2311-2328 (1984).

11. Myers, P. & Bastiani, M. Cell-cell interactions during the migration of an identified commissural growth cone in the embryonic grasshopper. *Journal of Neuroscience* **13**, 115-26 (1993).

12. Bastiani, M., Raper, J. A. & Goodman, C. S. Pathfinding by neuronal growth cones in grasshopper embryos. III. Selective affinity of the G growth cone for the P cells within the A/P fascicle. *Journal of Neuroscience* **4**, 2311-2328 (1984).

13. Taghert, P. H., Bastiani, M., Ho, R. K. & Goodman, C. S. Guidance of pioneer growth cones: filopodial contacts and coupling revealed with an antibody to Lucifer Yellow. *Developmental Biology* **94**, 391-399 (1982).

14. Bastiani, M., Pearson, K. G. & Goodman, C. S. From embryonic fascicles to adult tracts: organization of neuropile from a developmental perspective. *Journal of Experimental Biology* **112**, 45-64 (1984).

15. Raper, J., Bastiani, M. & Goodman, C. Pathfinding by neuronal growth cones in grasshopper embryos II. Selective fasciculation onto specific axonal pathways. *The Journal of Neuroscience* **3**, 31-41 (1983).

16. Sun, Q., Bahri, S., Schmid, A., Chia, W. & Zinn, K. Receptor tyrosine phosphatases regulate axon guidance across the midline of the Drosophila embryo. *Development* **127**, 801-812 (2000).

17. Desai, C. J., Gindhart, J. G. J., Goldstein, L. S. & Zinn, K. Receptor tyrosine phosphatases are required for motor axon guidance in the Drosophila embryo. *Cell* **84**, 599-609 (1996).

18. Bate, C. Pioneer neurones in an insect embryo. *Nature* **260**, 54-55 (1976).

19. Bentley, D. & Keshishian, H. Pathfinding by peripheral pioneer neurons in grasshopper. *Science* **218**, 1082-1087 (1982).

20. Boyan, G., Therianos, S., Williams, L. & Reichert, H. Axogenesis in the embryonic brain of the grasshopper Schistocerca gregaria: an identified cell analysis of early brain development. *Development* **121**, 75-86 (1995).

21. Klose, M. & Bentley, D. Transient pioneer neurons are essential for formation of an embryonic peripheral nerve. *Science* **245**, 982-983 (1989).

22. Hidalgo, A. & Brand, A. H. Targeted neuronal ablation: the role of pioneer neurons in guidance and fasciculation in the CNS of Drosophila. *Development* **124**, 3253-3262 (1997).

23. LoPresti, V., Macagno, E. R. & Levinthal, C. Structure and development of neuronal connections in isogenic organisms: cellular interactions in the development of the optic lamina of Daphnia. *Proc. Nat. Acad. Sci. USA* **70**, 433-437 (1973).

24. Kaprielian, Z., Runko, E. & Imondi, R. Axon guidance at the midline choice point. *Developmental Dynamics* **221**, 154-181 (2001).

25. Colamarino, S. & Tessier-Lavigne, M. The role of the floor plate in axon guidance. *Annual Reviews in Neuroscience* **18**, 497-529 (1995).

26. Kim, G. J., Shatz, C. J. & McConnell, S. K. Morphology of pioneer and follower growth cones in the developing cerebral cortex. *Journal of Neurobiology* **22**, 629-642 (1991).

27. Chien, C. B., Rosenthal, D. E., Harris, W. A. & Holt, C. E. Navigational errors made by growth cones without filopodia in the embryonic *Xenopus* brain. *Neuron* **11**, 237-251 (1993).

28. McConnell, S., Ghosh, A. & Shatz, C. Subplate neurons pioneer the first axon pathway from the cerebral cortex. *Science* **245**, 978-981 (1989).

29. Bovolenta, P. & Mason, C. Growth cone morphology varies with position in the developing mouse visual pathway from retina to first targets. *The Journal of Neuroscience* **7**, 1447-1460 (1987).

30. Bovolenta, P. & Dodd, J. Guidance of commissural growth cones at the floor plate in embryonic rat spinal cord. *Development* **109**, 435-447 (1990).

31. Mason, C. & Wang, C. Growth cone form is behavior-specific and consequently position-specific along the retinal axon pathway. *The Journal of Neuroscience* **17**, 1086-1100 (1997).

32. Mason, C. & Erskine, L. Growth cone form, behavior, and interactions in vivo: retinal axon pathfinding as a model. *Journal of Neurobiology* **44**, 260-270 (2000).

33. Wilson, S. & Easter, S. Stereotype pathway selection by growth cones of early epiphysial neurons in the embryonic zebrafish. *Development* **112**, 723-746 (1991).

34. Chitnis, A. & Kuwada, J. Axonogenesis in the brain of zebrafish embryo. *The Journal of Neuroscience* **10**, 1892-1905 (1990).

35. Chitnis, A. & Kuwada, J. Elimination of a brain tract increases errors in pathfinding by follower growth cones in the zebrafish embryo. *Neuron* **7**, 277-285 (1991).

36. Chitnis, A., Patel, C., Kim, S. & Kuwada, J. A specific brain tract guides follower growth cones in two regions of the zebrafish brain. *The Journal of Neurobiology* **23**, 845-854 (1992).

37. Ross, L., Parrett, T. & Easter, S. Axonogenesis and morphogenesis in the embryonic zebrafish brain. *The Journal of Neuroscience* **12**, 467-482 (1992).

38. Dynes, J. & Ngai, J. Pathfinding of olfactory neuron axons to stereotypes glomerular targets revealed by dynamic imaging in living zebrafish embryos. *Neuron* **20**, 1081-1091 (1998).

39. Jontes, J., Buchmanan, J. & Smith, S. Growth cone and dendrite dynamics in zebrafish embryos: early events in synaptogenesis imaged in vivo. *Nature Neuroscience* **3**, 231-237 (1999).

40. Pike, S., Melancon, F. & Eisen, J. Pathfinding by zebrafish motoneurons in the absence of normal pioneer axons. *Development* **114**, 825-831 (1992).

41. Greenspoon, S., Patel, C., Hashmi, S., Bernhardt, R. & Kuwada, J. The notochord and floor plate guide growth cones in the zebrafish spinal cord. *The Journal of Neurobiology* **15**, 5956-5965 (1995).

42. Wilson, S., Ross, L., Parrett, T. & Easter, S. The development of a simple scaffold of axon tracts in the brain of the embryonic zebrafish, *Branchydanio rerio*. *Development* **108**, 121-145 (1990).

43. Bak, M. & Fraser, S. E. Axon fasciculation and differences in midline kinetics between pioneer and follower axons within commissural fascicles. *Development* **130**, 4999-5008 (2003).

44. Hutson, L. & Chien, C.-B. Pathfinding and error correction by retinal axons: the role of astray/robo2. *Neuron* **33**, 205-221 (2002).

45. McDonald, R. et al. The Pax protein Noi is required for commissural axon pathway formation in the restral forebrain.. *Development* **124**, 2397-2408 (1997).

46. Lichtman, J. W. & Fraser, S. E. The neuronal naturalist: waching neurons in their native habitat. *Nature Neuroscience* **4**, 1215-1220 (2001).

47. Koester, R. W. & Fraser, S. E. Tracing transgene expression in living zebrafish embryos. *Developmental Biology* **233**, 329-346 (2001).

48. Bastiani, M. & Goodman, C. S. Neuronal growth cones: specific interactions mediated by filopodial insertion and induction of coated vesicles. *Proc. Nat. Acad. Sci. USA* **81**, 1849-1853 (1984).

49. Alsina, B., Vu, T. & Cohen-Cory, S. Visualizing synapse formation in arborizing optic axons in vivo: dynamics and modulation by BDNF. *Nature Neuroscience* **4**, 1093-1001 (2001).

50. Kasthuri, N. & Lichtman, J. W. Structural dynamics of synapses in living animals. *Current Opinion in Neurobiology* **14**, 105-111 (2004).

51. Niell, C. M., Meyer, M. P. & Smith, S. In vivo imaging of synapse formation on a growing dendritic arbor. *Nature Neuroscience* **7**, 254-260 (2004).

52. Yoshikawa, S. & Thomas, J. Secreted cell signaling molecules in axon guidance. *Current Opinion in Neurobiology* **14**, 45-50 (2004).

53. Butler, S. J. & Dodd, J. A role for BMP heterodimers in roof plate-mediated repulsion of commissural axons. *Neuron* **38**, 389-401 (2003).

54. Yoshikawa, S., D., M. R., Kokel, M. & Thomas, J. Wnt-mediated axon guidance via the Drosophila derailed receptor. *Nature* **422**, 583-588 (2003).

55. Charron, F., Stein, E., Jeong, J., McMahon, A. & Tessier-Lavigne, M. The morphogen Sonic Hedgehog is an axonal chemoattractant that collaborates with Netrin-1 in midline axon guidance. *Cell* **113**, 11-23 (2003).

56. Ming, G. Cyclic-AMP-dependent growth cone guidance by netrin-1. *Neuron* **19**, 1225-1235 (1997).

57. Nishiyama, M. et al. Cyclic AMP.GMP-dependent modulation of CA2+ channels sets the polarity of nerve growth-cone turning. *Nature* **423**, 990-995 (2003).

58. Woo, K. & Fraser, S. E. Oder and coherence in the fate map of the zebrafish nervous system. *Development* **121**, 2595-2609 (1995).

59. Draper, B., Marcos, P. A. & Kimmel, C. B. Inhibition of zebrafish fgf8 pre-mRNA splicing with morpholino oligos: a quantifiable method for gene knockdown. *Genesis* **30**, 154-156 (2001).

60. Nasevicius, A. & Ekker, S. Effective targeter gene 'kockdown' in zebrafish. *Nature Genetics* **26**, 216-220 (2000).

61. Westerfield, M. The Zebrafish Book. *University of Oregon Press* **Eugene, OR.** (1995).

62. Wilson, S., Brennan, C., McDonald, R., Brand, M. & Holder, N. Analysis of axon tract formation in the zebrafish brain:the role of terrirories of gene expression and their boundaries. *Cell Tissue Research* **290**, 198-196 (1997).

63. Meng, A., Tang, H., Ong, B., Farrell, J. & Lin, S. Promoter analysis in living zebrafish embryos identifies a cis-acting motif required for neuronal expression of GATA-2. *The Proceedings of the National Academy of Science* **94**, 6267-6272 (1997).

64. Cohen-Cory, S and Fraser, S.E. Effects of brain-derived neurotrophic factor on optic axon branching and remodeling in vivo *Nature* **378,** 192-196 (1995).

Chapter 2 Cell labeling for imaging studies of early nervous system development

Magdalena Bak and Scott E. Fraser

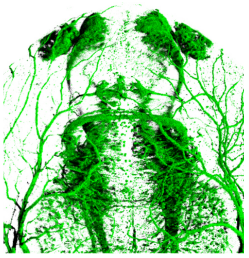

SUMMARY

Our understanding of biological processes and cell behavior(s) is increasingly linked to our ability to label cells. Recent advances in genetically encoded fluorescent proteins (FPs) as well as vital dyes are allowing us to highlight cells and observe them dynamically in a living embryo. Here we present a number of different approaches to cell labeling that can be used in zebrafish and discuss their usefulness for imaging studies.

2.1 Cell labeling in the zebrafish embryo

Cell labeling with genetic methods through the introduction of fluorescent proteins (FPs) and other vital dyes is rapidly advancing dynamic studies of nervous system development and embryo morphogenesis. These techniques allow researchers to highlight the cells of interest and follow their migration or behavior over time in a living embryo. Zebrafish development is relatively fast compared to other vertebrate model systems such as chicken or mouse. In a 24-hour period a fertilized zebrafish embryo develops into a small mini-adult with a clearly distinct brain. Development is also external allowing easy access for labeling the cells to be studied. Many cell markers such as dextrans, cDNA expression constructs or mRNAs for FPs can be injected into a large number (50-100) of single cell stage embryos quickly and relatively easily. In addition, a number of vital dyes including lipophilic and cell permeant dyes can be either injected or soaked into the embryo at different stages to highlight cell boundaries (bodipy dyes) or to trace axonal projections (DiI and its derivatives). Together these techniques provide a powerful arsenal of cell labeling methods that can be further intermixed to achieve more intricately labeled cell patterns.

The work described in this dissertation was motivated by the need to understand the early phases of forebrain circuitry development in vertebrates using zebrafish. We first studied axon behaviors during commissure formation and second gained insight into molecular signals that guide this process. These types of studies benefit from reproducibly labeled cells so that their behavior(s) can be subsequently characterized using dynamic imaging. Detailed descriptions of this sort can be later used to perform functional studies and assay specific phenotypes. We were specifically interested in

following the behaviors of early axons and their growth cones. Toward this goal we experimented with a number of cell labeling techniques. Here we describe these methods in more detail and discuss their usefulness for imaging studies.

2.2 Lipophilic and cell permeant dyes

Many of the dyes employed today have a long history of being used to reveal the structures of the nervous system. This is especially the case for the group of lipophilic carbocyanines fluorescent tracers DiI, DiO and DiD (Molecular Probes). Low toxicity of these dyes makes them well suited for labeling neurons. When applied to live brain tissue or near nerve endings, DiI dyes are taken up by axon terminals and transported back to cell bodies. In fixed samples, the dye diffuses in the membrane and is able to label axons along considerable distances. For this reason, they have been extensively used for tracing early neuronal projections in a number of different systems[1,2]. Usually a small injection site is made and the dye is picked up by axons or the cell body. Because these dyes have slightly different excitation and emission profiles, they can be used in combination for multicolor imaging.

To label axons in the early zebrafish brain we initially experimented with DiI and made small injections into different regions of the zebrafish brain in wildtype embryos. However, we found this method of labeling axons not ideal for our purpose. Because of the lipophilic nature of DiI, the injection site usually ended up being too large and the DiI stained other cells in the vicinity of the injection site (Figure 2-1a,a'). This made it difficult to visualize the morphologies of DiI labeled neurons in detail. Also the location of injection had to be well targeted in order to mark axon bundles. This was difficult in

an otherwise unlabeled embryo. Finally, because we injected DiI using a pressure picospritzer we judged this method not ideal for studies in which we wanted to observe axon behaviors dynamically soon after the injection. This together with the improvements in other cell labeling methods made us look for alternative ways to mark early neurons in the zebrafish brain.

In our later studies we returned to DiI tracing to demonstrate that the postoptic (POC) GFP expressing axons we were observing were indeed the first axons along the POC axon tract (Chapter 3). To demonstrate this, we injected DiI into fixed embryos at a timepoint when the first GFP positive growth cone appeared along the future POC. This was done to label other POC axons that might not express GFP but which should be easily visualized with the DiI. In these embryos, DiI only labeled the GFP positive axons. However, similar injections into one of the ventrorostral cell clusters labeled many POC axons in slightly older embryos. Thus DiI and its relatives continue to be very useful cell labeling dyes.

We also used the family of bodipy fluorescent dyes useful in highlighting cell boundaries. These dyes are excellent for providing a counter cell labeling method in both fixed and live embryos because they can be taken up by soaking the embryo in a solution containing the dye. The green fluorescence bodipy ceramide is particularly effective at penetrating and labeling cell membranes in one to two day old zebrafish embryos. However, it is not at all robust to bleaching during repetitive imaging. Instead, the dye can be used to highlight cells at less frequent intervals to provide a framework for the architecture of the tissue in a specific part of the embryo. Because the dye intercalates into the cell membrane, it can also be used to visualize cell division in the early

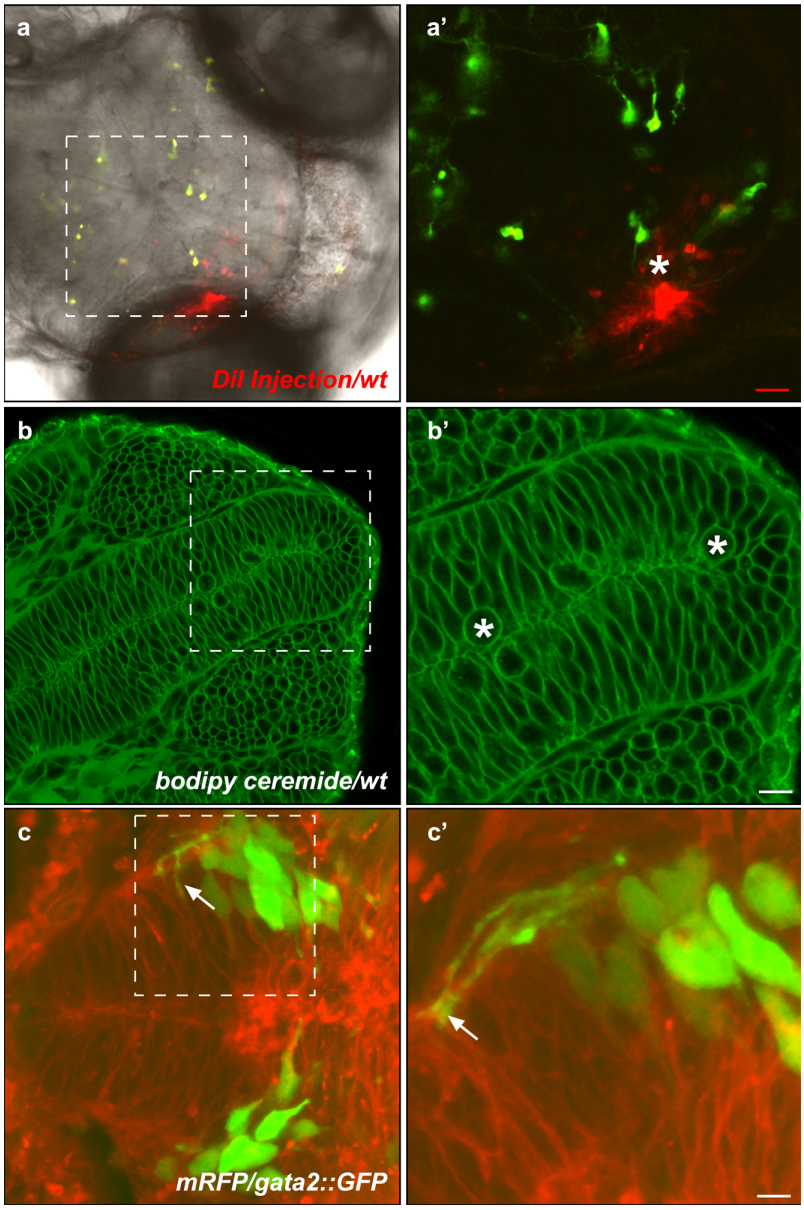

Figure 2-1 Methods for labeling cells in living zebrafish embryos.

(a,a') Example of DiI injection (star) into the tectum of a three day old zebrafish embryo. Green cells represent neurons that have been labeled with GFP using transient expression. The intense DiI signal makes it difficult to visualize labeled axonal processes nearby.**(b,b')** 20-21hpf zebrafish embryo soaked in bodipy ceremide dye used to visualize cell boundaries. Prior to division, early neuroepethelial cells round up for mitosis (star). This can be effectively visualized with this dye and the sequence of events during division followed over time.**(c,c')** gata2::GFP embryo injected with mRNA encoding mRFP. GFP expression can be seen in the ventro-rostral cell clusters and initial POC axons (arrow). This type of co-labeling allows the interaction between the green growth cones and surrounding cells to be followed in time.

neuroepithelium (Figure 2-1b,b'). Also, while not practical for continuous imaging studies, the embryos can be repeatedly re-soaked for further imaging.

In summary, vital dyes continue to be useful for cell labeling and they continues to serve as a good complement to recently developed genetic cell labeling methods using FPs which we discuss below.

2.3 Transient transgenics

The zebrafish embryo is well suited for cDNA and mRNA injections that can serve as means to introduce fluorescent proteins (FPs) to label cells for imaging studies.

Labeling cells with FPs mRNA

Injecting mRNA directly into one-four cell stage zebrafish embryos is a rapid way of labeling cells early on in development. This method is particularly attractive for researchers wanting to study developmental processes during early embryogenesis such as gastrulation movements. Because the embryo is injected early, the mRNA that will be translated into a particular FP is ubiquitously distributed. Additional targeting sequences can be added to express FPs in specific subcellular structures allowing multiple features of the cell to be labeled and followed in time simultaneously. This was recently performed to follow cell division and its contribution to axis elongation in zebrafish embryos[3]. mRNA injection of FPs can be used for labeling cells in order to create mosaic embryos which are particularly useful for dissecting whether a given gene functions autonomously or is needed in neighboring cells and for transplants. However injected mRNA is in a limited supply and gets degraded over time which means that the labeling

will become more dilute as embryos develop. Therefore, labeling cells with mRNA FPs works best for following early developmental events in zebrafish that are up to one day old. FPs expressed from mRNA are also very sensitive to repeated imaging and quickly bleach. Injecting mRNA that encodes FP proteins that have localization sequences that target them to specific cellular compartments such as the nucleus, mitochondria, or cell membrane can slow down the bleaching. Such FPs are more resistant to bleaching because the FP ends up being more concentrated.

Another use for mRNA cell labeling with FPs is to highlight background cells similarly to cell permeant dyes mentioned earlier. For example, in our studies the ventro-rostral neuronal clusters and their axons express GFP allowing us to observe early POC axon behaviors as they grow towards and across the midline. However, in these timelapse experiments the rest of the cells are not labeled. Thus while we can observe the behaviors of POC growth cones, we cannot visualize the neuroepethelial cells they grow on. To highlight both cell types and follow their interactions we used mRNA cell labeling methods to introduce membrane targeted red fluorescent protein (mRFP) into gata2::GFP embryos that express GFP in the POC axons. This way we could visualize the GFP expressing growth cones in context of the developing brain and track the interactions between them and the neighboring cells (Figure 2-1c,c'). A limit on these studies however, was that during frequent scans the signal was completely lost in 2 hours while acquiring z stacks every 6min. Further improvements in FPs in terms of their brightness and photo stability might allow similar studies to be done in the future.

Labeling cells with cDNAs encoding FPs

While mRNA tends to be rapidly degraded, DNA plasmids are more stable in fish embryos[4]. Also, by using tissue-specific regulatory elements, cell labeling can be spatially and temporally controlled in contrast to mRNA. Presently however, the temporal control in particular is very difficult because of the lack of sufficient numbers of temporally restricted promoter elements that would offer this type of flexibility other than the heatshock promoter. Perhaps the most elegant advantage of this method is that because the injected plasmid results in a mosaic labeling pattern, this allows small groups of cells or even individual cells to be analyzed in a background of unlabeled or wildtype cells. This can be advantageous for studies of cell migration, for example where labeling all the cells might make resolving their individual behaviors during migration difficult (see below). The mosaic aspect of this technique also readily lends itself to studies of gene function. In spite of these advantages, until recently DNA plasmids were not broadly employed because the resulting expression was very low[5].

A great advance for long term imaging has been the development of amplified gene expression cDNA constructs based on the Gal4UAS system used in Drosophila[6]. In this case, a gene of interest or a fluorescent protein is placed behind a number of UAS binding sites. A Gal4 transcriptional activator driven by a specific promoter, controls the expression of the effector gene or FP. Once made, Gal4 binds to UAS sites and increases the transcription level of the effector gene. This results in higher expression levels of the gene or FP of interest[5,6]. In addition, this system is highly versatile as the activator and effector components can reside on different plasmids. In zebrafish Koester and Fraser found that fusion of the yeast Gal4 domain to the herpes simplex virus transcriptional

activation domain (VP16) results in high levels of effector gene expression[5] and can be successfully used for following cell behaviors using extended timelapse imaging[7]. Using transient expression, Koester and Fraser were able to follow fates of neuronal precursor cells generated within the upper rhombic lip directly[7].

Another characteristic of this technique is that the actual number of labeled cells in each embryo injected with the same plasmid is variable which can be advantageous for certain experiments. Using transient expression of EGFP we were able to label early neurons in the zebrafish forebrain and follow a number of different cell behaviors from how early neruons delaminate and begin to grow an axon, to axon behavior during

Figure 2-2 Transient GFP labeled cells in the early developing zebrafish brain (next page)

(a) 20hpf zebrafish embryo with high number of cells labeled in the developing neuroepithelium. Labeled cells on both sides of the midline (red broken line) are arranged in parallel and are in contact with the midline via a single process (arrows). Cells can be seen loosing contact as they move laterally (last panel arrow).

(b) 19-20hpf zebrafish embryo where a delaminating early neuron has been labeled with GFP. This neuron is in contact with the midline but also is extending an axon-like process (arrow). The process connecting the cell to the midline is eventually withdrawn when the axon reaches a cell cluster (circle).

(c) 27hpf zebrafish embryo in which cells in one of the neuronal clusters in the brain have been labeled. These cells have active protrusions (arrows) that they extend towards one another. This type of contact between cells is transient but appears to be ongoing.

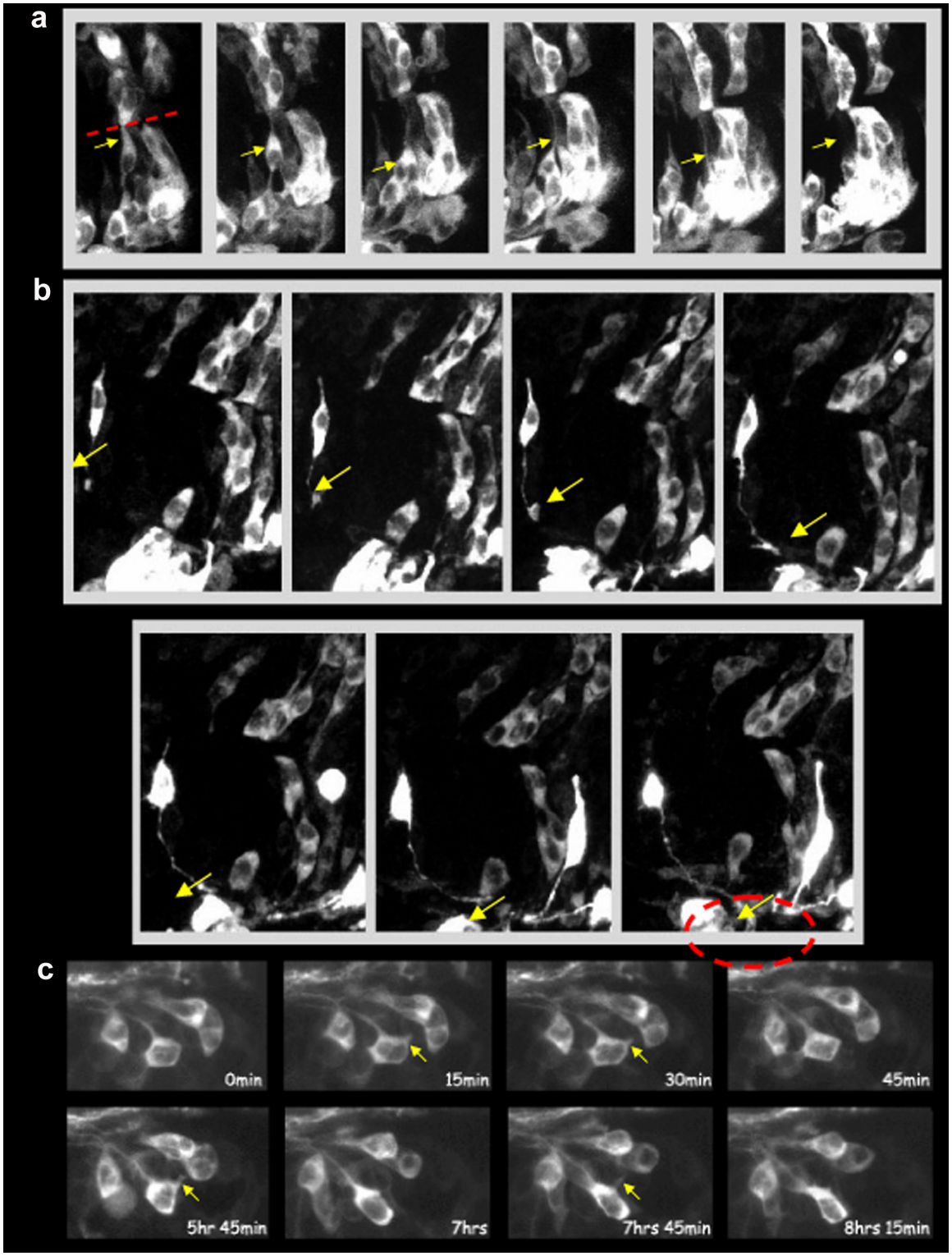
a
b
c
0min
15min
30min
45min
5hr 45min
7hrs
7hrs 45min
8hrs 15min

navigation and dynamics of cell protrusions (Figure 2-2). However this type of labeling was not ideal for our purposes because the cells being labeled were truly random, which prevented us from repeatedly imaging the behaviors of a single group of cells. This meant that to understand a given behavior we would need to always find an embryo that had a subset of the proper cells labeled and perform a large number of studies to generalize the behavior of a given group of cells. While this is slightly easier for studies of a large population of neurons such as in the cerebellum of older embryos, it is less practical for labeling the early neuronal clusters. This led us to examine a number of stable zebrafish lines that had neuron specific GFP expression and which we hoped would be most useful for our studies.

We were able to use the transient cell labeling method for another set of experiments in which we wanted to ectopically express netrin in cells that would be positioned in close proximity to the GFP expressing growth cones of POC axons. This in turn would allow us to assay the behavioral responses of POC growth cones to netrin (Chapter 5). Because the GAL4VP16UAS system allows for more than one effector gene to be expressed[5], we created a plasmid that contained mRFP and netrin1a under separate UAS sites on the same plasmid thus ensuring that cells expressing netrin would be marked red (Chapter 5). The variability in position and number of labeled cells common to this method of cell labeling was ideally suited for this purpose.

Currently there are many fluorescent proteins commercially available to the experimenter[8-12], greatly increasing both the flexibility of choosing a particular fluorescent protein based on the laser(s) available in a given imaging setup as well as the combinatorial multi color imaging schemes[13,14]. Thus transient cell labeling can already

provide us with multicolor imaging to study cell interactions *in vivo* before similar multicolor stable transgenic fish are made. Further improvements in the relative brightness of different spectral FPs along with identification of additional tissue specific promoter and enhancer elements will further increase the power of this cell labeling method.

2.4 Electroporation method for labeling cells

Electroporation is a voltage-assisted method of transferring DNA into cells that has in recent years allowed genetic analyses to be performed in more classical embryological model systems like chicken and Xenopus in which transgenic techniques are not readily available[15,16]. By having control over the time when DNA is injected into cells, electroporation allows both spatial and temporal control for labeling cells, which is not completely possible with DNA plasmid injections into single cell embryos (see above). Furthermore, electroporation alleviates some of the requirements for having tissue specific promoters needed for spatial or temporal targeting of a FP cell marker or for functional studies of proteins in an otherwise normal embryo. This can be particularly advantageous for studying later functions of genes that have roles in both early and later development of the embryo.

Electroporation applied to zebrafish offers several specific benefits for cell labeling and functional studies. Different cell types can be labeled with different FPs to allow dynamic cell interaction studies and to analyze the functions of specific proteins in a mosaic population of cells in a chosen window of development and particular location. Also, while a number of transgenic zebrafish lines, including the gata2::GFP line we used

in our studies exist, most of them use GFP as a cell marker. This means that even when the cells of interest are sufficiently labeled, observing them might be difficult because they cannot be resolved from one other. We encountered this problem with GFP expressing POC axons. Because these axons fasciculate with each other, our observations were mostly limited to initial axons, because later in development we could not reliably distinguish and track individual POC growth cones for extended time periods. In such cases electroporation could be used to increase the effective resolution of a single bundle of axons or cell groups by introducing another FP into the area. A similar approach has been used in chimaeric mice expressing different FPs or double transgenics allowing cell interactions to be studies dynamically[8].

While this technique has obvious benefits for developmental studies in zebrafish, electroporation has not been widely used in this system. A partially successful application documented the delivery of GFP into the regenerating fin nerve, albeit with low efficiency[17]. However, more recently another approach has achieved more promising results using a “Gene Pulser” cuvette[18].

We adopted the electroporation technique for use in zebrafish embryos based on the external electrodes method commonly used in the chicken (Figure 2-3) in order to be able to label cells selectively. In this method, the DNA is injected into the neural tube for labeling cells in the nervous system followed by a voltage pulse. Because the DNA is negatively charged, it will be transferred to the side of the embryo adjacent to the positive electrode (Figure 2-3). This allows an elegant internal control on the side that is not electroporated.

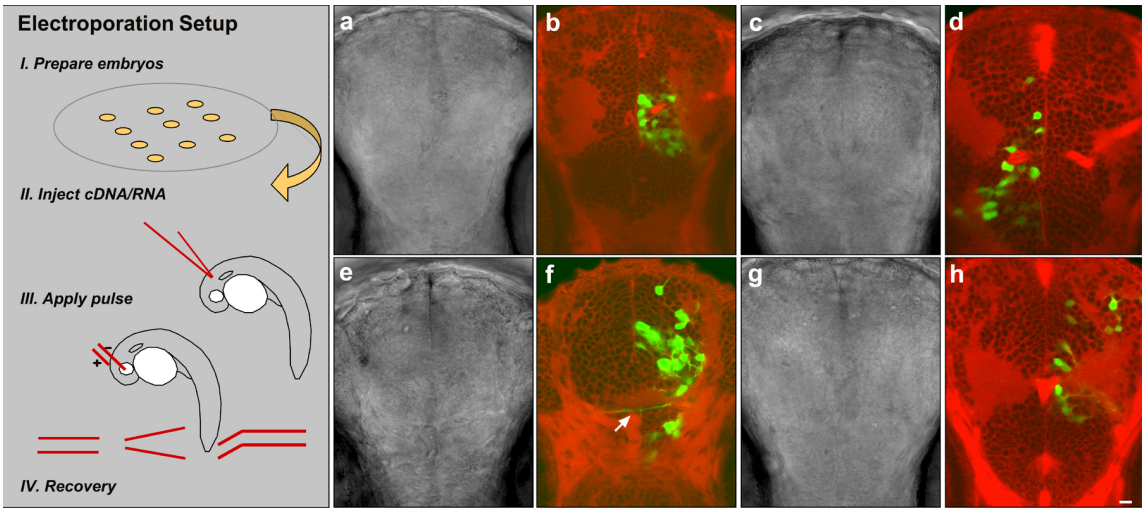

Figure 2-3 Electroporation in zebrafish

(left) Diagram illustrating the electroporation procedure. Embryos are mounted in low melt agorose and injected with DNA (0.5-1µg/ml) followed by a 15-25mV voltage pulse. Embryos are subsequently taken out of the gel and allowed to recover at 28°C.

(b,d,f,h) 24hpf wildtype zebrafish embryos that have been electroporated with a DNA plasmid encoding GFP into the forebrain region. Electroporation results in specific transfer of DNA to one side of the embryo as visualized here with a red fluorescence bodipy ceramide dye. The number and position of labeled cells with respect to the midline varies. The GFP is expressed at high level and allows visualization of axon processes (f). **(a,c,e,g)** Corresponding brightfield images taken at the same position.

Our method in the zebrafish allows rapid and selective labeling of the nervous system along any section of the anterior-posterior axis of the embryo. Cells labeled with electoporated cDNAs encoding different FPs can be subsequently timelapsed for extended times, similarly to embryos injected with GALVP16UAS plasmids. The DNA is delivered into the neural tube using pressure injection followed by a voltage pulse. The duration of the pulse as well as the spacing of the electrodes have to be empirically determined for embryos at different stages. We were successful at electroporating embryos between 16hpf-5dpf. Typical survival rates at these stages were between 50-75% with half the surviving embryos having FP expression. Lower survival was obtained

in embryos at younger stages (16-19hpf) largely due to the embryos being small and more sensitive to the injection procedure.

Unlike the cuvette method which lacks good spatial control, we were able to selectively electroporate DNA into the forebrain, midbrain and hindbrain sections of the zebrafish brain as well as the eye, ear, spinal cord and tail regions of the embryo (Figure 2-4).

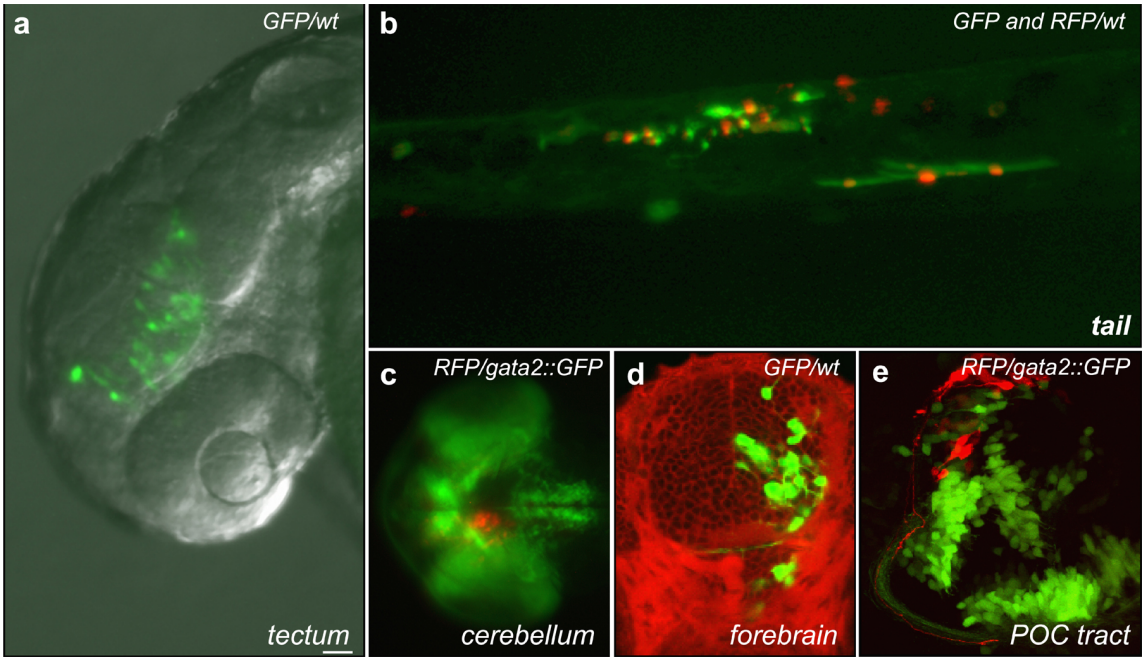

Figure 2-4 Electroporation in zebrafish can be targeted to different areas of the embryo.

(a) 24hpf wildtype embryo electroporated with DNA encoding GFP into the tectum **(b)** 2dpf wildtype embryo that has been co-electroporated with two different FPs (GFP and RFP) into the tail region. **(c)** 36hpf gata2::GFP stable trangenic electroporated with DNA encoding RFP into the cerebellum **(d-e)** 24-27hpf embryos that were electroporated with DNA encoding FPs under a neuron specific promoter. Introduction of a second color greatly increases the resolution as demonstrated by the RFP expressing axons in the gata2::GFP background.

This electroporation method can be applied to stable transgenic lines as a way to introduce more cell labels. Co-injection of different FPs resulted in multicolor cell labeling, however the extent to which the colors are co-localized remains to be examined in detail.

Cell labeling with this method appears to be very stable, and embryos could be imaged days after the electroporation. Interestingly, electroporation of DNA plasmid where the EGFP was under the control of a ubiquitous cytomegalovirus (CMV) promoter that would normally produce weak transient labeling resulted in expression yields comparable to embryos that were electroporated with a construct where EGFP expression level was expected to be boosted by the Gal4VP16UAS amplification system. This might result from enough DNA entering the cell during electroporation that initial differences in expression are difficult to observe. We did not carry out a thorough analysis to fully evaluate this further. This result is very encouraging and suggests that plasmids encoding FPs or other genes of interest would not need to be first subcloned into the amplification vectors to be effectively used for expression using electroporation.

A few further improvements are needed to make zebrafish electroporation highly reproducible and universally used for cell labeling and functional studies. In particular, better control over the pulse strength is needed. Currently both the voltage intensity and the distance between electrodes need to be re-adjusted. At present, electroporation is limited to tissues that are located in close proximity to a cavity where DNA can be injected. In the future, the technique might allow DNA to be transferred from outside the embryo using a gel matrix or some other DNA holding medium. This will greatly increase the versatility of labeling tissues in much older embryos that are not close to a

cavity without the need to inject DNA into the cells themselves. With these developments it might be soon possible to electroporate other functional molecules into subsets of cells such as morpholinos, as has been demonstrated in chicken[19].

In summary, electroporation should be added to the zebrafish tool box of cell labeling methods. It allows for multicolor labeling of cells in wildtype or readily available GFP stable expressing lines. Its use offers a potential similar to that found in chicken and Xenopus embryos for gain of function and loss of function experiments (using dominant negative expression constructs). It provides several advantages to other presently available labeling methods. First, a subset of cells can be labeled at any time. Second, using a mixture of DNAs coding for different FPs the structural morphologies and behaviors of adjacent cells can be visualized and their projections traced with increased resolution. Third, free control over the orientation of the electrodes allows electroporation to be manipulated to direct the expression of FPs or other constructs specifically to dorsal or ventral structures. Given these advantages, this technique can be used for a number of exciting studies. For example, in combination with mutants that have different components of the same signaling pathways mutated, electroporation can be used to dissect the hierarchical levels of a signaling cascade in terms of their function by allowing the specific components to be restored to different subsets of cells in the same embryos. This would allow for combinatorial analysis of signaling while simultaneously imaging cell behavior(s). In another scenario, electroporation will be the ideal method for tracing neuronal connections trans-synaptically because in this case only a small source of transsynaptic marker should be present. Because electroporation is unilateral this type of labeling can be nicely exploited for tracing projections. Thus,

electroporation will be a useful technique used to probe many developmental processes and the function of the nervous system.

2.5 Stable transgenics with neuron specific expression

After testing a number of different cell labeling techniques, we decided to examine available stable transgenics with nervous system specific expression and evaluate their suitability for live imaging studies of early forebrain neuronal scaffold development. This is possible because many transgenic lines have broad expression patterns that are not always completely characterized and some have not been used in imaging studies so far. We examined three specific lines: the αtubulin::GFP [20], HuC::GFP [21], and gata2::GFP[22] and evaluated their suitability for in vivo imaging.

The α1 tubulin fragment fused to GFP results in GFP expression in neuronal progenitor cells and their differentiated progeny[20]. As the maximal GFP expression was reported to occur at 24hpf, which correlates with the formation of the early neuronal scaffold, this was our most promising candidate. Timelapse analysis revealed that homozygous embryos had sufficient GFP expression to allow visualization of the early forebrain neuronal clusters. However, at 24hpf GFP expression in early axons was absent.

The HuC::GFP line was similar to the αtubulin::GFP line, having relatively well labeled early differentiating neuronal cells in the forebrain, but had weak GFP expression in the axonal processes. However, the expression was too low to visualize growth cones. At later stages the GFP expression became significantly brighter. While not suitable for

studying axon behaviors, both of these lines and especially the HuC::GFP line are well suited for following the formation of early neuronal clusters. They are also well suited for performing detailed tracings of the early connections between cell clusters that could be done with different color dextrans and iontophoresis.

The third line (gata2::GFP) proved well suited for our studies. GATA2 is a transcription factor normally expressed in the hematopoietic lineage and the nervous system[22]. In the central nervous system (CNS), GATA2 is implicated in specifying neurotransmitter phenotype[23]. The gata2::GFP line had the highest level of GFP expression compared to the other two lines. During early stages of the neuronal scaffold formation, GFP is strongly expressed in the ventro-rostral neuronal clusters and the axons forming the POC[24], but many other neuronal cells also express GFP throughout the CNS. Strong GFP expression in the gata2:;GFP embryos allowed us to perform detailed studies of the behavior of early POC commissural axons [24] (Chapter 3), functional studies revealing the role of DCC and netrin in POC formation [24] (Chapter 4) and measurements of local protein diffusion in early navigating growth cones[25] (Chapter 5). Based on these results we believe that the gata2::GFP line along with the islet1::GFP[26] (which we did not mention here) represents the best currently available stable transgenics for imaging the developing nervous system.

Recent progress in imaging techniques [13,14,27-29] and improvements in fluorescent proteins[8-12] has been paralleled by an equal expansion in stable transgenic zebrafish lines[30]. A substantial subset of these stable lines has a nervous system specific GFP expression[20-22,26,30-32]. Nevertheless, a relatively small number of research reports so far have utilized them for in vivo imaging of nervous system development. Instead, transient

GFP expression and/or lipophilic dye tracing were used[3,7,33-38]. This observation highlights one of the present problems that researchers wanting to employ stable lines continue to face, namely that the level of GFP expression required must be sufficiently high to allow repeated illumination with relatively low laser power so as not to cause photodamage. Further developments to create brighter FPs with rapid maturation and/or varied degradation kinetics to allow them to serve as temporal reporters of gene expression, additional monomeric spectral variants, and functionalized FPs acting as cellular sensors offer great potential for the field of stable zebrafish transgenics. For example, Halloran et al. made transgenic lines in which the inducible hsp70 (heat shock promoter) has been linked to GFP, demonstrating that GFP or any other gene expression can be regulated in both space and time[32]. However, the suitability of the hsp70 driven GFP expression for live imaging has not been directly evaluated. Another thus far relatively unexplored area in zebrafish transgenics has been to make stable lines that express different spectral variants of fluorescent proteins in the same embryo. These multicolor lines would be particularly useful for developmental neurobiology by both increasing resolution and allowing studies of cellular and subcellular components that interact with each other.

In summary, presently available labeling methods and stable lines are making it easier to follow and understand cell behaviors in a wide variety of developmental processes dynamically. The near future of dynamic studies looks bright and multicolored.

Acknowledgements

We would like to thank Shuo Lin (gata2::GFP), T-L Huh (Huc::GFP), and Dan Goldman (αtubulin::GFP) for providing us with the transgenic fish. We thank Rajan Kulkarni and Helen McBride for critical reading and discussions.

2.6 References

1. Mastick, G. & Easter, S. E., Jr. Initial organization of neurons and tracts in the embryonic mouse fore and midbrain. *Developmental Biology* **173**, 79-94 (1996).
2. McConnell, S., Ghosh, A. & Shatz, C. Subplate neurons pioneer the first axon pathway from the cerebral cortex. *Science* **245**, 978-981 (1989).
3. Gong, Y., Mo, C. & Fraser, S. E. Planar cell polarity signalling controls cell division orientation during zebrafish gastrulation. *Nature* **430**, 689-693 (2004).
4. Winkler, C., Vielkind, J. R. & Schartl, M. Transient expression of foreign DNA during embryonic and larval development of the medaka fish (Oryzias latipes). *Mol. Gen. Genet* **226**, 129-140 (1991).
5. Koester, R. W. & Fraser, S. E. Tracing transgene expression in living zebrafish embryos. *Developmental Biology* **233**, 329-346 (2001).
6. Fischer, J. A., Giniger, E., Maniatis, T. & Ptashne, M. Gal4 activates transcription in *Drosophila*. *Nature* **332**, 853-856 (1988).
7. Koester, R. W. & Fraser, S. E. Direct imaging of in vivo neuronal migration in the developing cerebellum. *Current Biology* **27**, 1858-1863 (2001).
8. Hadjantonakis, A.-K., Dickinson, M. E., Fraser, S. E. & Papaioannou, V. E. Technicolour trangenics: imaging tools for functional genomics in the mouse. *Nature Reviews in Genetics* **4**, 613-625 (2003).
9. Guerrero, G. & Isacoff, E. Y. Genetically encoded optical sensors of neuronal activity and cellular function. *Current Opinion in Neurobiology* **11**, 601-607 (2001).

10. Miyawaki, A. Fluorescence imaging of physiological activity in complex systems using GFP-based probes. *Current Opinion in Neurobiology* **13**, 591-596 (2003).

11. Pozzan, T., Mongillo, M. & Rudolf, R. Investigating signal transduction with genetically encoded fluorescent probes. *European Journal of BIochemistry* **270**, 2343-2352 (2003).

12. Zhang, J., Campbell, R. E., Ting, A. Y. & Tsien, R. Y. Creating new fluorescent probes for cell biology. *Nat Rev Mol Cell Biol* **3**, 906-918 (2002).

13. Lansford, R., Bearman, G. & Fraser, S. E. Resolution of multiple green fluorescent protein color variants and dyes using two-photon microscopy and imaging specroscopy. *Journal of Biomedical Optics* **6**, 311-8 (2001).

14. Dickinson, M. E., Bearman, G., Tille, S., Lansford, R. & Fraser, S. E. Multi-spectral imaging and linear unmixing add a whole new dimension to laser scanning fluorescence microscopy. *Biotechniques* **31**, 1272, 1274-6, 1278 (2001).

15. Sasagawa, S., Takabatake, T., Takabatake, Y., Mauramatsu, T. & Takeshima, K. Improved mRNA electroporation method in Xenopus neurula embryos. *Genesis* **33**, 81-85 (2002).

16. Swartz, M., Eberhart, J., Mastick, G. S. & Krull, C. E. Sparking new frontiers: Using in vivo electroporation for genetic manipulations. *Developmental Biology* **233**, 13-21 (2001).

17. Echeverri, K. & Tanaka, E. M. Elecroporation as a tool to study in vivo spinal cord regeneration. *Developmental Dynamics* **226**, 418-425 (2003).

18. Teh, C., Chong, S. W. & Korzh, V. DNA delivery into anterior neural tube of zebrafish embryos by electoporationi. *BioTechniques* **35**, 950-954 (2003).

19. Kos, R., Tucker, R., Hall, R., Duong, T. D. & Erickson, C. A. Methods for introducing morpholinos into the chicken embryo. *Developmental Dynamics* **226**, 470-477 (2003).

20. Goldman, D., Hankin, M., Dai, X. & Ding, J. Trangenic zebrafish for studying nervous sytem development and regeneration. *Transgenic Research* **10**, 21-33 (2001).

21. Park, H.-C. et al. Analysis of upstream elements in the HuC promoter leads to the establishment of transgenic zebrafish with fluorescent neurons. *Developmental Biology* **227**, 279-293 (2000).

22. Meng, A., Tang, H., Ong, B., Farrell, J. & Lin, S. Promoter analysis in living zebrafish embryos identifies a cis-acting motif required for neuronal expression of GATA-2. *The Proceedings of the National Academy of Science* **94**, 6267-6272 (1997).

23. Groves, A. K. et al. Differential regulation of transcription factor gene expression and phenotypic markers in developing sympathetic neurons. *Development* **121**, 887-901 (1995).

24. Bak, M. & Fraser, S. E. Axon fasciculation and differences in midline kinetics between pioneer and follower axons within commissural fascicles. *Development* **130**, 4999-5008 (2003).

25. Bak-Maier, M., Kulkarni, R. & Fraser, S. E. One and Two-Photon FRAP reveals differences in mobility of cytosolic GFP in growth cones in vivo. *Manuscript submitted to Science* (2004).

26. Higashijima, S., Hotta, Y. & Okamoto, H. Visualization of cranial motor neurons in live transgenic zebrafish expressing green fluorescent protein under the control of the Islet-1 promoter/enhancer. *The Journal of Neuroscience* **20**, 206-218 (2000).

27. Lippincott-Schwartz, J. et al. Monitoring the dynamics and mobility of membrane proteins tagged with green fluorescent protein. *Methods in Cell Biology* **58**, 261-281 (1999).

28. Lippincott-Schwartz, J., Snapp, E. & Kenworthy, A. Studying protein dynamics in living cells. *Nature Reviews in Molecular Cell Biology* **2**, 444-456 (2001).

29. Megason, S. G. & Fraser, S. E. Digitizing life at the level of the cell:high performance laser-scanning microscopy and image analysis for in toto imaging of development. *Mechanisms of Development* **120**, 1407-1420 (2003).

30. Udvadia, A. J. & Linney, E. Windows into development: historic, current, and future perspectives on transgenic zebrafish. *Developmental Biology* **256**, 1-17 (2003).

31. Yoshida, T. & Mishina, M. Neuron-specific gene manipulations in transparent zebrafish embryos. *Methods in Cell Science* **25**, 15-23 (2003).

32. Halloran, M. C. et al. Laser-induced gene expression in specific cells of trangenic zebrafish. *Development* **127**, 1953-1960 (2000).

33. Das, T., Payer, B., Cayouette, M. & Harris, W. In vivo time-lapse imaging of cell divisions during neurogenesis in the developing zebrafish retina. *Neuron* **37**, 597-609 (2003).

34. Dynes, J. & Ngai, J. Pathfinding of olfactory neuron axons to stereotypes glomerular targets revealed by dynamic imaging in living zebrafish embryos. *Neuron* **20**, 1081-1091 (1998).

35. Fetcho, J. & O'Malley, D. M. Imaging neuronal networks in behaving animals. *Current Opinion in Neurobiology* **7**, 832-838 (1997).

36. Hutson, L. & Chien, C.-B. Pathfinding and error correction by retinal axons: the role of astray/robo2. *Neuron* **33**, 205-221 (2002).

37. Jontes, J., Buchmanan, J. & Smith, S. Growth cone and dendrite dynamics in zebrafish embryos: early events in synaptogenesis imaged in vivo. *Nature Neuroscience* **3**, 231-237 (1999).

38. Niell, C. M., Meyer, M. P. & Smith, S. In vivo imaging of synapse formation on a growing dendritic arbor. *Nature Neuroscience* **7**, 254-260 (2004).

Chapter 3 Axon kinetics in the zebrafish forebrain

Magdalena Bak and Scott E. Fraser

SUMMARY

Early neuronal scaffold development studies suggest that initial neurons and their axons serve as guides for later neurons and their processes. While this arrangement might aid axon navigation, the specific consequence(s) of such interactions are unknown in vivo. We follow forebrain commissure formation in living zebrafish embryos using timelapse fluorescence microscopy to quantitatively examine commissural axon kinetics at the midline: a place where axon interactions might be important. While it is commonly accepted that commissural axons slow down at the midline, our data shows this is only true for leader axons. Follower axons do not show this behavior. However, when the leading axon is ablated, follower axons change their midline kinetics and behave as leaders. Similarly, contralateral leader axons change their midline kinetics when they grow along the opposite leading axon across the midline. These data suggest a simple model where the level of growth cone exposure to midline cues and presence of other axons as a substrate shape the midline kinetics of commissural axons.

3.1 Introduction

During development of the central nervous system (CNS), neurons differentiate and connect with one other, enabling information processing and the establishment of specific behavioral patterns. A better understanding of the early events in neuronal connectivity in the forebrain is a fundamental step in understanding how the brain assembles itself and functions. Unlike their adult counterparts, early embryonic brains are relatively simple, with a small number of neurons and neuronal tracks, offering unique advantages for mechanistic studies. Detailed studies of tract formation in invertebrate nervous systems have shown that a small number of early neurons, termed pioneers, lay down an axonal scaffold that later axons and their growth cones follow [1-5]. Removal of these pioneers adversely affects the pathfinding of later axons [6-9]. Growth cones of pioneer and later axons differ in their morphology: early axons posses larger and more complex growth cones [3,10]. Furthermore, growth cone morphology changes correlate with specific choice points along the axon route [11].

Analogous mechanisms may be involved in establishing the initial neuronal circuitry in vertebrates. For example, connections between the cerebral cortex and the thalamus originate from a transient population of subplate neurons that establish this connection during embryonic stages [12]. Using fluorescent lipophilic dye tracers, growth cone morphology differences between these early axons and later axons found in this projection have been observed in ferrets and cats [13]. Growth cone morphology has been correlated with axon decision making, especially at choice points such as the optic chiasm and the floor plate. In these regions, growth cone morphology and sometimes growth behavior significantly change with pioneering growth cones assuming complex

shapes while later axons have more streamlined growth cones [14-16]. Similar to invertebrate systems, the earliest axons in vertebrates are in the right place and at the right time to establish initial projections that later axons can then follow. For example, in zebrafish, secondary motoneurons in the absence of primary motoneurons are not able to correctly pattern dorsal nerves but do form correct, albeit delayed, ventral projections [17]. Taken together, these data support the hypothesis that initial axons might play a pioneer-like role in establishing later axonal tracts, perhaps similar to their role in invertebrates. In vivo time-lapse analysis of axonal tract formation is needed to directly address how the initial axons affect later axons during early neuronal scaffold formation.

At one day of development, the zebrafish forebrain neuronal scaffold contains several distinct bilaterally symmetrical clusters of neurons, interconnected by a limited number of neuronal tracts and commissures [18-20] (Figure 3-1B), analogous to the early neuronal scaffold of mouse embryos [21]. During the next few days, the scaffold increases in size as more neurons and axons are added to the existing tracts, but few new axonal tracts appear. For example, initially the postoptic commissure (POC) connects two clusters of ventral neurons (the left and right ventrorostral cluster; vrc) in the forebrain [20] (Figure 3-1B) with additional axons from other brain regions projecting across it at later stages [15]. In zebrafish, cell labeling methods in combination with surgical manipulations reveal that early brain tracts aid in axon guidance for initial axons of other tracts [15,22,23]. Whether early axons influence later axons inside the same axon fascicles has not been addressed.

Here we build upon studies of the retinotectal projection [24], olfactory neuron pathfinding [25] and growth cone and dendrite dynamics of spinal cord motor neurons [26] to

examine the role of early axon guides on midline kinetics of commissural axons. Using a stable transgenic zebrafish line [27] and timelapse confocal laser-scanning microscopy we reveal a new level of complexity in commissural axon kinetics at the midline. Our data shows that midline kinetics in vertebrate commissural axons result from the combination of highly adaptive axons, dynamic interaction between them and the different exposure of each growth cone to other axons and the local cues.

3.2 Results

gata2::GFP labels a specific neuronal cluster of the forebrain

Neuronal differentiation and axonogenesis in the zebrafish forebrain have been shown to begin between 17-28hpf [18-20]. The relative arrangement of the early neuronal clusters inside the brain and their tracts, deduced from antibody staining against the neuron specific acetylated alpha tubulin [18-20], is schematically illustrated (Figure 3-1A,B). To permit reproducible in vivo imaging, we employ a stable transgenic line in which the cis-regulatory domain of the transcription factor GATA-2 drives GFP (gata2::GFP) [27], and shows early expression in the earliest differentiating cells in the forebrain (Figure 3-1C,D). The GFP positive cells, 8-10 μm in diameter, form bilateral clusters in the ventral forebrain that extend along the optic recess from the anterior diencephalon towards the ventral flexure (Figure 3-1C,D). Staining with acetylated alpha tubulin antibody at 18-28hpf reveals two distinct clusters of acetylated alpha tubulin positive ventrorostral cluster (vrc) neurons (red); many of these cells express GFP (green) (Figure 3-1E). By 24hpf all vrc neurons express GFP (Figure 3-1F).

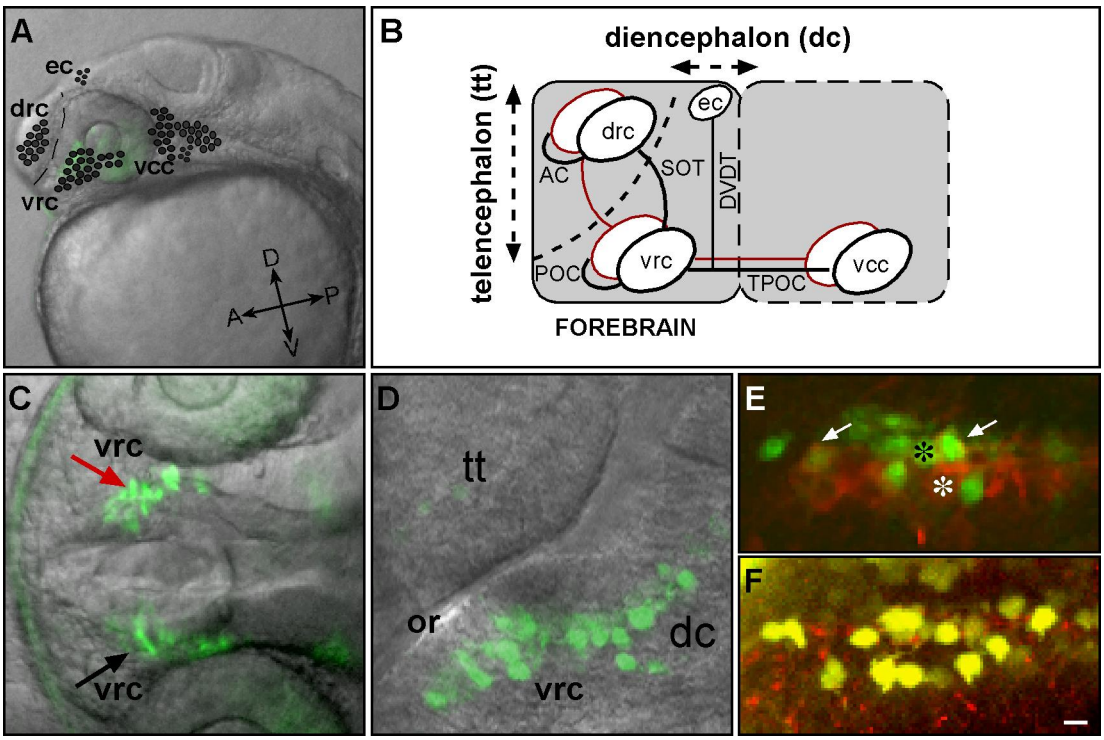

Figure 3-1 Zebrafish forebrain primary neuronal scaffold contains gata2::GFP positive neurons

(a) 24hpf zebrafish transmitted light view. The approximate location of the early neuronal clusters in the forebrain are schematically shown. **(b)** Schematic drawing illustrating the position of the major neuronal clusters and the axon tracts that connect them in the anterior CNS in zebrafish (based on [18-20]). **(c-d)** Confocal images of dorsal **(c)** and lateral **(d)** view of a 24hpf gata2::GFP zebrafish showing the location of GFP positive cells in relation to forebrain morphology. The cells are located bilaterally **(c)** and occupy the rostro-ventral part of the diencephalon along the optic recess (or) **(d)**. **(e-f)** Fluorescent confocal images showing the vrc stained with acetylated alpha tubulin antibody (red) to reveal the identity of gata2::GFP expressing cells (green). At 20hpf some vrc cells (white asterisk) express GFP (black asterisk). White arrows point to cells where colocalization of the neuronal antibody and the GFP can be seen **(e)**. At 24hpf all vrc cells express GFP and appear yellow due to spectral overlap between the green GFP and the neuronal antibody **(f)**. Scale: **(a)** 80µm, **(c)** 20µm, **(d-f)** 10µm. tt-telencephalon, dc-diencephalon, drc-dorso-rostral cluster, vrc-ventro-rostral cluster, vcc-ventro-caudal cluster, ec-epiphysial cluster, SOT-supraoptic track, TPOC-track of postoptic commissure and POC–postoptic commissure, AC–anterior commissure, or–optic recess.

The first axons to form the POC are gata2::GFP positive

Immunohistochemistry with the acetylated alpha tubulin (AT) antibody shows that the postoptic commissure (POC) is set up between 21 and 23hpf (Figure 3-2A-D). In addition to labeling the axons of the early neuronal scaffold, AT also labels the cell bodies of cells undergoing axonogenesis, ependymal processes and cilia [18] as well as the superficial network of nerve fibers running just beneath the ectoderm. At the early stages of POC formation these labeled processes are closely juxtaposed and can appear as axon-like processes. Thus, our detailed analyses of the earliest POC axons were performed on individual optical sections.

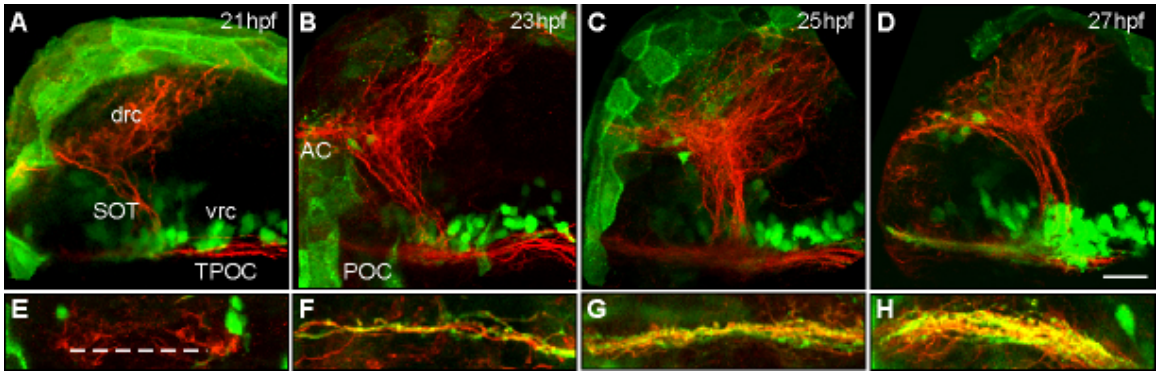

Figure 3-2 gata2::GFP positive axons pioneer the POC and also mark the majority of later POC axons

Gata2:GFP cells and their axons are depicted in green and the primary neuronal scaffold in red. Rostral is to the left and dorsal is to the top. Images are maximum intensity projection (MIP) views of confocal z stacks. Scale = 20μm. **(a-d)** Lateral images at 21,23,25 and 27hpf showing the relative position of gata2:GFP cells (green) with respect to the neuronal scaffold revealed with acetylated alpha tubulin (red). **(e-h)** Corresponding frontal views of the POC show gata2::GFP expressing axons pioneer the POC. At 21hpf only early neurons differentiating away from the neuroepithelium can be seen but no axons are present where the POC will form (dashed white line) **(e)**. At 23hpf a small number of axons can be seen across the POC; these early axons express GFP although due to fixation some of the GFP signal is too weak to be visible in the overlay image **(f)**. At 25 and 27hpf respectively the POC thickens. GFP positive axons can be seen spanning the entire width of the commissure **(g-h)**. The small number of axons that appear to not express GFP reflects axons from other brain regions that project their axons along this tract.

Double label studies show that these earliest axons of the POC, detected by AT, are GFP positive. At 21hpf no axonal staining with either AT or GFP can be seen along the future POC trajectory except for the cell bodies and ependymal processes of delaminating neuroepethelial cells (Figure 3-2E). At 23hpf a small number of axons slightly beneath the surface ectoderm are visible across the POC (Figure 3-2F). Analysis and rendering of these double labeled preparations is often challenging because the GFP expression levels in axons are weak after fixation. To confirm that all of the initial axons growing across the POC are GFP positive, we employed spectral analysis using a Zeiss LSM-510 META microscope. Given the low levels of GFP expression, some axons appear reddish in the double overlay even though they express distinct GFP fluorescence. Analysis of the individual z sections further confirms that both ependymal processes and superficial nerve fibers extend near the commissural axons and these do not express GFP. At later stages, more GFP positive axons appear (Figure 3-2H), as well as a small number of axons which do not express GFP, likely originating from other neuronal clusters as previously described [15].

DiI labeling experiments were performed to confirm that the first GFP axon is the first axon along the future POC tract. Transgenic gata::GFP fish were timelapsed until the first GFP-expressing growth cone appeared (Figure 3-3A), at which time the embryos were fixed briefly to retain GFP and growth cone morphology. DiI injection into the vrc cluster (Figure 3-3C) reliably labeled the first GFP expressing axon including its growth cone; no DiI-labeled axons were visible ahead of the leading GFP positive process (Figure 3-3B). Thus the first GFP positive axon is the initial axon that grows along the POC trajectory.

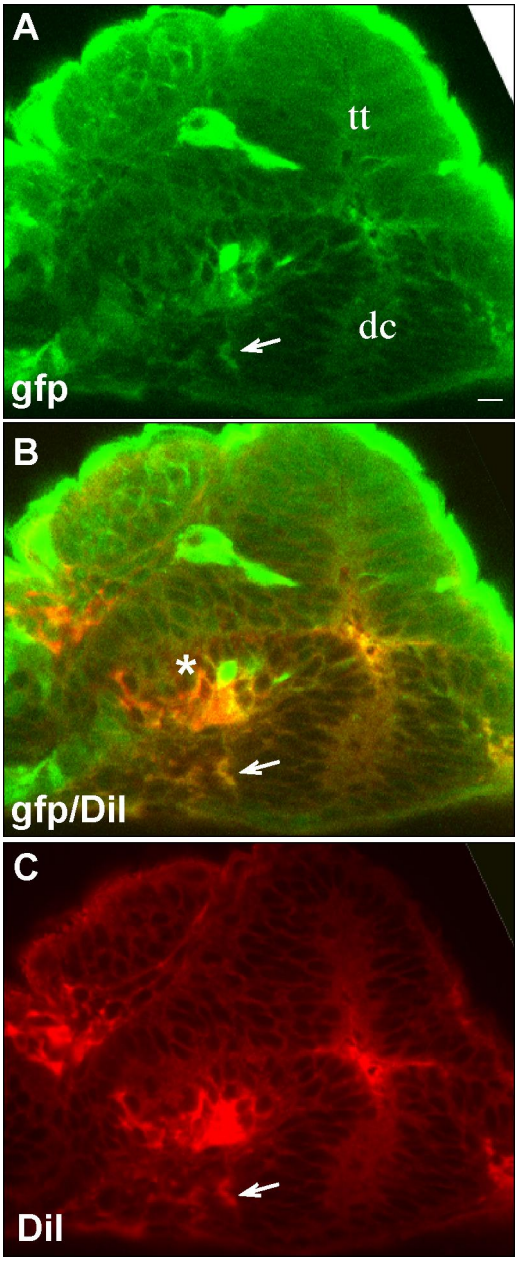

Figure 3-3 DiI filled gata::GFPpositive cluster where first GFP axon has just started to grow to midline shows no red axons ahead of the GFP

gata::GFP embryo fixed immediately after the first GFP positive axon began growing to midline and the vrc cluster (star) was filled with DiI to label axons from the vrc. **(a)** Front view of the green channel showing the GFP positive vrc cells and the first GFP expressing growth cone (arrow) projecting towards the midline. **(b)** Merged green and red emission channels showing the injected vrc cluster (star) and the labeled growth cone (arrow). No other DiI fileld axons are visible ahead of the GFP expressing axon. **(c)** Red channel showing the DiI fill and the labeled DiI growth cone (arrow).

Axon kinetics during POC formation in vivo

To characterize the growth behavior of POC axons, we performed a series of time-lapse confocal microscopy experiments (n=22) using gata2::GFP zebrafish embryos. At 22-23hpf, 1-3 discernable axons from the bilateral vrcs advance rostrally along the POC path (Figure 3-4A).

Within one hour, these axons meet, creating a continuous axon arc along the future POC trajectory (the early axon from the right is indicated with pink arrow in (Figure 3-4A,B). Later axons from both sides (blue arrows in Figure 3-4A-D) fasciculate with the initial axons at various points along the commissure and follow them across the midline (Figure 3-4).

These movies reveal two distinct classes of behaviors. The first axon that emerges maintains its leading position towards the midline and across it (Figure 3-4A,B pink arrow); the trailing axons stay close behind, crossing the midline after the first axon crosses (Figure 3-4C,D blue arrow). To analyze the dynamics of axons along the POC trajectory, length and position along the POC trajectory was measured at every time point for each axon visible in our timelapse recordings. To allow easier comparison of axon behaviors, axon growth was plotted as distance from midline along the POC trajectory as a function of time (Figure 3-4E). At the midline, the first visible axon (pink line) has an almost flat slope, signifying that this axon slows down in this region (pink boxed area). In contrast, a later axon (blue line) has a continuous, steep slope at the midline (blue boxed area) showing that it does not slow down. Thus the two types of axons show different behaviors at the midline, an important intermediate target for commissural axons [28].

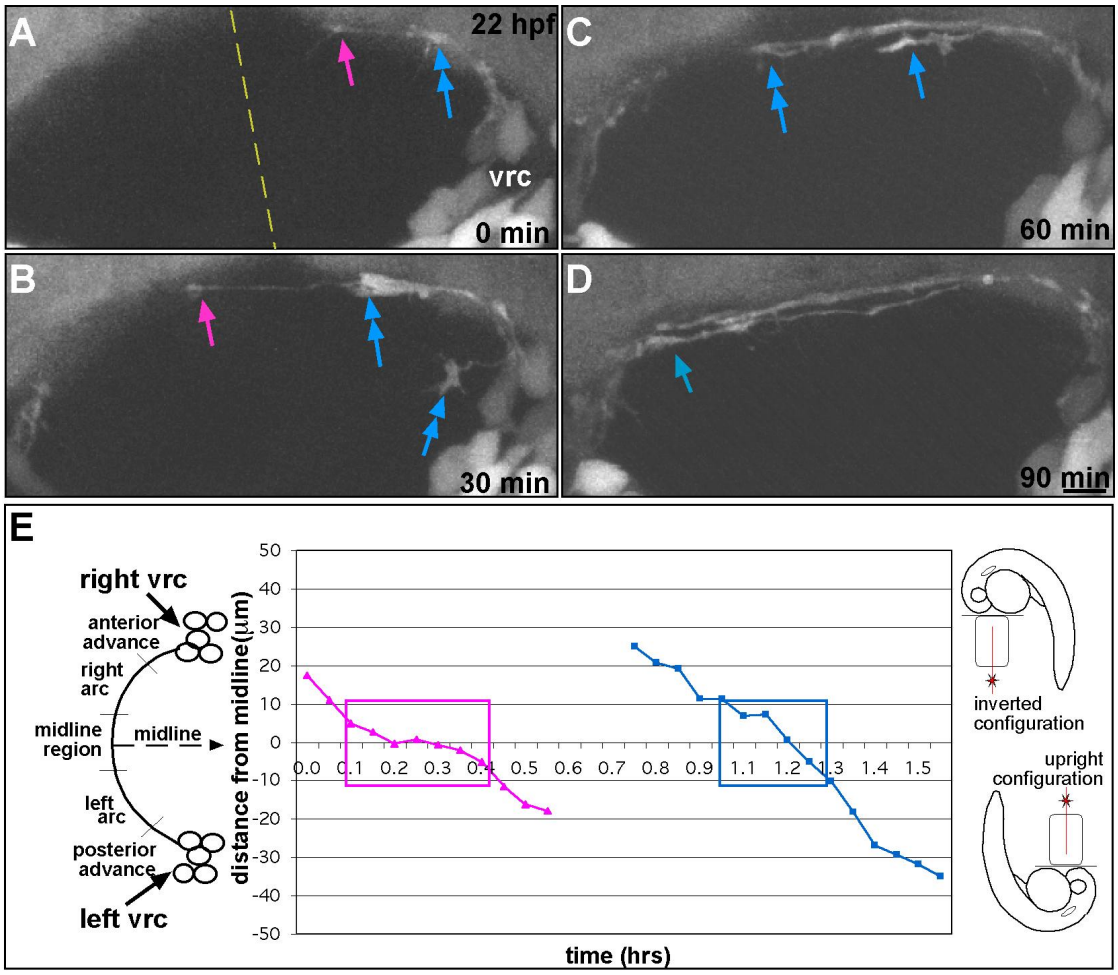

Figure 3-4 Timelapse imaging of a wildtype gata2::GFP growth cones crossing the ventral forebrain and forming the POC

(a-d) Selected images of single time points from one 3 min interval timelapse sequence showing a typical leading growth cone (pink arrow in a and b) from the vrc cluster navigating towards and past the midline where it is joined by the growth cone from the opposite cluster (not visible in b because it is masked by fluorescence from more dorsal sections). Subsequently, later growth cones (blue arrows in b-d) also cross the midline and grow across the POC. Midline location is denoted by a dashed line based on transmitted light images taken during each timelapse and time is shown in minutes. Scale=10µm. **(e)** A typical distance from midline along the POC trajectory axon plot. Axon length at each time point is plotted as distance from midline along the POC trajectory. The leading growth cone is plotted in pink and a later (follower) axon is plotted in blue corresponding to the growth cones marked with pink and arrows in panels a-d. The axons shown here start from the right vrc (top of the plot) and cross over to the left vrc (bottom of the plot) as indicated in the schematic to the left of the graph. The two axons spend different amounts of time at the midline (see pink and blue boxed regions). On the right two microscope configurations are shown for how the imaging was performed. The timelapse shown in panels a-d was obtained in the inverted configuration.

POC axon nomenclature

In view of the order in which the axons reached and crossed the midline, we have defined the first axon from either side to cross the midline as a leader axon; all later axons observed along the POC are defined as follower axons. In 25% of the cases, axons originating from the two opposite vrcs arrived at the midline at approximately the same time and both were defined as leader axons. In the rest of the cases, one axon arrived early at the midline and grew across it. In these cases the initial axon was defined as a leader and the contralateral axon was defined as a follower.

Quantitative analysis of leader and follower axons reveals differences in their behavior at the midline

Quantitative analysis of POC axons (n=46) reveals a behavioral difference between leader and follower axons in the midline region (± 10μm from the midline). Within this region, leading axons slow significantly (Figure 3-5A) compared to follower axons (Fig. 3-5B), correspondingly their average slopes in this region are markedly different. This difference is robust: the difference between leader and follower axon behavior at the midline is maintained even when they are averaged (Figure 3-5C). The extended time that leading axons spend within the midline region is due to a more than 50% reduction in growth by the leader axons at the midline. At the midline, leader axons grow at an average rate of 35±5μm/hr as opposed to 85±5μm/hr, the average growth rate of leader axons along the rest of the POC trajectory (Figure 3-5D). Follower axons do not display this behavior; their average growth rates inside (91.6 ± 7.1 μm/hr) and outside (93.7 ± 6.2 μm/hr) are equivalent (Figure 3-5D). Thus, leader and follower axons grow at

comparable rates outside the midline region, but display drastically different growth rates near the midline.

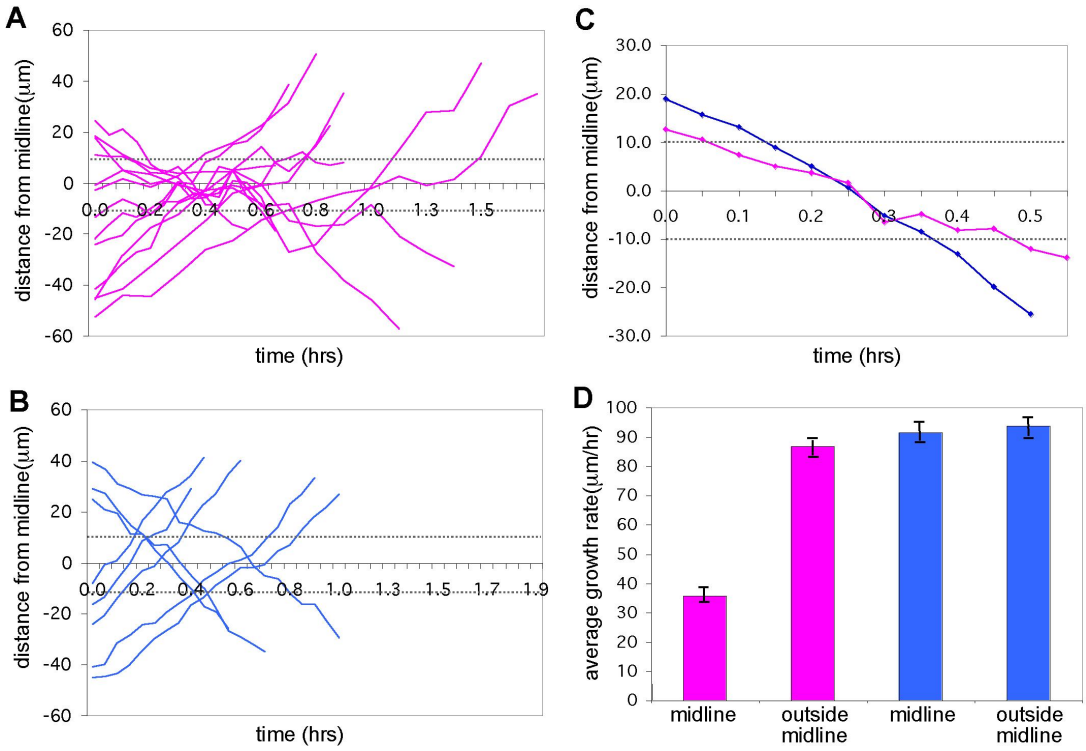

Figure 3-5 POC axon dynamics with respect to the midline

Quantitative analysis of axon growth rates reveals a difference in axon behavior around the midline not readily apparent from direct observation of timelapse experiments. **(a-b)** Representative plots of distance from the midline along the POC trajectory vs time for leader **(a)** and follower **(b)** axons. Leader axons spend considerably more time within ±10μm of midline (dashed black line in **a-c**) while later axons do not slow down in this region. **(c)** Plot showing the average behavior of leader (n=16) and follower (n=24) axons at the midline. Leader and follower axon plots were centered on the timepoint when each axon crossed the midline and averaged showing a more than two fold difference between the duration of time leader and follower axons spend at the midline. Individual plots of all axons from the left vrc were reflected around the x axis. **(d)** Average growth rates ± s.e.m for leader (pink) and follower (blue) axons with respect to the midline and outside midline region. Leading axons grow significantly slower at the midline compared to their average growth away from midline and compared to follower axons at the midline ($p<0.001$, Student's t-test corrected for multiple comparison).

Both slower speeds and higher frequency of retractions contribute to lower average growth

Axon growth rate reflects both the absolute *speed* and *direction* of growth. Thus, two factors could contribute to the apparent slowing of leader axons at the midline: 1) a decrease in axon growth *speed* and 2) higher number of growth cone retractions around the midline without a necessary reduction in growth speed. To examine the relative importance of these two factors we determined the frequency of brief retractions of the leader and follower growth cones within the midline region and outside of it. 90% of leader axons displayed retraction behavior at the midline; in contrast, only 15% of follower axons showed retraction in this region.

	N	MIDLINE		AWAY FROM MIDLINE	
		Average (μm/hr)	Absolute Average (μm/hr)	Average (μm/hr)	Absolute Average (μm/hr)
Leader	17	35.6 ± 4.5 * =	58.2 ± 9.2 * =	86.9 ± 6.9 *	95.3 ± 5.7 *
Follower	22	91.6 ± 7.1 =	97 ± 5.3 =	93.7 ± 6.2	102.9 ± 9.9

Table 3-1 Longer midline interaction for leader axons is due to decrease in speed as well as higher frequency of retraction in leader axons

Mean ± SEM of average growth rates and absolute growth rates for leader and follower axons at and away from the midline. To ensure that different leader and follower axon retraction frequency did not vary with our sampling interval, timelapse data were collected at 1.5, 3 and 6min intervals. The table above is based on pooled data as similar retraction percentages for both classes of axons were obtained independent of the sampling interval. The growth rates, either compensated for the increased retractions (absolute growth) or not (average growth) are slower at the midline for leaders (* $p<0.001$, Student's t-test). Similarly, the growth rates of the leaders are slower than follower axons at the midline (= $p<0.001$, Student's t-test).

When higher retraction frequency was compensated for, the resulting average absolute growth rate for leading axons was still significantly lower at the midline (58 ± 9.2μm/hr) compared with followers (97± 5.3μm/hr) (Table 3-1). Outside the midline, leader and

follower growth cones retracted with similar low frequencies and their average growth rates do not change significantly even when we account for these retractions (Table 3-1).

Leader and follower axons differ in growth cone morphology

Our time-lapse imaging allowed us to resolve entire growth cone shapes along with a number of filopodia for all leader growth cones and a fraction of follower growth cones (Figure 3-6A-C).

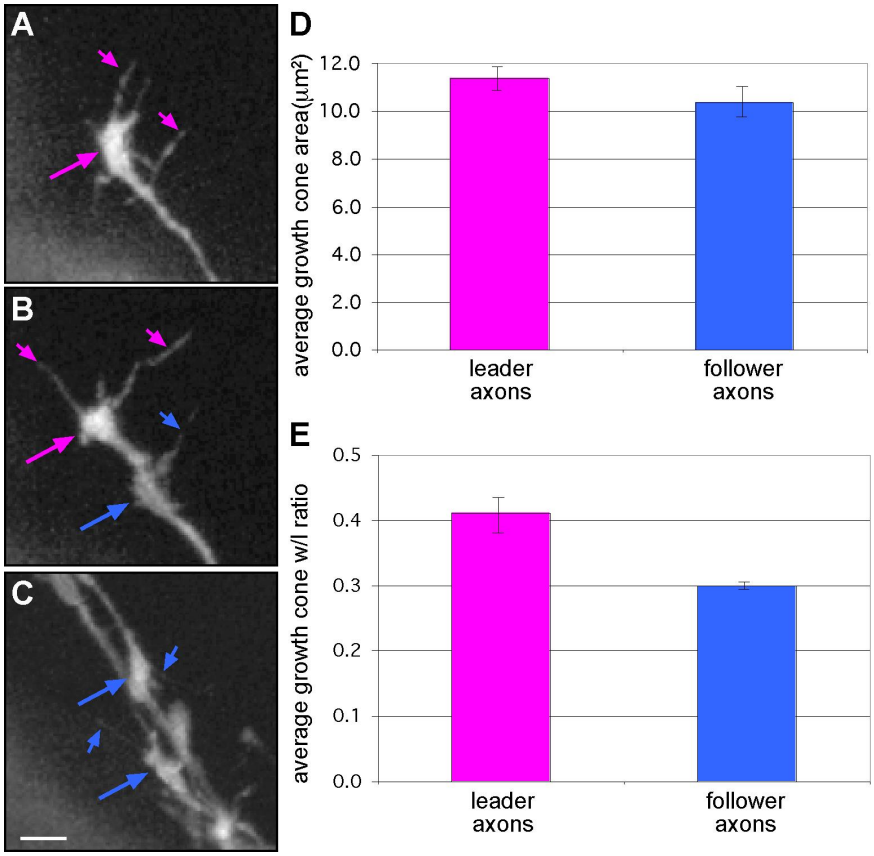

Figure 3-6 Growth cone morphology analysis for POC axons

Growth cone morphology can be visualized during timelapse imaging of the POC axons. **(a-c)** Representative growth cones of leader (long pink arrow) and follower (long blue arrow) axons are shown. Filopodia present on both types of growth cones are also indicated with smaller arrows (pink for leader and blue for follower). Scale bar =10μm **(d)** Average growth cone areas do not differ between leader (n=12) and follower (n=8) axons. Only clearly visible follower axons were chosen for this analysis. **(e)** Average width to length (w/l) ratio plot shows a significantly higher ratio for leader axons (n=12) compared to follower axons (n=8) ($P<0.05$, Student's t-test).

To test if growth cones of leader and follower axons differ in complexity, we computed width/length (w/l) ratios for the two classes of axons. Leading growth cones (Figure 3-6A,B long pink arrow) were consistently wider and shorter (higher w/l ratio) than the elongated shape of the follower growth cones (Figure 3-6B,C blue long arrow). At the midline, leader growth cone w/l ratios (0.43±0.2 , n=12) were 50% larger than follower growth cone w/l ratios (0.24±0.1 , n=8) (Figure 3-6D). The average growth cone areas for leader and follower axons did not differ (Figure 3-6E), consistent with what has been found in growth cones of corticothalamic projections in ferrets and cats [13].

In the midline region, leading axons had up to 50% more filopodia than the follower axons (average filopodia length did not differ). The filopodia on leaders were arranged at all angles to the growth cone (Figure 3-6A short pink arrows); in contrast, the filopodia of follower axons were mostly oriented in a forward direction (Figure 3-6A short blue arrows). Together these data show that the growth cones of leader and follower axons display marked differences as judged by the different w/l ratios and number and orientation of their filopodia.

Direct interaction between leader and follower axons

Since follower axons grew in close contact with the leader axon and had different midline kinetics we examined how the presence of the leader axon affects follower axons in vivo. For this purpose, we examined follower axons in samples where the leader axon was damaged by intense laser light. Repeated high laser illumination of single leader growth cones to the point of saturation causes permanent damage to single axons and has been used as a tool to ablate cells and their processes [11,17].

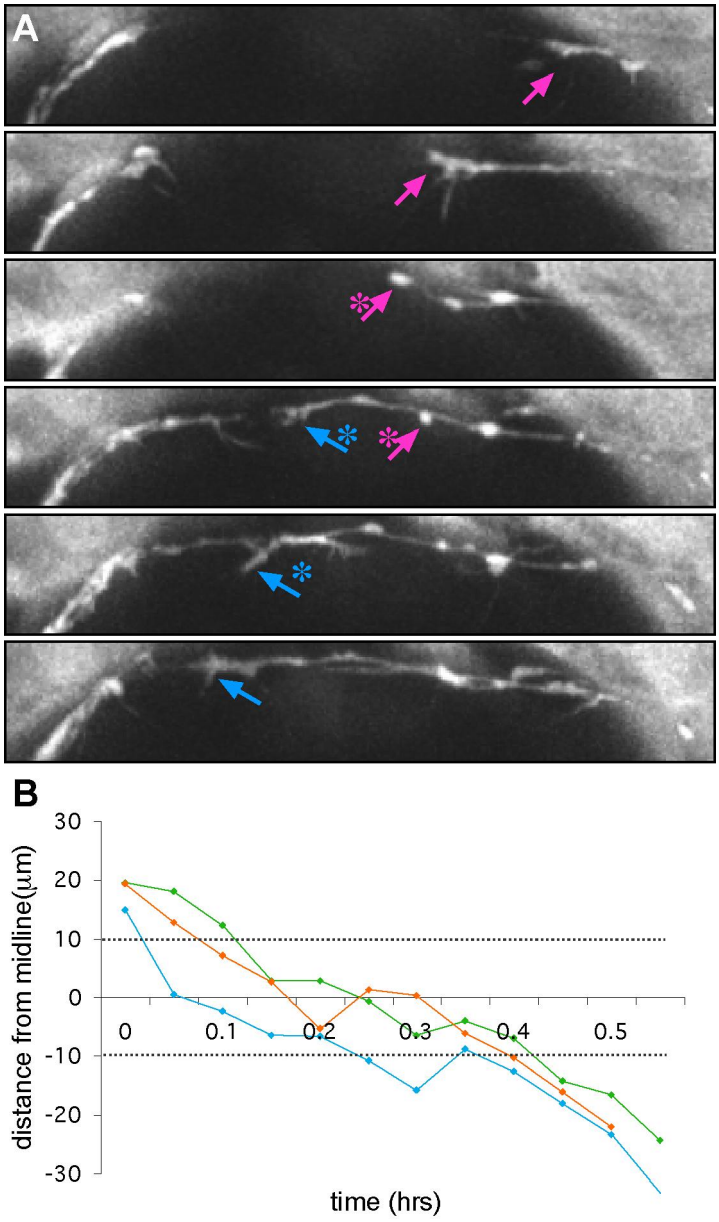

Figure 3-7 In absence of a leader axon follower axons slow down at the midline

(a) Single time point images showing a leader axon (pink arrow) that projects towards the midline and is injured right before crossing it (pink arrow with asterisk). A follower axon behind it (blue arrow) overtakes the leader axon and crosses the midline (blue arrow with asterisk). After this axon crosses the midline another axon from the left vrc also grows across the midline. The two growth cones: the new leader from the right vrc (blue arrow with asterisk) and the first axon from the left vrc have just underwent their stereotypic behavior and are not aligned with the POC trajectory until the last image where their growth cones establish contact with the opposite axon shaft. **(b)** Axon distance from midline along the POC trajectory graph showing three separate cases where follower axon was analyzed after the leader axon was damaged. The axon graphed in blue corresponds to the follower axon shown above (blue arrow in a).

Strong laser illumination over 3-5 consecutive time points resulted in leader axons whose growth cones rounded up and did not recover (n=3; Figure 3-7). After the leader's growth cone was damaged and collapsed in vivo at or before the midline (Figure 3-7 pink arrow with an asterisk), the nearest follower axon changed its behavior and slowed down within the midline region (Figure 3-7 blue arrow with an asterisk), while later follower axons behaved as they normally would (i.e., crossed the midline swiftly). Thus early POC axons can adopt leader-characteristic midline behavior. As long as one axon becomes a leader, subsequent axons that grow along this tract behave as followers at the midline.

Axon fasciculation can explain the differences between midline kinetics of leader and follower axons

Leader axons slow down at the midline because they must interpret and navigate through a complex environment of positive and negative midline cues. Since follower axon growth cones can use leaders as guides to cross the midline, they are less exposed to midline signals allowing them to cross the midline swiftly. Thus, a simple difference in growth cones exposure to local cues can explain the difference between leader and follower axon kinetics at the midline. Both growth cone morphology differences and the ablation experiments support this model. To further test this hypothesis we turned to an experiment in nature. As mentioned earlier, in 75% of the cases, a leader axon from one side crosses the midline alone. The contralateral first axon grows along the leader across the midline displaying fast kinetics in this region. Since leader and follower growth cone morphology differences correlate with their midline kinetics, we examined growth cone morphology of these contralateral axons before and after they encountered the leader

axon. If fasciculation of the growth cone with the leader axon alters its interaction with the environment resulting in faster growth at the midline, then we would expect to see a growth cone morphology change in the contralateral axon accompanying the fast kinetics we observe in these cases. This change would be expected to occur even before the growth cone crosses the midline simply because it now grows along another axon. Following initial contact with a leading axon that has crossed the midline, growth cones of contralateral axons undergo a drastic change in shape from complex to elongated even before they themselves cross the midline (Figure 3-8). Thus simple growth cone shape change brought about by the newly available opposite commissural axon substrate can switch the midline kinetics of these axons from leader to follower.

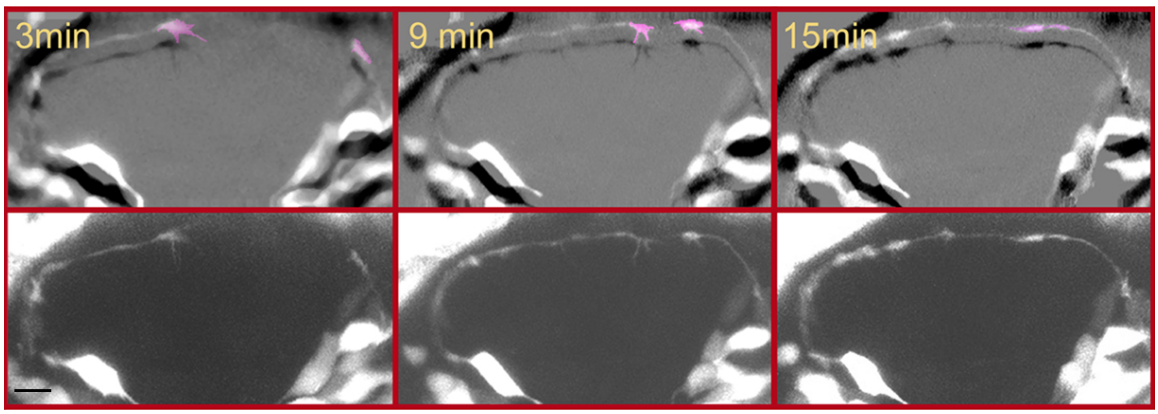

Figure 3-8 Leader axon alters midline kinetics of first contralateral axon at the midline during commissure formation

Single time point images showing stereotypic interaction between the initial POC growth cones. Two growth cones, one from each of the vrc, project toward the midline and one has already crossed the midline (left). Up to this point both growth cones have complex morphologies. Upon contact however (middle panel), both growth cones change shape and become elongated (right) even though the second growth cone has not yet crossed the midline. When this second axon grows across, it has fast midline kinetics similar to a follower axon. Scale = 10µm.

3.3 Discussion

Here, in vivo microscopy of embryonic zebrafish expressing GFP in the ventrorostral clusters (vrc's) of cells in the embryonic forebrain permits the early events involved in establishing the postoptic commissure (POC) to be followed. The labeled cells in the gata2::GFP fish send their axons along the POC earlier than any others (22-23hpf). As the initial axons course towards the midline, one of them becomes the leader axon, approaching and crossing the midline first. After a characteristic slowing at the midline the two leader axons pass one another and continue on towards their contralateral targets. Later axons follow the leaders but do not overtake them or behave like them at the midline. Thus, the leading axons from the vrc's are in the correct place and show the correct behaviors to serve as the early pioneers of the POC.

Commissural axons have been studied in invertebrates [5,11] and in vertebrate spinal cord [14], and appear to share similar mechanisms for building the early neuronal scaffold. However, little is known about commissural axon kinetics during early brain development in vertebrates in vivo. Our dynamic imaging results show behaviors that might not have been expected from invertebrate studies. First, we find that follower axons can adopt a pioneering role if the leader is eliminated, contrary to the case in invertebrates where defined pioneer(s) play a central role in guiding later axons to their targets [6-9]. Consistent with this data, removal of some of the primary motoneurons in the zebrafish spinal cord does not affect the establishment of correct projections in the remaining population of primary axons [29]. This suggests that the vrc cells that send their axons along the early POC act as an equivalence group, with only one or two of the axons serving as leaders. The signals that promote the leaders or that permit leaders to suppress

leader behavior in followers have yet to be defined. Second, unlike invertebrates, where bilateral homologues of early commissural axons arrive at the midline together [5,11], and where cooperative fasciculation between contralateral homologues of commissural axons appears to be essential for allowing each axon to cross the midline [11], we find that this is not always the case in zebrafish POC formation. In 75% of the timelapses (n=22), an initial axon emerging from one of the ventral clusters arrived at and crossed the midline before the contralateral axon got within 15-20μm of the midline suggesting that leader axons can navigate the midline territory alone. Further while contralateral Q1 commissural growth cones in grasshopper exhibit strong affinity for each other at the midline [11], growth cones of leading POC axons do not appear to have equally high affinity for each other. Contact of leader axon growth cones via their filopodia makes one or both growth cones jog to the side so that rather than facing each other they are parallel to each other. As they advance forward, each growth cone makes contact with the opposite axon shaft directly behind its growth cone, and then follows it to the other side to establish the initial POC axon fascicle (data not shown).

Direct interaction between axons has been suggested to influence follower axon growth direction and growth cone morphologies in retinal ganglion cells in vitro [30]. Here we report a clear behavioral consequence for axons following an already established track that can be seen in terms of their growth cone morphology and their midline kinetics in vivo. Similar, growth cone morphology differences between the initial and later axons have been noted in invertebrates [6,10]and in fixed tissues in vertebrate systems [13,15]. We find that axon kinetics and growth cone morphology correlates with whether the axon is a pioneer or a follower. The fact that upon elimination of a leader axon, follower axons

change their midline kinetics, and that simple interaction between bilateral leader axons can alter their growth cone shape and midline kinetics, demonstrates that pioneering axons and the early follower axons growing along them interact with one another in vivo. While it remains possible that these interactions are indirect, through the leader altering the midline environment, we favor the interpretation that the difference in kinetics results from direct interaction between these axons.

One way this might work is that fasciculation between the follower growth cones and the leader axon simply changes their exposure to the positive and negative growth signals found at the midline (Figure 3-9). In support of this model, we observe that only the initial leader axon that pioneers a commissure displays drastic slowing at the midline and has a complex growth cone. Later axons following this pioneer do not show the same complex growth cone morphology, nor do they slow down at the midline. This model predicts that when the leader is ablated, the substrate it provides for the next axon is removed, and the next axon becomes more exposed to the environmental cues. As a result its growth cone morphology as well as its midline kinetics change to that of a pioneer as observed. Similarly, contralateral leading axons upon fasciculation change their growth cone morphology and midline kinetics to that of followers even before crossing the midline as would be expected from this model. It is also possible that the differences reported here, result from the balance between positive and negative midline cues that growth cones interpret, as characterized in vitro in several studies of growth cone guidance [31]. In this case axon fasciculation would speed the kinetics of followers through the midline milieu, skewing the balance more sharply and resulting in less retractions and pausing.

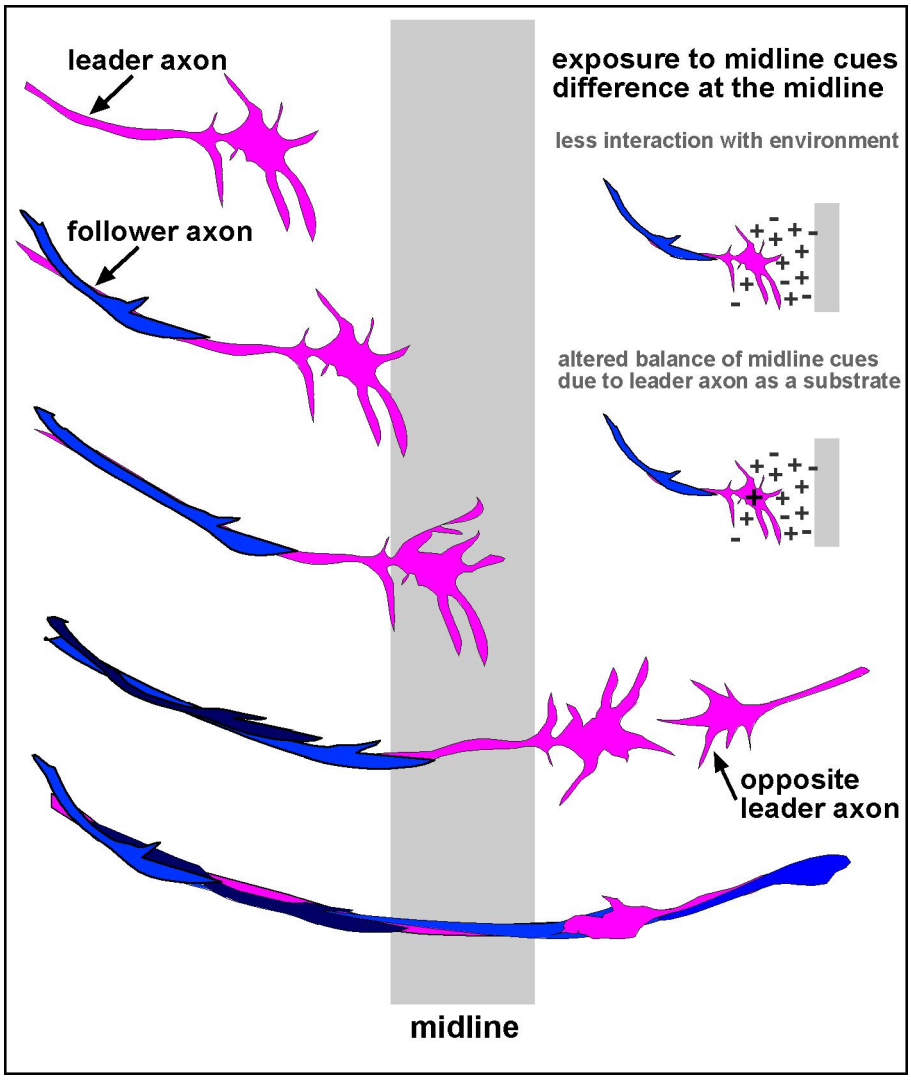

Figure 3-9 How fasciculation between commissural axons alters their midline kinetics

A schematic drawing shows a leader axon (pink) and a number of follower axons (light and dark blue) growing through the midline. The leading axon being the first, is completely exposed to the guidance cues in the environment. Its growth cone must sense all the positive and negative midline cues and interpret them accordingly which results in slow kinetics of leader axons at the midline where these cues are found. By growing along the leader, follower axons are less exposed to midline cues. This can happen because their growth cones are shaped differently which limits their exposure to conflicting midline signals and/or because the substrate that the leader axon provides contributes an extra signal that allows them to grow across the midline swiftly.

In either scenario leader-follower axon fasciculation ensures that all commissural axons stay sensitive to the midline cues but permits later axons to swiftly cross the midline and expedite commissure formation.

Studies in invertebrates and vertebrates strongly suggest that midline cells play an important role in axon guidance [32-35]. Mutations affecting midline signaling [36] or the presence of midline cells [29,36]result in axon pathfinding defects. The present focus on the complex midline domain has assumed that all axons react similarly to these positive and negative cues, thus slowing down at the midline [14,16]. Our demonstration that axon kinetics are shaped by an ongoing interaction between leader and follower axons, in addition to any midline cues, highlights the importance of investigating the molecular underpinnings of midline crossing in vertebrates in vivo.

3.4 Experimental methods

Fish maintenance

Raising and spawning of adult zebrafish were performed as outlined in the Zebrafish book [37] and in accordance with the guidelines of the California Institute of Technology.

Whole-mount immunohistochemistry and confocal microscopy

Embryos at stages 19-27hpf were fixed, blocked and incubated with primary antibodies as previously described [19]. Acetylated alpha tubulin antibody (Sigma) was used to label neuronal cell bodies and their axons [19,20]. For some experiments a cocktail of neuron specific antibodies zn1,8,12 (Developmental Studies Hybridoma Bank) was used for neuronal cell body labeling. The neuron specific antibodies were detected with secondary TRITC antibody (Jackson Lab). Inherent GFP was imaged. Embryos were deyolked prior to imaging and the head region (anterior to hindbrain) was dissected for imaging. Embryo heads were placed in bridge slides, covered with coverslips and imaged using the Zeiss LSM510 laser scanning confocal microscope at 40x.

Timelapse confocal microsopy

Embryos at 20-22 hpf were anesthetized with tricane in sedative amounts (0.01%) and embedded in a drop of 1-1.2% ultralow melt agarose on a cover slip-bottom petri dish in 30% danieau/0.01%tricane/0.15 mM PTU (to bleach pigment). Imaging was performed using inverted Zeiss Pascal confocal with a Plan-Neuofluar 40X/N.A1.3 Oil objective as well as Zeiss 510 confocal with Achroplan IR 40X/0.8 W, 63X/0.9W and C-Apochromat 40X/N.A 1.2 objectives. 3D stacks of the forebrain were taken at 6, 3 and 1.5 spanning

the vrc and the POC. Temperature was maintained at 28-29 °C throughout all imaging. GFP positive cells were excited with the 488 nm argon laser line using 505LP chroma filter set. Typical imaging experiment (n=22 separate live speciments) lasted between 3-5 hours. A z stack spanning approximately 60μm was collected at each time point with individual sections being 1μm apart. The pinhole settings were at 2.0-2.77 airy units. Refocusing was minimal but needed to be done occasionally to make sure the growth cones were imaged in full. Z-stack images were imported into Object Image and maximum intensity projections (MIPs) were made at each time point. These were later assembled into movies.

Axon growth rates analysis

Time-lapse data were analyzed with a 4D visualization software Slidebook Intelligent Imaging Innovations, Inc.), which allowed us to import our movies from Object Image and trace individual axon lengths at each time point during the time-lapse. Midline was found using a transmitted light image from each timelapse. Axons were traced, measured and plotted as variation in position (distance) from midline along the arc of the POC trajectory (Fig. 3g). Axon lengths were also used to compute average growth rates. All axon length data was divided into two groups: axons with no commissure, i.e., leading axons (n=16) and those where a commissure was already in place, i.e., follower axons (n=24). For each axon, the average growth rate ± s.e.m at midline, defined as ±10μm on each side of the midline was calculated. The growth rate was compared to the average growth rate ± s.e.m outside the midline for both axon groups. To confirm that our sampling time interval was adequate timelapses were done at 1.5, 3 and 6 minute

intervals and the numbers were analyzed separately for each group. Because all data was consistent across the different sampling frequencies the data were pulled together for final analysis.

DiI labeling

Gata::GFP embryos were prepared for timelapse experiment and imaged until the first GFP expressing growth cone appeared. The embryos were removed and immediately fixed in 4% PFA for 1.5 hours at RT. Fixed embryos were remounted in 1% agarose in PBS and injected under fluorescent microscope with DiI into the GFP positive vrc cluster in order to label axons from the vrc cells. DiI injected embryos were incubated at RT for 12-24 hours to allow the dye to diffuse throughout the axons and growth cones. Embryos heads were removed and remounted in agarose for analysis. Imaging was done using Zeiss Pascal inverted confocal scanning microscope, using 488 nm and 543 nm excitation sequentially using multitrack mode and a C-Apochromat 40x/1.2 water objective.

Growth cone morphology analysis

The highest quality time-lapses were selected for this analysis. Growth cone morphology was analyzed using ImageJ measurement and analysis software. Growth cone areas were measured by outlining the growth cone excluding filopodia. For width/length ratio measurements, the lengths of the growth cones were measured from tip of the leading edge of the lamelipodium to the base of the growth cone tip along a trajectory of the proximal region of that growth cone's axon. The width was measured in each case as the perpendicular segment positioned at the widest point for each growth cone. The average

growth cone area ± s.e.m and w/l ratio value were calculated and compared between leading and follower growth cones. The number and lengths of filopodia were recorded for each time frame of a movie for leading axons (n=10) and follower axons. In the later case only axons with clearly discernable filopodia were chosen (n=8).

Data analysis

Quantitative axon growth rates data was analyzed to test for significant differences using Student's t-test analyses with Origin software. In cases where one average growth rate was compared to two different growth rates the P value was corrected for multiple comparisons.

Acknowledgments:

We would like to thank Andres Collazo and Olivier Bricaud for suggesting the gata2::GFP line as candidate for our work as well as Shuo Lin for the gata2::GFP adults. We thank Kai Zinn, Reinhard Köster, Cyrus Papan and Helen McBride for discussions and critical reading of the manuscript.

3.5 References

1. Bate, C. Pioneer neurones in an insect embryo. *Nature* **260**, 54-55 (1976).
2. Bentley, D. & Keshishian, H. Pathfinding by peripheral pioneer neurons in grasshopper. *Science* **218**, 1082-1087 (1982).
3. Bastiani, M., Raper, J. & Goodman, C. Pathfinding by neuronal growth cones in grasshopper embryos III. Selective affinity of the G growth cone for the P cells within the A/P fascicle. *The Journal of Neuroscience* **4**, 2311-2328 (1984).
4. Jacobs, J. & Goodman, C. Embryonic development of axon pathways in the Drosophila CNS:IV. Behavior of pioneer growth cones. *The Journal of Neuroscience* **9**, 2412-2422 (1989).
5. Boyan, G., Therianos, S., Williams, L. & Reichert, H. Axogenesis in the embryonic brain of the grasshopper *Schistocerca gregaria*: an identified cell analysis of early brain development. *Development* **121**, 75-86 (1995).
6. Raper, J., Bastiani, M. & Goodman, C. Pathfinding by neuronal growth cones in grasshopper embryos: IV. The effects of ablating the A and P axons upon behavior of the G growth cone. *The Journal of Neuroscience* **4**, 2329-2345 (1984).
7. Klose, M. & Bentley, D. Transient pioneer neurons are essential for formation of an embryonic peripheral nerve. *Science* **245**, 982-983 (1989).
8. Gan, W. & Macagno, E. Developing neurons use a putative pioneer's peripheral arbor to establish their terminal fields. *The Journal of Neuroscience* **15**, 3254 (1995).

9. Hidalgo, A. & Brand, A. H. Targeted neuronal ablation: the role of pioneer neurons in guidance and fasciculation in the CNS of *Drosophila*. *Development* **124**, 3253-3262 (1997).

10. LoPresti, V., Macagno, E. R. & Levinthal, C. Structure and development of neuronal connections in isogenic organisms: cellular interactions in the development of the optic lamina of *Daphnia*. *Proc. Nat. Acad. Sci. USA* **70**, 433-437 (1973).

11. Myers, P. & Bastiani, M. Growth cone dynamics during the migration of an identified commissural growth cone. *The Journal of Neuroscience* **13**, 127-143 (1993).

12. McConnell, S., Ghosh, A. & Shatz, C. Subplate neurons pioneer teh first axon pathway from the cerebral cortex. *Science* **245**, 978-981 (1989).

13. Kim, G., Shatz, C. & McConnell, S. Morphology of pioneer and follower growth cones in teh developing cerebral cortex. *The Journal of Neurobiology* **22**, 629-642 (1991).

14. Bovolenta, P. & Dodd, J. Guidance of commissural growth cones at the floor plate in embryonic rat spinal cord. *Development* **109**, 435-447 (1990).

15. Wilson, S. & Easter, S. Stereotype pathway selection by growth cones of early epiphysial neurons in the embryonic zebrafish. *Development* **112**, 723-746 (1991).

16. Mason, C. & Wang, C. Growth cone form is behavior-specific and consequently position-specific along the retinal axon pathway. *The Journal of Neuroscience* **17**, 1086-1100 (1997).

17. Pike, S., Melancon, F. & Eisen, J. Pathfinding mby zebrafish motoneurons in teh absence of normal pioneer axons. *Development* **114**, 825-831 (1992).

18. Chitnis, A. & Kuwada, J. Axonogenesis in the brain of zebrafish embryo. *The Journal of Neuroscience* **10**, 1892-1905 (1990).

19. Wilson, S., Ross, L., Parrett, T. & Easter, S. The development of a simple scaffold of axon tracts in the brain of the embryonic zebrafish, Branchydanio rerio. *Development* **108**, 121-145 (1990).

20. Ross, L., Parrett, T. & Easter, S. Axonogenesis and morphogenesis in the embryonic zebrafish brain. *The Journal of Neuroscience* **12**, 467-482 (1992).

21. Mastick, G. & Easter, S. E., Jr. Initial organization of neurons and tracts in the embryonic mouse fore and midbrain. *Developmental Biology* **173**, 79-94 (1996).

22. Chitnis, A. & Kuwada, J. Elimination of a brain tract increases errors in pathfinding by follower growth cones in the zebrafish embryo. *Neuron* **7**, 277-285 (1991).

23. Chitnis, A., Patel, C., Kim, S. & Kuwada, J. A specific brain tract guides follower growth cones in two regions of the zebrafish brain. *The Journal of Neurobiology* **23**, 845-854 (1992).

24. Hutson, L. & Chien, C.-B. Pathfinding and error correction by retinal axons: the role of astray/robo2. *Neuron* **33**, 205-221 (2002).

25. Dynes, J. & Ngai, J. Pathfinding of olfactory neuron axons to stereotypes glomerular targets revealed by dynamic imaging in living zebrafish embryos. *Neuron* **20**, 1081-1091 (1998).

26. Jontes, J., Buchmanan, J. & Smith, S. Growth cone and dendrite dynamics in zebrafish embryos: early events in synaptogenesis imaged in vivo. *Nature Neuroscience* **3**, 231-237 (1999).

27. Meng, A., Tang, H., Ong, B., Farrell, J. & Lin, S. Promoter analysis in living zebrafish embryos identifies a cis-acting motif required for neuronal expression of GATA-2. *The Proceedings of the National Academy of Science* **94**, 6267-6272 (1997).

28. Kaprielian, Z., Runko, E. & Imondi, R. Axon guidance at the midline choice point. *Developmental Dynamics* **221**, 154-181 (2001).

29. Pike, S. & Eisen, J. Identified primary motoneurons in embryonic zebrafish select appropriate pathways in the absence of other primary motoneurons. *The Journal of Neuroscience* **10**, 44-49 (1990).

30. Devenport, R., Thies, E. & Cohen, M. Neuronal growth cone collapse triggers lateral extensions along trailing axons. *Nature Neuroscience* **2**, 254-259 (1999).

31. Song, H. & Poo, M. Signal transduction underlying growth cone guidance by diffusible factors. *Current Opinion in Neurobiology* **9**, 355-363 (1999).

32. Hatta, K. Role of the floor plate in axonal patterning in the zebrafish CNS. *Neuron* **9**, 629-642 (1992).

33. Colamarino, S. & Tessier-Lavigne, M. The role of the floor plate in axon guidance. *Annual Reviews in Neuroscience* **18**, 497-529 (1995).

34. Greenspoon, S., Patel, C., Hashmi, S., Bernhardt, R. & Kuwada, J. The notochord and floor plate guide growth cones in the zebrafish spinal cord. *The Journal of Neurobiology* **15**, 5956-5965 (1995).

35. Matise, M., Lustig, M., Sakurai, T., Grumet, M. & Joyner, A. Ventral midline cells are required for teh local control of commissural axon guidance in the mouse spinal cord. *Development* **126**, 3649-3659 (1999).

36. Varga, Z. et al. Zebrafish smoothened functions in ventral neuronal tube specification and axon tract formation. *Development* **128**, 3497-3509 (2001).

37. Westerfield, M. The Zebrafish Book. *University of Oregon Press* **Eugene, OR.** (1995).

Chapter 4 Netrin and its receptor deleted in colorectal cancer (DCC) pattern early forebrain commissural axons

Magdalena Bak-Maier and Scott E. Fraser

SUMMARY

Despite the identification of numerous candidate guidance molecules and elucidation of their signaling pathways, the challenge has been to understand how growth cones integrate external guidance cues *in vivo* to form the stereotypical axon tracts common to early vertebrate brains. Here, loss- and gain-of-function experiments are combined with in vivo microscopy to elucidate the role of DCC and netrin in forebrain commissure formation. Timelapse imaging of a stable GFP expressing zebrafish line reveals that instead of acting as a midline attractor as expected from their role in spinal cord, netrin signaling via DCC serves as a repellent cue keeping postoptic commissural (POC) axons in a single fascicle. Interference with the expression of *DCC* or *Netrin1a* leads to defasciculation of the POC axons, extensive projections into the axon free domain between the POC and anterior commissure, and ectopic midline crossing errors. Ectopic expression of the ligand either globally or in a small population of neuroepethelial cells, produces growth cone collapse and increased avoidance behavior consistent with the loss-of-function studies. Our data identify netrin as an important boundary delineating guidance molecule in the zebrafish forebrain.

4.1 Introduction

Early in development vertebrate brains are relatively simple, containing only a small number of cell clusters and axon tracts [1-3]. The early forebrain in zebrafish, an optically and genetically tractable vertebrate model, contains only two commissural axon tracts: the anterior (AC) and the postoptic commissure (POC) [2-4] which are separated by an axon free zone. This spatial arrangement requires that axons navigate correctly along specific trajectories. The growth cone, a specialized structure at the axon tip, largely carries out these functions. Vertebrate [4-10] and invertebrate [11-17]studies of early axon navigation have revealed that both external guidance cues and/or axons themselves (reviewed in [18] [19] [20,21]) influence axon growth and behavior. For example, in a previous analysis [4], we have shown that POC axon behavior at the midline is largely shaped by the interaction between leader and follower POC axons.

Another mechanism for establishing correct axon projections is the growth cone's plasticity as displayed during adaptation[22] and error correction[23]. A wealth of embryonic and culture studies have demonstrated that navigating growth cones are highly adaptable and explorative structures. In order to sense guidance molecules, growth cones continuously readjust their sensitivity to a given signal[22]. Growth cone errors are also common but they end up being corrected[23,24]. It remains unclear however, how growth cones react to external guidance cues in vivo to form clearly distinct axon tracts, and which specific molecular signals are involved and their specific role(s).

In mice, studies of the spinal cord commissural neurons have established netrin as a guidance cue for midline crossing axons [25,26]. In the spinal cord, netrin is mostly confined to the ventral midline where it acts to attract axons of commissural neurons to

extend towards and across the ventral midline [27]. Consistent with this role, netrin-1 mutant mice display defects in commissural projections in both the spinal cord and the entire nervous system, which suggests that netrin plays a role in axon guidance for multiple commissural tracts[28]. Additionally, netrin might also act as a repellent by directing axons away from cells expressing netrin [27]. In fact, the growth cone turning response to netrin in culture can be manipulated by varying the cytosolic level of cAMP[29]. Deleted in colorectal cancer (DCC) is a transmembrane protein that has been shown to directly bind netrin [30,31]. In the central nervous system *DCC* expression is localized to both commissural and non-commissural projecting axon[30,32,33]. DCC knockout mice show similar defects as netrin-1 mutant mice lending support to the hypothesis that this receptor-ligand pair has a role in midline axon guidance [30]. However, little is known about how netrin affects commissural axons in the developing brain.

Forebrain *netrin* expression is dynamic and appears to be expressed in orthogonally-arranged domains of brain cells close to early axon tracts [34-36]. Analysis of a number of gene expression patterns in the zebrafish shows that axons grow at the borders of such expression domains [37]. In zebrafish, *netrin* expression correlates with the location of the primary axon tracts [35]. *DCC* is expressed exclusively in the early neuronal forebrain clusters in one day old embryos [33], which suggests that netrin might play a role in establishing the early neuronal scaffold. These data are consistent with the hypothesis that *netrin* expressing cells might help delineate the arrangement of early axon tracts by providing attractive or repulsive cues to early growth cones.

However it is also possible that the Netrin protein is actively redistributed. For example, the DCC orthologue Frazzled was shown to rearrange the netrin protein into a

completely different spatial pattern in the ventral cord of Drosophila embryos[38]. Further, the intact brain is likely to have different cues with overlapping functions. Such overlaps make testing the roles of individual molecules potentially difficult, especially in a highly dynamic structure like a growing axon or growth cone. To tease apart the role of guidance cues on growth cones in vivo, timelapse analysis is needed to provide temporal resolution to observe these individual effects.

Previously, we have defined a powerful approach for assessing the dynamic behaviors of axons that form the early scaffold [4]. Targeted gene knockdown via antisense morpholino oligonucleotides (MOs)[40] allows this approach to be applied towards functional studies. Here we combine loss- and gain-of-function experiments with in vivo timelapse microscopy to elucidate the role of DCC and netrin in forebrain commissure formation. Our results demonstrate that netrin does not act as a midline attractor as might be expected from spinal cord studies. Instead, netrin signaling via DCC is important for keeping POC axons in a single fascicle by establishing a repulsive zone that prevents POC axons from making independent dorsal projections. Interference with the expression of *DCC* or *Netrin1a* leads to defasciculation of the POC axons, extensive projections into the upper domain and ectopic midline crossings.

4.2 POC axon behavior during commissure formation in unperturbed gata2::GFP embryos

We have previously described the behavior and kinetics of POC axons in the gata2::GFP zebrafish line which expresses GFP in the early ventorostral cell clusters (vrc) neurons [4]. After emerging in front of the vrc, early POC axons turn slightly upwards and medial to grow towards the midline creating an arc-like projection (Figure 4-1). POC axon growth is directed, with axons making few stereotypic errors (see below) and follower axons staying in close contact with earlier axons. The majority of misprojection errors made by wildtype (wt) POC axons are short-distance explorations of the area dorsal to the POC; these however, are short lasting, and growth cones rapidly rejoin the main POC axon fascicle. In fact, such brief errors are difficult to detect in fixed embryos stained with neuron specific antibody (data not shown). Timelapse analysis allows us to observe and assay these growth cone behaviors in detail.

In wildtype embryos, growth cone errors occur with highest frequency in the lateral segments of the commissure where axons emerge in front of the vrc and turn towards the midline. Elsewhere along the commissure filopodia can be found extending both forward and dorsally along the POC (Figure 4-1C control-MO). These behaviors suggest that later POC axons use the earlier axons as guides.

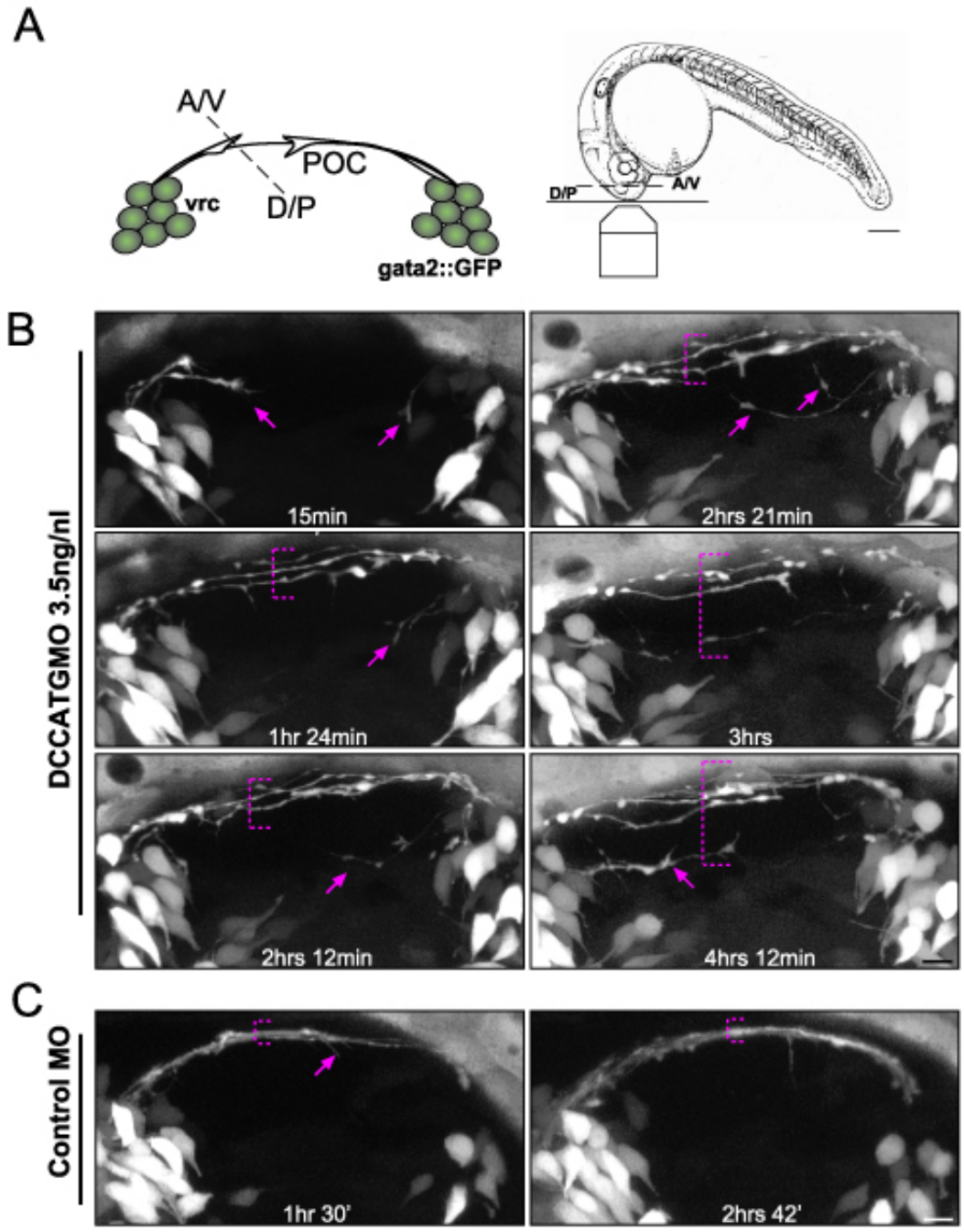

Figure 4-1 Timelapse imaging of POC axons reveals that translation-inhibiting DCC MOs cause POC axon defasciculation, growth cone errors and ectopic midline crossings.

(A) Schematic diagram showing the arrangement of the POC tract (left) and the imaging set up (right) **(B)** Selected single timepoint frames from a timelapse movie showing POC commissure development in DCCATG-MO injected embryo and control MO injected embryo. The early POC growth cones defasciculate (broken line bracket) from the onset and later axons instead of following earlier processes grow independently to midline (see arrows). **(C)** POC tract grows as a single bundle of axons in embryos injected with control-MO. Scale bar:10µm.

4.3 The DCC receptor aids in POC axon tract formation by keeping POC axons together.

To examine whether netrin and DCC are involved in establishing early brain tracts we used MOs against the zebrafish *DCC* coding sequence to block its expression. MOs are well established as powerful inhibitors of mRNA translation[40]. At 16-24 hours post fertilization (hpf), DCC is expressed exclusively in the early neuronal clusters[33]. Thus we were confident that the effects of DCC gene knockdown at this developmental stage would be specific to the early neurons. MOs complementary to the 5'UTR sequence of the zebrafish DCC receptor (5'UTR-MO), the translation initiation codon (ATG-MO), and the first intron splice site (splice-MO) result in similar phenotypes described below.

In embryos injected with DCC-MO, the growth cones of POC axons grow independently away from the main commissural tract and extend dorsally into the axon-free domain (Figure 4-1B). This dorsal bias is first visible as the initial POC axons emerge in front of the vrc, which results in some early POC axons growing at an angle while other POC axons maintain correct position (Figure 4-1B, see arrows in first left panel). Aberrant follower growth cone projections are either initiated from the onset, with axons failing to follow the commissural path pioneered by earlier POC axons, or occur later as axons detach from the main fascicle and begin to pioneer their own path across the midline. Often, the aberrant axon(s) rejoin the main commissure at a later position along the POC arc. However, in most severe cases axons that lose contact with the POC main fascicle succeed in making ectopic midline crossings. These aberrant projections result in widening of the commissural fascicle (Figure 4-1B brackets).

To further assess the trajectory of these ectopic POC growth cones, we analyzed the resulting POC tracts using depth-coded images. Aberrant POC axons found in embryos injected with DCC specific MOs continue to grow in an arc-like trajectory, similar to unperturbed axons, but fail to respect their dorsal boundary (Figure 4-2A arrows). Thus, POC axons increasingly defasciculate and begin to project to midline earlier and independently of other POC axons. Their growth cones are complex and resemble those of POC leader axons that pioneer the commissure. Some growth cones found in the wrong territory are round and collapsed, suggesting that this area is not normally permissive to POC axons (Figure 4-2A). In contrast, POC axons in embryos injected with control MO, form a single commissural tract similar to wildtype embryos (Figure 4-2A, control).

As there is no DCC antibody available against the zebrafish DCC receptor, we made EGFP fusion constructs to the 5'UTR and ATG DCC coding sequences to demonstrate sequence-specific knockdown for the corresponding MOs (Figure 4-2BC). Co-injection of the sequence-matched pair of mRNA and MO into one-cell stage zebrafish embryos leads to complete inhibition of GFP expression. The same MO has no effect on GFP expression fused to the non-complementary sequence (Figure 4-2B) or another nonspecific mRNA up to 2 days post fertilization (dpf) (data not shown). In these experiments small MO dose was able to completely abolish the expression of up to 0.4µg/µl of mRNA suggesting that it should also cause significant decrease, or loss of DCC receptor expression in vivo. Splice-MO resulted in POC axons defasciculation and independent projections to the midline similar to the other DCC MOs (Figure 4-2A). RT-PCR analysis of embryos injected with the DCC splice-MO reveals a hidden splice site

inside intron1 of DCC gene that results in addition of 27 amino acids to the N terminus of the protein (supplementary data, also see Suli and Chien). While this is likely to interfere with the function of the protein, the specific consequence of this insertion remains to be examined. Thus, in all embryos where the DCC expression is perturbed POC axons make independent projections instead of fasciculating with each other resulting in a widening of the POC tract.

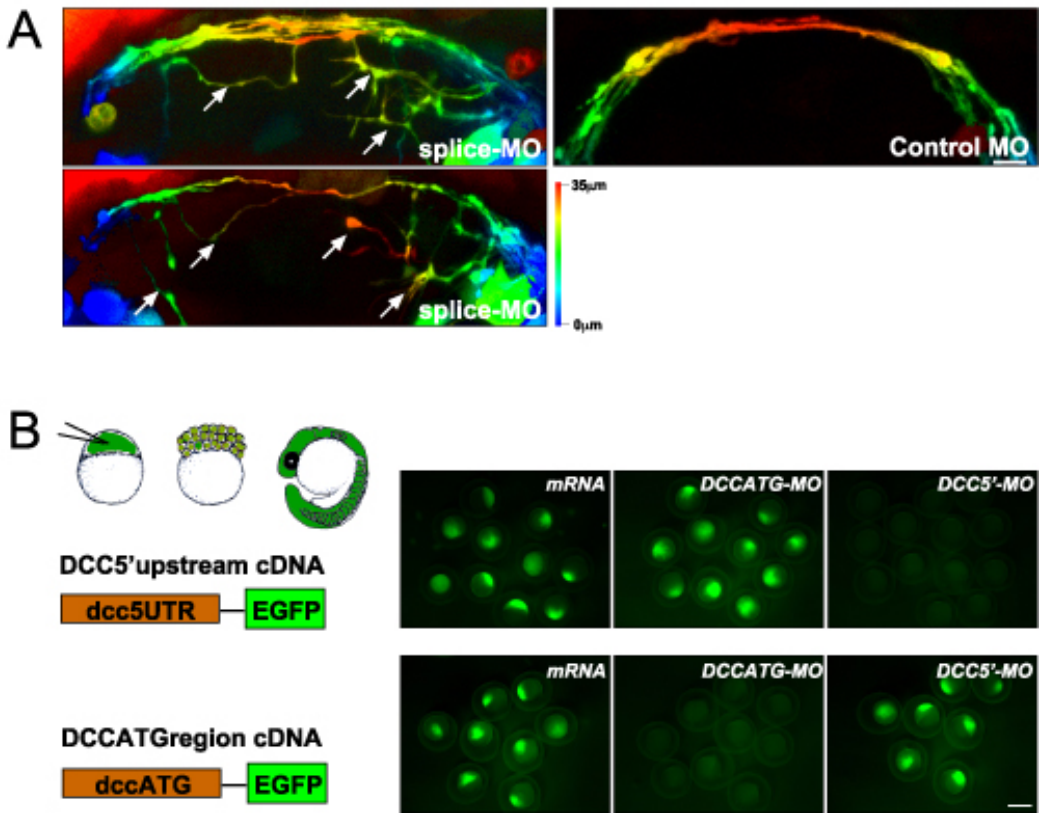

Figure 4-2 DCC-MO results in POC axons making independent projections to midline

(A) Depth coded images of POC axons in embryos injected with DCC splice-MO highlight that ectopic growth cones project in a similar arc like manner (as indicated by the color change from blue at periphery to yellow-red at the midline) but are displaced dorsally in relation to the main POC as indicated by the black space separating them. Scale bar: 10µm. **(B)** Fusion constructs made to test the sequence specificity of the DCC-translation-inhibiting MOs. Injection of the complementary fusion mRNA and MO pair results in complete prevention of GFP expression in a sequence specific manner. Images show zebrafish embryos at epiboly stage. Scale bar:400µm.

4.4 DCC depletion increases the overall number of POC axon misprojections, their duration and location along the commissure

DCC depletion greatly increases the number of POC axon errors and randomizes their position along the POC tract. Whereas only 35% of control embryos show any visible errors (n=35), 95% of embryos injected with the translation inhibiting MO (n=12) display clear errors where POC growth cones detach and project more dorsally (Figure 4-3A). On average, five times as many growth cone errors were found in DCC MO injected embryos compared to control embryos (data not shown).

Error duration is also affected. 90% of error projections in control embryos are short-lived, with half of them spending between 3-6 minutes away from the POC before rejoining it (Figure 4-3B). In contrast, in embryos injected with DCC MOs, POC growth cones are significantly delayed (Figure 4-3B) with over 35% of the growth cones spending more than one hour away from the POC tract before either joining back or crossing the midline on their own. In these latter cases, follower POC axons become new pioneers, establishing a new commissural tract that is then explored and followed by later POC axons.

As mentioned, our timelapse experiments in the wildtype embryos made it appear that the POC growth cones that detach from the POC commissure do so at specific points. We quantified areas where such detachments took place. Two main areas emerged in wildtype embryos: the initial POC arc region where axons first turn onto the future POC tract and the midline area particularly as axons approach the midline but not after they cross it (Figure 4-3C). To test whether DCC signaling is connected with these hotspots,

we performed similar analysis in embryos injected with various MOs. POC axon errors in embryos injected with the control MO are indistinguishable from uninjected embryos.

Figure 4-3 Phenotype of DCC depletion is revealed by quantitative analysis of POC axon growth cone behaviors and axon growth rate in the presence of DCC-specific MOs (next page).

(A) Percentage of total embryos in which at least one growth cone error was observed during the timelapse experiment. **(B)** Percentage distribution histogram showing the durations of errors made by POC misprojecting growth cones in control and DCC-specific MO injected embryos reveals a shift in duration length in presence of the MO towards longer time lengths. **(C)** Percentage disribution histogram showing the predominant location where growth cones of POC axons can be found making errors along the POC tract. Axons from both sides were pooled and the data reflected about the midline point to show the resulting pattern of error in POC axons. DCCMO injected embryos display no preference for any given spot along the POC (compare black dash line with orange line). **(D)** The average maximal distance ±s.d. of a POC growth cone projecting away from the POC. ($p<0.0001$ Student's t-test) **(E)** Average growth rates ± s.d. for leader axons of control and DCC MOs injected embryos within the midline region and elsewhere along the POC tract. ($p<0.0001$, one-way analysis of variance (ANOVA) test and $p<0.001$Tukey-Kramer Multiple Comparison Test) **(F)** Average growth rates ± s.d. for follower axons within the midline region and outside the midline. The followers pool represents axon that grew along the main POC tract most of the time together and axons that grew independently along any portion of the main POC. ($p<0.0001$ (ANOVA) test and $p<0.001$Tukey-Kramer Multiple Comparison Test)

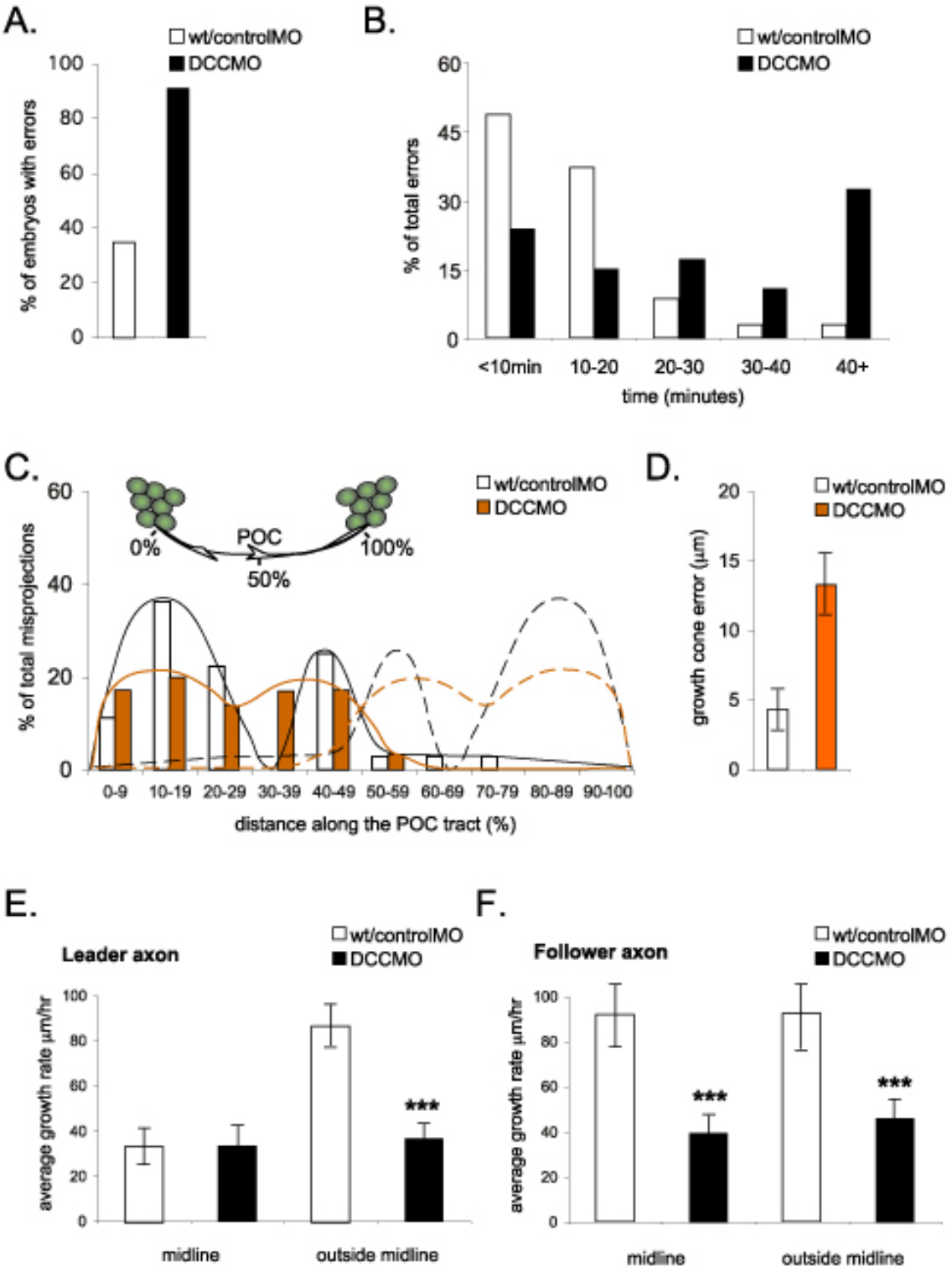
A.
wt/controlMO
DCCMO
% of embryos with errors
100
80
60
40
20
0
B.
wt/controlMO
DCCMO
% of total errors
60
45
30
15
0
<10min
10-20
20-30
30-40
40+
time (minutes)
C.
wt/controlMO
DCCMO
0%
POC
100%
50%
% of total misprojections
60
40
20
0
0-9
10-19
20-29
30-39
40-49
50-59
60-69
70-79
80-89
90-100
distance along the POC tract (%)
D.
wt/controlMO
DCCMO
growth cone error (µm)
20
15
10
5
0
E.
Leader axon
wt/controlMO
DCCMO
average growth rate µm/hr
100
80
60
40
20
0
***
midline
outside midline
F.
Follower axon
wt/controlMO
DCCMO
average growth rate µm/hr
100
80
60
40
20
0
***
***
midline
outside midline

However, in the presence of DCC-MO the hotspots are eliminated. Instead, POC axons make errors along the entire POC arc (Figure 4-3C). Analysis of POC growth cone errors and their location in embryos injected with the splice-MO reveals similar randomness of these projections (data not shown). Thus DCC depletion appears to lead POC axons to increasingly detach away from the POC fascicle.

To further assess the effect of DCC depletion on POC growth cones' projection, we measured the maximum distance and duration of projections away from the POC tract. Aberrant growth cones in control embryos and wildtype embryos extended dorsally for brief periods and over short distances (4±2μm). In DCC-MO injected embryos however, growth cones extended significantly further (13.5±3μm, $p<0.001$ student t-test) (Figure 4-3D). This data suggests that the repulsive netrin cue normally inhibits POC axons from detaching from the POC tract and that its function is not midline specific, in accordance with netrin mRNA expression in zebrafish [35]. Thus dynamic imaging reveals that wildtype POC axons are actively discouraged from growing away from the POC by possible inhibitory cues present around the axon fascicle.

4.5 Quantitative analysis of POC axon kinetics and growth cone errors shows that DCC depletion significantly affects axon growth rate.

We have previously measured POC axon growth rates and showed that pioneer POC axons grow significantly slower at the midline compared to later axons that grow along them [4]. If DCC depletion results in more ectopic POC growth cone projections, their growth rates would be expected to be slower. To confirm this, we measured and

compared the growth rates of leader and follower POC axons in control and DCC-MO injected embryos.

Leader axons in control embryos grow at a rate of 86.9±19.5μm/hr outside the midline and at a rate of 35.5±17.2μm/hr inside the midline region. At the midline the average growth rate of leader axons in DCC depleted embryos is comparable with control pioneers (33.2±19μm/hr, Figure 4-3E). However, outside the midline the average growth rate of leader axons in DCC-MO injected embryos is greatly reduced and resembles the growth of wt pioneers at the midline (36.6±14.5μm/hr, Figure 4-3E). This slower growth rate reflects the prolonged explorations of the area dorsal to the POC before turning towards the midline. One reason for the lack of a difference in growth rate at the midline might be that wt leader axons also grow slowly through this region spending more time exploring the midline area and often growing dorsally before continuing forward along the POC.

Previously, we have shown a behavioral consequence for follower axons that used earlier POC axons as a substrate especially at the midline[4]. As DCC depletion results in follower axons making independent dorsal projections we next wanted to examine the growth rate of follower axons in DCC-depleted embryos. While control POC follower axons grow at rates of 92±28μm/hr at the midline, in DCC-MO injected embryos followers at midline grow at a rate of 39.2±17.9μm/hr (Figure 4-3E). Similarly, outside the midline area while control followers grow at a rate of 92±34μm/hr outside the midline region, in DCC-MO injected embryos followers grow at a rate of 45.6±19.4μm/hr (Figure 4-3F). Thus follower axons grow significantly slower in DCC depleted embryos at all points. This slower growth reflects follower growth cones that

attempt to navigate through the dorsal region before either successfully crossing the midline independently or rejoining the main commissural tract (Figure 4-1B, Figure 4-2A). Taken together, these data provide evidence that netrin signaling in the zebrafish forebrain is not a midline specific cue but instead acts as a repulsive domain-delineating cue to keep the POC axons together in the diencephalon and effectively separate them from the more dorsal axons of the anterior commissure.

4.6 Interference with netrin expression results in phenotypes similar to those obtained with DCC specific MOs

So far, all of these effects resulted from perturbations of DCC receptor expression. To confirm that netrin signaling via DCC regulates POC axon projections we tested the function of its ligand netrin. Netrin1 knockout mice show severe defects in commissural axon extension in the spinal cord [28,43]. The zebrafish *netrin1a* shares a high level of sequence homology with *netrin1* of chicken and mouse[35] and *netrin1a* expression pattern correlates with early axon tracts in zebrafish [35]. To test the influence of netrin1a (net1a) on early POC axon growth cone behavior, we depleted net1a with MO.

At comparable doses to the DCC-MOs, the netrin1a MO (Net1a-MO) results in visible necrosis of the vrc cells (data not shown), in agreement with studies showing that netrin is required for cell survival[44] and that netrin receptors can act as dependence receptors [45,46]. However, at lower MO doses (see Methods) embryos appear to develop normally. We thus decided to examine whether any decrease in net1a will affect POC axons. At smaller doses, Net1a-MO injection resulted in similar projection errors as those found in DCC-MO injected embryos (Figure 4-4A). Leader POC axons grew more dorsally from

the start and many follower axons grew away from the POC. In some cases, ectopic midline crossings were visible (Figure 4-4A). Our data supports the idea that netrin has a role in both axon guidance and cell survival, as previously suggested[46] depending on its concentration. At high doses netrin provides a survival signal to the early vrc cells and at a lower dose it serves as a repulsive axon guidance cue for POC axons.

We next assayed the behavior of POC axons quantitatively. We expected that netrin depletion should both increase and randomize ectopic dorsal POC axon projections, which would affect the axon growth rates. Assaying the frequency of growth cone projections away from the POC revealed that Net1a-MO results in randomized misprojections, similar to DCC depletion (Figure 4-4A). In Net1a-MO injected embryos growth cones dissociate and begin to make independent dorsal projections along the entire length of the POC (Figure 4-4B).

Figure 4-4 Effects of netrin1a-MO on POC axons

(A) Single live timepoint (left) and depth coded (right) projection of a typical Net1aMO injected embryo showing ectopic dorsally projecting POC axons (arrows) Scale bar:10μm **(B)** Percentage distribution histogram showing the locations where POC growth cones make errors along the POC tract. Net1a-MO injected embryos do not appear to display a preference for any given spot along the POC (compare black and green dash lines). **(C)** Average growth rates ± s.d. for leader axons within the midline region and elsewhere along the POC tract of control and Net1a-MO injected embryos. ($p<0.0001$, one-way analysis of variance (ANOVA) test and $p<0.001$Tukey-Kramer Multiple Comparison Test). **(D)** Average growth rates ± s.d. for follower axons within the midline region and outside the midline. Followers represent a pool of axon that grew along the main POC tract at start and those that grew independently and either rejoined the tract later on or pioneered an ectopic midline crossing. ($p<0.0001$ (ANOVA) test and $p<0.001$Tukey-Kramer Multiple Comparison Test).

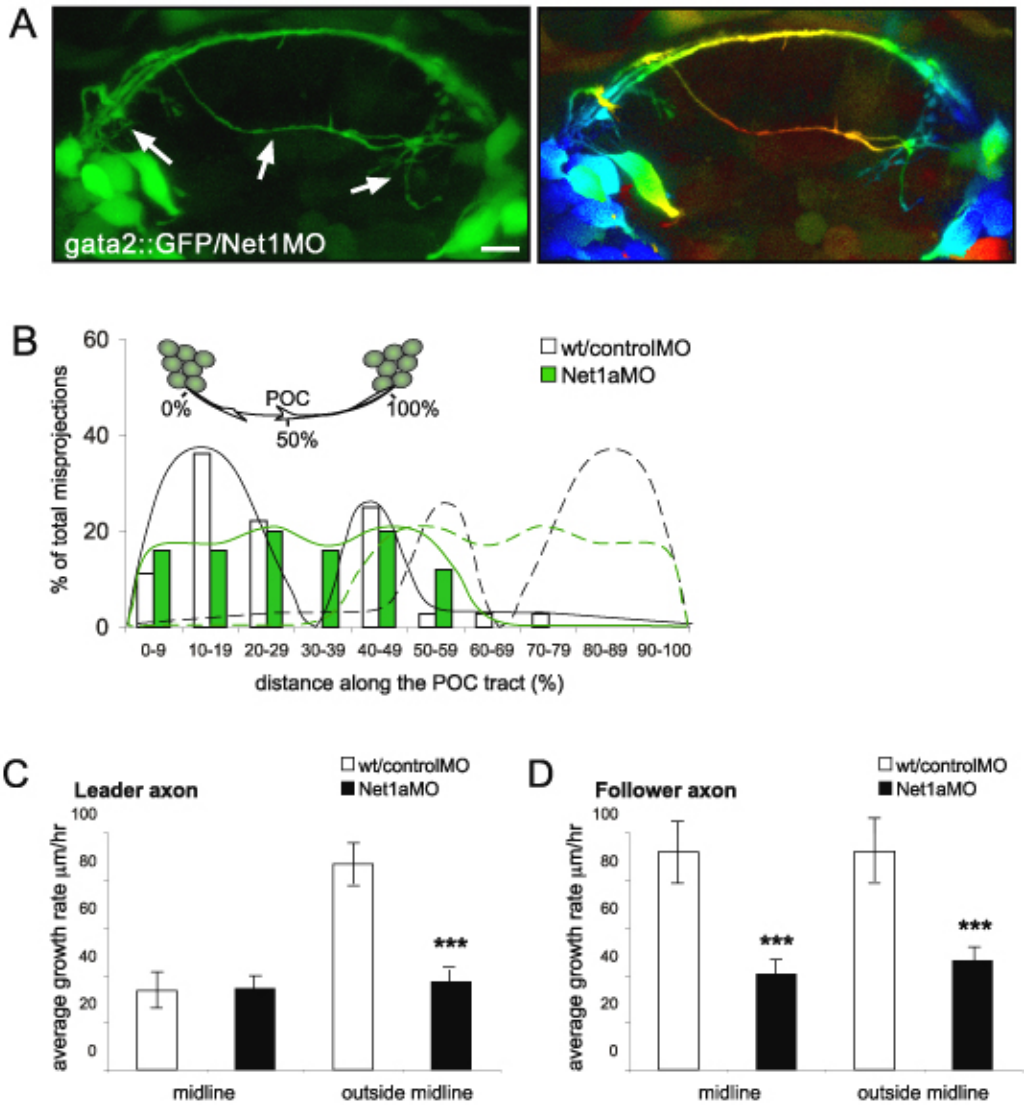

Next we examined the effects of netrin depletion on POC axon growth rate. Outside the midline, the average growth rate of leader axons in embryos injected with Net1a-MO is 37.2±3.8µm/hr (Figure 4-4C) and resembles pioneer axons in DCC-MO injected embryos (Figure 4-3E) while at the midline POC axons in Net1a-MO injected embryos have similar growth rates as control-MO injected pioneers (Figure 4-4C). Follower axons are severely affected along the entire POC tract. Follower axons in Net1aMO injected embryos grow at the rate of 40±16.5µm/hr at the midline and

46±8.6μm/hr outside the midline area (Figure 4-4D). These growth rates are half the normal rate for follower axons (Figure 4-4D). In summary, decrease in *netrin1a* expression correlates with more leader and follower POC growth cones projecting dorsally into a cell domain they do not normally invade. This results in slower growth rates as more axons attempt to pioneer the path to midline alone. Taken together, these data are consistent with the hypothesis that the *netrin1a* expressing cells in the forebrain discourages POC axons from projecting dorsally and away from the POC axon fascicle and aids in separating these projections from the AC axons.

4.7 Netrin1a overexpression either globally or ectopically produces POC growth cone collapse and increased avoidance behavior

The above findings suggest that netrin works as a repulsive cue for POC axons and limits their dorsal growth cone projections. To assess this repulsive effect on growth cones, we overexpressed *netrin1a* in zebrafish embryos and examined axon behavior during POC formation. We predicted that global overexpression of netrin1a should interfere with POC axon growth. Single live timepoints of POC axons in these embryos showed a disorganized POC tract (Figure 4-5A). Unlike in the case of MOs to either DCC (Figure 4-1B, Figure 4-2A) or Netrin1a (Figure 4-4A) in previous experiments, the axons appeared to grow stochastically (Figure 4-5A), suggesting that these aberrant trajectories resulted from a repulsive cue. Embryos injected with RFP alone as a control looked similar to unperturbed POC tracts (Figure 4-5B).

Another possibility however, is that netrin1a overexpression could affect cell patterning through its other receptor neogenin whose expression pattern is broader in the developing neuroepithelium. To address this possibility, we engineered two cDNA expression constructs to ectopically express either RFP alone as a control or co-express RFP and netrin1a in a small number of cells using the Gal4UAS system established in zebrafish [47]. Timelapse analysis (n=15) of POC leader growth cones with either RFP (control) or Netrin and RFP expressing cell allowed us to observe the specific effect of netrin on the growth cones. The data shows that when Netrin1a positive cell is in close proximity or directly in the path of a POC growth cone the likely result is growth cone collapse and avoidance behavior (Figure 4-5C).

Figure 4-5 Early POC growth cones exhibit increased collapse and avoid contact with ectopic netrin1a expressing cells.

(A) Live timepoints of gata2::gfp embryos injected with Net1a mRNA and control RFP mRNA show aberrant POC projecting growth cones (arrows) Scale bar:10µm. **(B)** gata2::gfp embryos injected with control RFP mRNA resemble unperturbed embryos. Scale bar:10µm. **(C)** (left) Wildtype growth cone (arrows) contacts and has extensive interaction with RFP only expressing cell and displays complex growth cone morphology throughout the whole interaction . Scale bar: 5µm. (right) Growth cones (arrows) interacting with RFP positive cells that co-express netrin1a have collapsed shapes and have limited contact with these cells. Scale bar: 10µm. **(D)** Percentage of timelapsed growth cones with complex shapes in presence of a netrin1a expressing cell. Growth cones judged complex had large spread out lamelopodia and at least 3-5 filopodia**.**

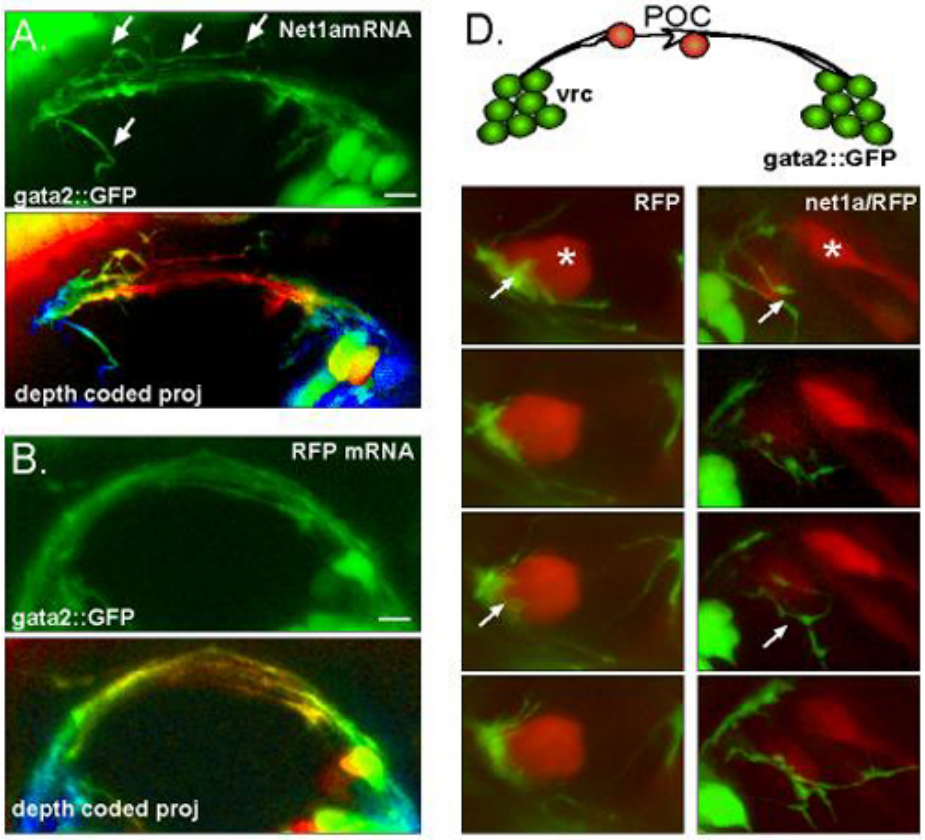
A.
Net1amRNA
gata2::GFP
depth coded proj
B.
RFP mRNA
gata2::GFP
depth coded proj
D.
POC
vrc
gata2::GFP
RFP
net1a/RFP
C.
100
80
60
40
20
0
complex growth cone shapes (%)
RFP
net1a/RFP

While wildtype growth cones extensively interacted with RFP-expressing cells and exhibited complex growth cone morphologies with many long filopodia and broad lamelipodia (Figure 4-5C arrows and Figure 4-5D), 78% of growth cones examined in the presence of netrin1a-expressing cells had collapsed shapes (Figure 4-5C,D). Growth cones that contacted Netrin1a cells withdrew but would at times try to contact the cells again. Repeated contact resulted in growth cones stalling for long periods of time. Occasionally, following the initial repulsion, the growth cone would grow past the netrin expressing cell. Growth cones that were in contact with a netrin1a expressing cell through their axon did not appear to be affected in terms of their ability to grow forward (data not shown). Taken together, these data are consistent with our earlier hypothesis that netrin is a repulsive cue for POC axon growth cones, thus serving to keep them away from projecting towards the netrin expressing domain. In doing so, netrin and DCC appear to work together to delineate a boundary for the early commissural tract in the zebrafish forebrain.

4.8 Discussion

Analysis of gene expression patterns in relation to the neuronal scaffold in zebrafish has led to the idea that specific gene expression domains might help delineate the early axon tracts[37,48-50]. Our timelapse data suggest that in the early zebrafish forebrain, netrin belongs to a set of guidance cues that help establish the early neuronal scaffold and delineate where axon tracts form. Netrin is normally expressed between the anterior and POC tracts, with the AC axons growing on top of cells expressing netrin and the POC axons growing slightly below the netrin1a-expressing cells (Fig4-6A and also see [35]).

This arrangement suggests that netrin might be a permissive cue for anterior commissural axons but not for POC axons.

In this paper, in vivo dynamic imaging combined with gain- and loss-of-DCC and netrin1a function allowed the analysis of the role of this ligand-receptor pair in establishing the early brain tracts. We show that netrin is an important guidance cue that helps delineate the POC axon tract as a single fascicle. Normally POC axons make brief and short explorations into the upper domain (Figure 4-3D). Depletion of either the receptor or the ligand results in aberrant dorsal POC growth cone projections that are normally discouraged when the netrin-DCC signaling is functional (Figure 4-1B, Figure 4-2A, Figure 4-4A and Figure 4-6B). This leads to a defasciculation phenotype and ectopic midline crossings by new POC axon pioneers that end up projecting independently. Finally, ectopic expression of the ligand either globally or in a small population of neuroepethelial cells results in growth cone collapse and increased avoidance behavior.

These responses are in agreement with the predicted function of netrin as a repellent cue for POC axons and with the loss-of-function studies. The axonal phenotype obtained in zebrafish mutant *aussicht* (Fgf8 mutant) and through MO knockdown of fgf8 support this conclusion. In both cases, the AC and the POC either fail to form[49] [51] or in less severely affected embryos axons make projections that resemble those shown here [51]. In the *ace* mutant, the netrin expression domain is greatly expanded [49] suggesting that the increased presence of netrin in this region might inhibit axon growth. Taken together, our results support the hypothesis that netrin participates in patterning early forebrain commissural tracts not by acting as a midline guidance cue as it does in the spinal cord of

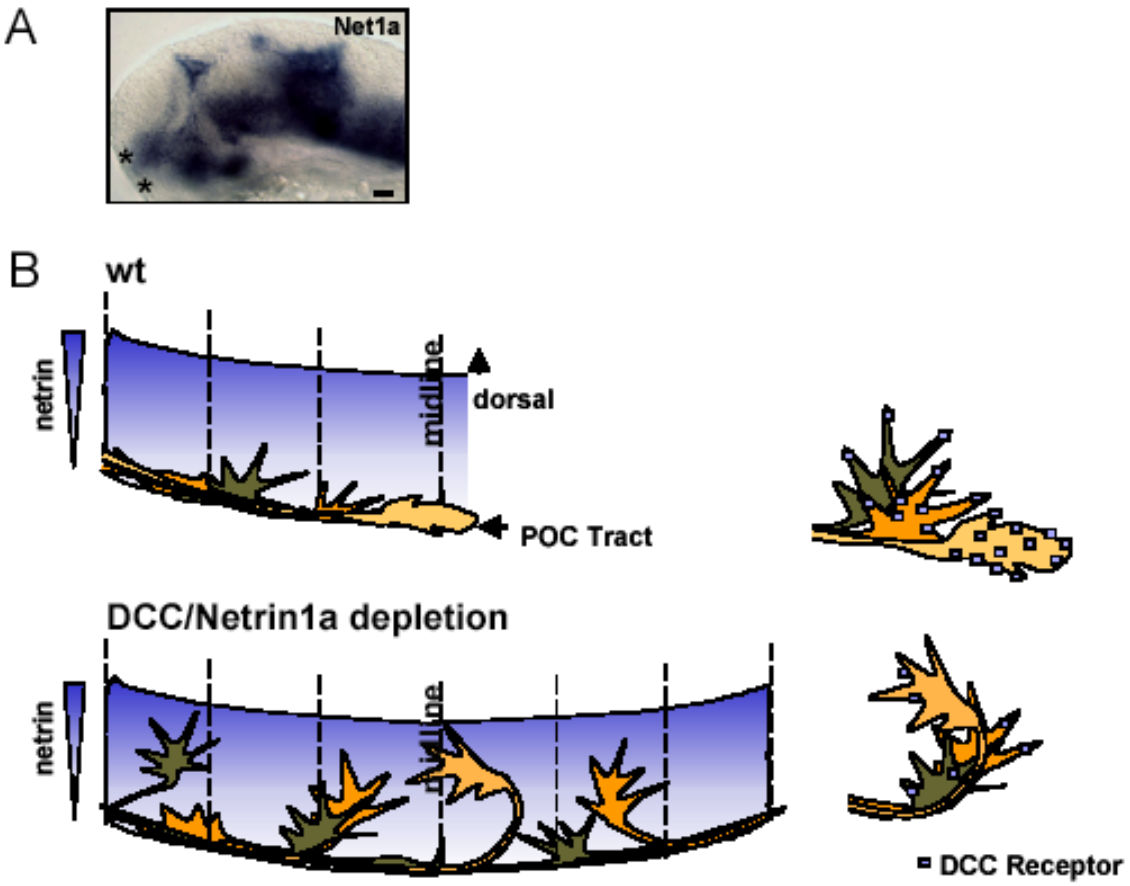

Figure 4-6 A model showing how netrin affects POC axons

(A) 24hpf zebrafish embryo stained to reveal the expression pattern of netrin1a. The location of the AC (dorsal) and POC (ventral) has been marked with asterisks.

(B) A schematic drawing depicting the affect of netrin expressing cells for early POC axons. Errors or detachments of growth cones from the main POC tract correspond to points where the netrin receptor might be low. When the receptor or the gradient is removed or significantly decreased POC growth cones errors increase.

other vertebrate systems but rather by delineating a repulsive boundary that keeps POC axons in their fascicle.

4.9 Experimental methods

Fish maintenance

Raising and spawning of adult zebrafish were performed as outlined in the Zebrafish book [52] and in accordance with the animal care guidelines of the California Institute of Technology.

In situ hybridization

Embryos were anaesthetized in 0.03% MS222 and fixed in 4% paraformaldehyde at room temperature for 4hrs. In situ hybridization was performed as previously described[53].

Plasmid construction

netrin1a expression vector: netrin1a was cloned into the pCS2 using and subsequently cloned into a pBluescriptSK containing a 14xUAS sequence with Xho1/Apa1. The membrane localization sequence of pCS2mRFP coding for monomeric red fluorescent protein (RFP) was removed creating pCS2RFP-membr. The RFP-membrPolyA was cloned into pBluescript containing 14xUAS with Xho1/Apa1. UASRFP-membPolyA was cloned in front of the UASNetrin1apolyA using Spe1/SmaI. All vectors were verified by transfection into 3T3 cells and assayed for fluorescence expression using Superfect® Trasfection Reagent (Qiagen) and also by injection into one-cell stage zebrafish embryos.

cDNA and RNA injections

Zebrafish embryos were injected at the one-cell stage with circular plasmid-DNA or mRNA using 0.8-1.4nl per embryo and air pressure. 2.5 pg of circular plasmid-DNA/embryo in 100 mM KCl was used and 0.1-0.4μg/μl of mRNA.

RNA for injection was prepared as follows: plasmids were linearized with appropriate restriction enzyme for 3hrs at 37°C and subsequently purified using the Nucleotide Removal Kit® (Qiagen). Complete digestion was verified by running a small sample on an agarose gel. RNA was made using Ambion mRNA kit at 37°C for 2hrs and further purified using RNAeasy® kit (Qiagen) and concentration obtained using spectrophotomoetry. Injected embryos were raised in 30% danieau solution/1% penicillin/streptomycin until imaging stage. Phenylthiourea (PTU) was added (0.15 mM) to the rearing medium between 12-14hpf.

Morpholino injections

Morpholinos (MOs) were designed to the three different complementary regions of the zebrafish DCC: (i) DCC5UTR-M0 (CGCGAAATCCGCTGCTAATCAATCAA) specific to the 5'UTR of DCC mRNA, (ii) DCCATG-MO (GAATATCTCCAG-TGACGCAGCCCAT) specific to the region overlapping the translation initiation codon (underlined) and (iii) DCCSplice-MO (GAG CAG CAC TGA CCG TGT GTG TAGA) overlapping the splice site in the DCC coding sequence and standard control MO, (CCT CTT ACC TCA GTT ACA ATT TATA) (Gene Tools LLC, Oregon, USA). All MOs were injected at a final concentration ranging from 3-5ng/nl in 120mM KCl and 20mM

Hepes solution at 1-4 cell stage. The volume injected was approximated by measuring the diameter of the injection in mineral oil and ranged between 0.8 and 1.4nl.

Timelapse experiments

Embryo Preparation:

Embryos at 20-22hpf were anesthetized with tricane in sedative amounts (0.01%) and embedded in a drop of 1-1.2% ultralow melt agarose on a cover slip-bottom petri dish in 30% danieau/0.01%tricane/0.15 mM PTU. Every effort was made to have each embryo in a similar orientation. Commissures that appear more arc-like compared to those that look more linear are a result of differences in the way the embryo was oriented and not an effect of any perturbations performed in this study.

Imaging details:

All imaging was performed using Inverted 510Meta Zeiss Confocal Scanning Microscope or a Zeiss Pascal inverted confocal scanning microscope with a Plan-Neuofluar 40X/N.A1.3 Oil objective. 3 D stacks of the forebrain were taken at 3-minute intervals previously determined to be optimal for observing POC axon kinetics [4], spanning the POC axon tract. Temperature was maintained at 28-29 °C throughout the imaging experiment. GFP positive cells were excited with the 488 nm argon laser line using 505LP chroma filter set. Typical imaging experiment lasted between 3-5 hours. A z stack spanning approximately 30-45μm was collected at each time point with individual sections being 1μm apart. The pinhole settings were at 1.5-2.77 airy units depending on the microscope used. Refocusing was minimal but needed to be done occasionally to

make sure the leading growth cones were imaged in full at all times. For observing growth cone responses to ectopic netrin1a expressing cells timelapse movies were acquired without time delay as short z-stacks (10-15µm) at 1µm interval to allow the growth cone morphology and its interaction with the *netrin1a* expressing cell(s) to be observed for up to 20min. These were later analyzed using Zeiss imaging software. Depth coded images were made using Zeiss software.

Axon growth error analysis

Z-stack images were imported into Object Image and maximum intensity projections (MIPs) were made at each time point and assembled into movies. Growth cone error position along the POC was obtained by taking the ratio between distance along the POC where the growth cone made an ectopic dorsal projection and the total distance of the POC. This ratio was converted to a percentage between 1 and 100%. All dorsal projection error positions were recorded with respect to the midline. As axons originating from the left and right side did not exhibit any biases in error position, total number of errors at each interval from both sides were added and plotted as one histogram. The trend outlines with a dash line was subsequently reflected over the midline to visualize the general behavior of growth cones along the POC. Maximal error projection length was measured as a perpendicular line connecting the place where the growth cone detached from the POC to the tip of the growth cone. Duration of individual errors was recorded as the number of time intervals that a given growth cone was away from the POC tract and binned into 10min intervals up to 40min. Growth cones that exceeded this last time bin

were binned into 40+ category. Axon growth rate analysis was performed as previously described[4].

Data analysis

Quantitative axon growth rates data was analyzed using GraphPad InStat 3.0 Software. In cases where one average growth rate was compared to more than one different growth rate, the p value was recalculated to adjust for multiple comparisons as indicated in figure legends. All p values are reported in text and figures.

Acknowledgements

We would like to thank Chi Bin Chien and Arminda Suli for the DCC MOs, John Kuwada for the Netrin1a cDNA and Helen Cooper for the mouse DCC cDNAs. We thank David Koos, Helen McBride, Rajan Kulkarni, Andres Collazo and Lisa Zimmer for discussions and critical reading of the manuscript and Tania Demyanenko and Aura Keeter for excellent technical assistance.

4.10 References

1. Mastick, G. & Easter, S. E., Jr. Initial organization of neurons and tracts in the embryonic mouse fore and midbrain. *Developmental Biology* **173**, 79-94 (1996).
2. Wilson, S., Ross, L., Parrett, T. & Easter, S. The development of a simple scaffold of axon tracts in the brain of the embryonic zebrafish, *Branchydanio rerio*. *Development* **108**, 121-145 (1990).
3. Chitnis, A. & Kuwada, J. Axonogenesis in the brain of zebrafish embryo. *The Journal of Neuroscience* **10**, 1892-1905 (1990).
4. Bak, M. & Fraser, S. E. Axon fasciculation and differences in midline kinetics between pioneer and follower axons within commissural fascicles. *Development* **130**, 4999-5008 (2003).
5. Wilson, S. & Easter, S. Stereotype pathway selection by growth cones of early epiphysial neurons in the embryonic zebrafish. *Development* **112**, 723-746 (1991).
6. McConnell, S., Ghosh, A. & Shatz, C. Subplate neurons pioneer the first axon pathway from the cerebral cortex. *Science* **245**, 978-981 (1989).
7. Devenport, R., Thies, E. & Cohen, M. Neuronal growth cone collapse triggers lateral extensions along trailing axons. *Nature Neuroscience* **2**, 254-259 (1999).
8. Chitnis, A. & Kuwada, J. Elimination of a brain tract increases errors in pathfinding by follower growth cones in the zebrafish embryo. *Neuron* **7**, 277-285 (1991).
9. Chitnis, A., Patel, C., Kim, S. & Kuwada, J. A specific brain tract guides follower growth cones in two regions of the zebrafish brain. *The Journal of Neurobiology* **23**, 845-854 (1992).

10. Bovolenta, P. & Dodd, J. Guidance of commissural growth cones at the floor plate in embryonic rat spinal cord. *Development* **109**, 435-447 (1990).

11. Raper, J., Bastiani, M. & Goodman, C. Pathfinding by neuronal growth cones in grasshopper embryos II. Selective fasciculation onto specific axonal pathways. *The Journal of Neuroscience* **3**, 31-41 (1983).

12. Myers, P. & Bastiani, M. Growth cone dynamics during the migration of an identified commissural growth cone. *The Journal of Neuroscience* **13**, 127-143 (1993).

13. Gan, W. & Macagno, E. Developing neurons use a putative pioneer's peripheral arbor to establish their terminal fields. *The Journal of Neuroscience* **15**, 3254 (1995).

14. Klose, M. & Bentley, D. Transient pioneer neurons are essential for formation of an embryonic peripheral nerve. *Science* **245**, 982-983 (1989).

15. Boyan, G., Therianos, S., Williams, L. & Reichert, H. Axogenesis in the embryonic brain of the grasshopper *Schistocerca gregaria*: an identified cell analysis of early brain development. *Development* **121**, 75-86 (1995).

16. Bastiani, M., Raper, J. & Goodman, C. Pathfinding by neuronal growth cones in grasshopper embryos III. Selective affinity of the G growth cone for the P cells within the A/P fascicle. *The Journal of Neuroscience* **4**, 2311-2328 (1984).

17. Bentley, D. & Keshishian, H. Pathfinding by peripheral pioneer neurons in grasshopper. *Science* **218**, 1082-1087 (1982).

18. Guan, K. & Rao, Y. Signaling mechanisms mediating neuronal responses to guidance cues. *Nature Reviews in Neuroscience* **4**, 941-956 (2003).

19. Song, H. & Poo, M. The cell biology of neuronal novigation. *Nature Cell BIology* **3**, E81-E88 (2001).

20. Tessier-Lavigne, M. & Goodman, C. The molecular biology of axon guidance. *Science* **274**, 11231133 (1996).

21. Kalil, K., Szebenyi, G. & Dent, E. w. Common mechanisms underlying growth cone guidance and axon branching. *Journal of Neurobiology* **44**, 145-58 (2000).

22. Ming, G. et al. Adaptation in the chemotactic guidance of nerve growth cones. *Nature* **417**, 411-418 (2002).

23. Hutson, L. & Chien, C.-B. Pathfinding and error correction by retinal axons: the role of astray/robo2. *Neuron* **33**, 205-221 (2002).

24. Mason, C. & Wang, C. Growth cone form is behavior-specific and consequently position-specific along the retinal axon pathway. *The Journal of Neuroscience* **17**, 1086-1100 (1997).

25. Kennedy, T. E., Serafini, T., de la Torre, J. R. & Tessier-Lavigne, M. Netrins are diffusible chemotropic factors for commissural axons in the embryonic spinal cord. *Cell* **78**, 425-435 (1994).

26. Serafini, T. et al. The netrins define a family of axon outgrowth-promoting proteins homologous to *C. elegans* UNC-6. *Cell* **78**, 409-424 (1994).

27. Colamarino, S. & Tessier-Lavigne, M. The role of the floor plate in axon guidance. *Annual Reviews in Neuroscience* **18**, 497-529 (1995).

28. Serafini, T. et al. Netrin-1 is required for commissural axon guidance in the developing vertebrate nervous system. *Cell* **87**, 1001-1014 (1996).

29. Ming, G. Cyclic-AMP-dependent growth cone guidance by netrin-1. *Neuron* **19**, 1225-1235 (1997).

30. Keino-Masu, K. Deleted in Colorectal Cancer (DCC) encodes a netrin receptor. *Cell* **87**, 175-185 (1996).

31. Geisbrecht, B. V., Dowd, K. A., Barfield, R. W., Longo, P. A. & Leahy, D. J. Netrin binds discrete subdomains of DCC and Unc5 and mediates interactions between DCC and Heparin. *Journal of Biological Chemistry* **278**, 32561-32568 (2003).

32. Shu, T., K.M., V., Seaman, C., Cooper, H. M. & Richards, L. J. Expression of the Netrin-1 receptor deleted in colorectal cancer (DCC), is largely confined to projecting neurons in teh developing forebrain. *Journal of Comparative Neurobiology* **416**, 201-212 (2000).

33. Hjorth, J. T., Gad, J., Cooper, H. M. & Key, B. A zebrafish homologue of deleted in colorectal cancer (zDCC) is expressed in the first neuronal clusters of teh developing brain. *Mechanisms of Development* **109**, 105-109 (2001).

34. Strahle, U., Fisher, N. & Blader, P. Expression and regulation of a netrin homologue in the zebrafish embryo. *Mechanisms of Development* **62**, 147-160 (1997).

35. Lauderdale, J. D., Davis, N. M. & Kuwada, J. Y. Axon tracts correlate with Netrin-1a expression in the zebrafish embryo. *Molecular and Cellular Neuroscience* **9**, 293-313 (1997).

36. MacLennan, J. A. et al. Immunohistochemical localization of Netrin-1 in the embryonic chick nervous sytem. *Journal of Neuroscience* **17**, 5466-5479 (1997).

37. McDonald, R. et al. Regulatory gene expression boundaries demarcate sites of neuronal differentiation in the embryonic zebrafish forebrain. *Neuron* **13**, 1039-1053 (1994).

38. Hiramoto, M., Hiromi, Y., Giniger, E. & Hotta, Y. The Drosophila netrin receptor Frazzled guides axons by controlling Netrin distribution. *Nature* **406**, 886-889 (2000).

39. Charron, F., Stein, E., Jeong, J., McMahon, A. & Tessier-Lavigne, M. The morphogen Sonic Hedgehog is an axonal chemoattractant that collaborates with Netrin-1 in midline axon guidance. *Cell* **113**, 11-23 (2003).

40. Nasevicius, A. & Ekker, S. Effective targeter gene 'knockdown' in zebrafish. *Nature Genetics* **26**, 216-220 (2000).

41. Ross, L., Parrett, T. & Easter, S. Axonogenesis and morphogenesis in the embryonic zebrafish brain. *The Journal of Neuroscience* **12**, 467-482 (1992).

42. Draper, B., Marcos, P. A. & Kimmel, C. B. Inhibition of zebrafish fgf8 pre-mRNA splicing with morpholino oligos: a quantifiable method for gene knockdown. *Genesis* **30**, 154-156 (2001).

43. Fazeli, A. et al. Phenotype of mice lacking functional deleted in colorectal cancer (DCC) gene. *Nature* **386**, 796-810 (1997).

44. Bloch-Gallego, E., Ezan, F., Tessier-Lavigne, M. & Sotelo, C. Floor plate and netrin-1 are involved in the migration and survival of inferior olivary neurons. *Journal of Neuroscience* **19**, 4407-4420 (1999).

45. Llamibi, F., Causeret, F., Bloch-Gallego, E. & Mehlen, P. Netrin-1 acts as a survival factor via its receptors UNC5H and DCC. *EMBO Journal* **20**, 2715-2722 (2001).

46. Mehlen, P. & Mazelin, L. The dependence receptors DCC and UNC5H as a link between neuronal guidance and survival. *Biology of the Cell* **95**, 425-436 (2003).

47. Koester, R. W. & Fraser, S. E. Tracing transgene expression in living zebrafish embryos. *Developmental Biology* **233**, 329-346 (2001).

48. McDonald, R. et al. The Pax protein Noi is required for commissural axon pathway formation in the restral forebrain.. *Development* **124**, 2397-2408 (1997).

49. Heisenberg, C.-P., Brennan, C. & Wilson, S. The zebrafish aussicht mutant embryos exhibit widespread overexpression of ace (fgf8) and coincident defects in CNS development. *Development* **126**, 2129-2140 (1999).

50. Wilson, S., Brennan, C., McDonald, R., Brand, M. & Holder, N. Analysis of axon tract formation in the zebrafish brain:the role of terrirories of gene expression and their boundaries. *Cell Tissue Research* **290**, 198-196 (1997).

51. Walshe, J. & Mason, I. Unique and combinatorial functions of Fgf3 and Fgf8 during zebrafish forebrain development. *Development* **130**, 1-14 (2003).

52. Westerfield, M. The Zebrafish Book. *University of Oregon Press* **Eugene, OR.** (1995).

53. Jowett, T. & Lettice, L. Whole-mount in -situ hybridization on zebrafish embryos using mixture of digoxigen- and fluorescein- labeled probes. *Trends in Genetics* **10**, 73-74 (1994).

Chapter 5 One and two-photon FRAP reveals differences in mobility of cytosolic GFP in growth cones in vivo

Magdalena Bak-Maier, Rajan P. Kulkarni and Scott E. Fraser

SUMMARY

Localized diffusion differences in growth cones are likely to be critical for delivery of molecular species into the growth cone tip, which in turn can influence the direction of axon growth. However, neither the kinetics of local protein movement nor the effects of cytoskeletal elements on protein mobility in a growth cone have been probed *in vivo*. Here, stable GFP expressing neurons and their growth cones were used in combination with one and two-photon fluorescence recovery after photobleaching (FRAP) method to determine the rates for lateral diffusion of molecules in growth cones *in vivo*. We find differences in local diffusion rates between actively pioneering growth cones and those that rely in part on other axons as substrate for guidance. Pharmacological perturbations of the actin and microtubule networks point to actin as the primary modulator of diffusion in growth cones. This experimental approach provides a powerful method for quantifying the mobility of specific proteins in growth cones in vivo and shows that diffusion is an important parameter during axon navigation.

5.1 Introduction

The wiring of the nervous system involves guided extension of neuronal processes, called axons, towards other neurons. A key structure at the end of the axon tip, called the growth cone, contains the sensory and motor functions necessary for axon guidance. Guidance signaling cascades are believed to converge on the cytoskeleton ensuring that growth cones properly steer towards or away from a given guidance cue. A major challenge is to understand how local diffusion might affect molecular species that play a role in guidance signaling[1]. Neither the kinetics of local protein movement nor the effects of cytoskeletal elements on protein mobility in a growth cone have been probed *in vivo*. Here, we have measured diffusion in growth cones during early neuronal scaffold formation in zebrafish embryos. We have uncovered differences in diffusion based on growth cone morphology that can be linked to the cytoskeleton.

5.2 Results

To measure the diffusion rates of small molecules in different regions of young neurons we employed one and two-photon fluorescent recovery after photobleaching (FRAP) to image GFP mobility using the gata2::GFP zebrafish line[2] and yellow fluorescent protein (YFP) as needed. Previously, we have shown that gata2::GFP zebrafish embryos express GFP in early differentiated brain cells and axons that form the postoptic commissure (POC) tract in the forebrain[3]. The high level of GFP expression allows the behavior of these early axons and growth cones to be observed *in vivo* as they navigate across the midline (Figure 5-1a)[3]. We have shown that the first axons (leader axons) that arrive at

the midline display different behaviors and growth cone shapes compared to later axons that grow along the leaders (follower axons)[3].

Two-dimensional (x and y) FRAP has been previously used to study the mobility, transport and sub-cellular organization of fluorescently tagged molecular species in cultured cells[4-9]. In FRAP, a small sample region is bleached using high intensity laser illumination and the recovery of non-bleached fluorescent molecules into this area is monitored using low-intensity illumination as before the bleach. Because fluorescence recovery depends on the movement of unbleached GFP in the surrounding areas, this allows us to monitor the fluorescence recovery kinetics and calculate a diffusion constant, D, of a given molecule[4,10-12]. Using the gata2::GFP zebrafish, FRAP experiments can be performed and the diffusion constant calculated for molecular species similar in size to GFP, inside navigating growth cones in vivo.

Neurons are highly compartmentalized cells designed to process and integrate multiple signals in a spatially and temporally distinct manner. Broadly, a young neuron can be subdivided into three regions based on its function: the cell body, the axon process and the growth cone. We first examined the diffusion of cytosolic GFP inside these three areas (Figure 5-1a) (n= 60 separate embryos). To measure fast diffusion, we analyzed lateral rates based on fluorescence recovery traces obtained from two-dimensional scans over time (Figure 5-1b). While the axon process and the growth cone are relatively flat structures, this FRAP measurement requires that they remain in the same axial plane (z dimension) over the time course of the experiment. To assess the stability of growth cones, we used depth color-coded z-stacks of the same growth cone at different time-points. Four dimensional (x,y, z and time) timelapse movies of early POC growth cones

show that early growth cones remain in the same axial plane for up to 2 minutes. During this time, the growth cone is actively sampling its environment as revealed by the appearance and disappearance of individual filopodia (Figure 5-1c, arrows). This allows sufficient time to perform FRAP measurements.

5.3 Quantitative FRAP analysis reveals difference in diffusion within neuronal compartments

Post-bleach traces in the three compartments (cell body, axon process and growth cone) show rapid recovery, occurring on the order of seconds (Figure 5-1di-iii). This resulted in diffusion values being fastest in the cell body and slowest in the growth cone (Table 5-1). Control experiments using fixed gata2::GFP embryos showed no recovery (data not shown). To verify that the observed diffusion was not affected by GFP expression levels, we performed similar FRAP measurements using the islet1::GFP line and obtained similar diffusion values (Table 5-2).

Due to the large nucleus, the cytoplasmic volume in early neurons is small, thus effectively reducing the cytoplasm to two-dimensions. This should allow direct comparison of diffusion across all three compartments. To test whether the out of focus light in one-photon mode FRAP significantly affected the calculated diffusion rate we employed two-photon FRAP and compared GFP and YFP diffusion in the same neuronal cell bodies using gata2::GFP embryos injected with YFP mRNA. Two-photon FRAP allows deeper penetration into the sample and reduced radiation outside of the focal plane of the laser beam. Further, two-photon FRAP permits different fluorophores to be

bleached simultaneously[1], allowing us to examine the GFP/YFP recovery kinetics at the same time. The bleach applied resulted in virtually identical fluorescence recovery traces and diffusion values for both fluorescent species as might be expected since the two molecules are almost identical in size (Figure 5-1div, Table 5-2). These values, are also similar to the one-photon results indicating that out of focus light does not significantly perturb axial diffusion measurements in these samples.

5.4 Diffusion differences between leader and follower growth cones

We have previously reported differences in leader and follower axon growth cones in terms of their morphologies and growth rates and found that kinetics of follower axons correlate with changes in growth cone shape[3]. Here we saw an opportunity to examine the correlation between growth cone shape and diffusion by applying FRAP to leader and follower growth cones. We found that leader growth cones consistently showed longer recovery times compared to follower growth cones. The typical recovery time of the leader growth cone was 6-8 sec compared to 3-4 sec for a follower growth cone. Thus, the diffusion constant was significantly slower in leader growth cones (0.278 $\mu m^2 s^{-1}$, Table 5-1) compared to follower growth cones (0.55 $\mu m^2 s^{-1(}$, Table 5-1) and remained unchanged irrespective of growth cone position along the commissural tract. To further investigate differences in GFP mobility between leader and follower growth cones, we next examined follower growth cones that lost contact with other POC axons. To

[1] This is due to the two-photon absorption cross sections of many common fluorophores (including the fluorescent proteins) being broad over the wavelength range of typical two-photon lasers (~750-950 nm).

distinguish them from the followers that grow along the POC, we named these followers 'off-tract'. FRAP measurements revealed a striking decrease in GFP mobility in off tract growth cones compared with regular follower growth cones. Off-tract growth cones had the slowest recovery times with an average diffusion of 0.144 $\mu m^2 s^{-1.}$ (Figure 5-2a,Table 5-1).

To confirm that GFP fluorescence recovery correlated with growth cone shape we assayed the same follower growth cone as it grew away from and along other axons using timelapse analysis and FRAP (Figure 5-2d). Fluorescence recovery was slow at all points when the growth cone lost contact with other axons (Figure 5-2d, pink lines). However, both before and after reestablishing contact, the fluorescence recovery was rapid and the diffusion constant characteristic of regular follower growth cones (Figure 5-2d, blue lines). These experiments indicate a strong correlation between GFP diffusion and growth cone shape. Complex growth cones of axons probing their environment independently have significantly slower diffusion values compared to growth cones that wrap around other axons.

Figure 5-1 Single and two-photon FRAP analysis of diffusion in early neurons (next page)

(a) (left) Schematic showing embryo preparation for imaging and FRAP analysis. (middle) Diagram of the POC commissural axon tract showing the three regions of the gata2::GFP neurons were FRAP measurements were taken: (1) cell body, (2) axon process and (3) growth cone. Ventor-rostral cluster (vrc). (right) 23hpf gata2::GFP embryo showing GFP positive vrc cells and early POC axons growing to midline. The POC growth cones have been highlighted by color. Black regions correspond to non-fluorescing cells. **(b).** The image sequence represents a typical FRAP experiment performed on a leader growth cone. Pre-bleach sequences are acquired to provide baseline fluorescence, followed by the bleach (star). Fluorescence recovery is then recorded as a function of time and can be plotted as shown on the right**. (c)** Depth coded z-stack of a leader growth cone showing no significant change in the axial position of the growth cone during the length of a typical FRAP experiment. Arrows indicate filopodia. **(d)** Average fluorescence recovery traces obtained with either single or two-photon FRAP imaging in different compartments of young neurons in vivo. (i) cell body, (ii) axon process, (iii) leader growth cone. The non-bleached control for each compartment is plotted in gray. (iv) YFP/GFP cell-body two-photon comparison. The YFP average trace was normalized to the GFP. Scale: 10μm.

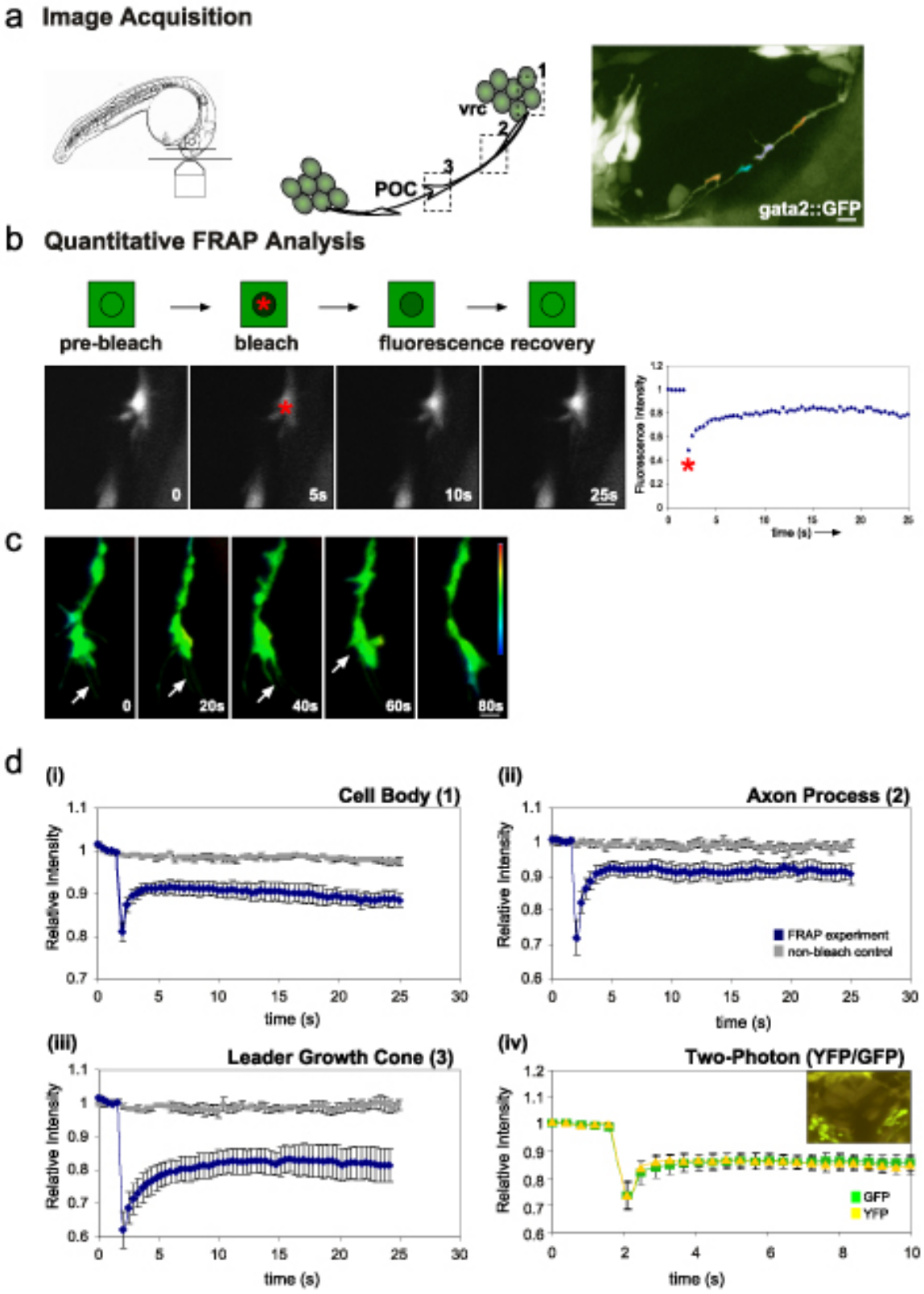
a Image Acquisition
vrc
1
2
3
POC
gata2::GFP
b Quantitative FRAP Analysis
pre-bleach
bleach
fluorescence recovery
0
5s
10s
25s
Fluorescence Intensity
time (s)
c
0
20s
40s
60s
80s
d
(i)
Cell Body (1)
(ii)
Axon Process (2)
FRAP experiment
non-bleach control
(iii)
Leader Growth Cone (3)
(iv)
Two-Photon (YFP/GFP)
GFP
YFP
Relative Intensity
time (s)

5.5 Role of actin and microtubule networks in GFP diffusion in early POC growth cones

The observed differences in GFP mobility suggest the presence of a diffusion barrier that is either more extensive or longer lasting in growth cones having slower diffusion. Previous measurements have shown that the actin network can slow down the diffusion rate of long-chain dextrans in cultured neurons[13]. The leading edge of the growth cone is actin rich, containing a meshwork of actin bundles that project radially out and into the filopodia[1]. Cytochalasins are well characterized actin depolymerizing agents[14,15] used to study the effects of the actin network on diffusion in *Dictyostelium* and cultured neurons[16,17]. To examine whether the actin network affects diffusion in the growth cone we used cytochalasin B to perturb actin organization and assayed the resulting GFP fluorescence recovery rate. Growth cones in embryos injected with cytochalasin B begin to lose filopodia and become less motile compared to uninjected embryos. Cytochalasin B significantly increased the diffusion rate in both leader and off- tract growth cones (Figure 5-2b, Table 5-1). This results in all growth cones having similar recovery kinetics (Figure 5-2b). Similar results were obtained with latrunculin (data not shown). The observed increase in GFP mobility upon actin depolymerization suggests that actin plays a role in local diffusion in growth cones.

The central region of the growth cone and axon process contain microtubule bundles mainly utilized for axoplasmic transport of organelles and general structural integrity[1]. To determine how the microtubule scaffold affects diffusion in growth cones we treated the gata2::GFP embryos with nocodazole. Nocodazole treatment caused progressive growth cone collapse. However, fluorescence recovery traces did not reveal

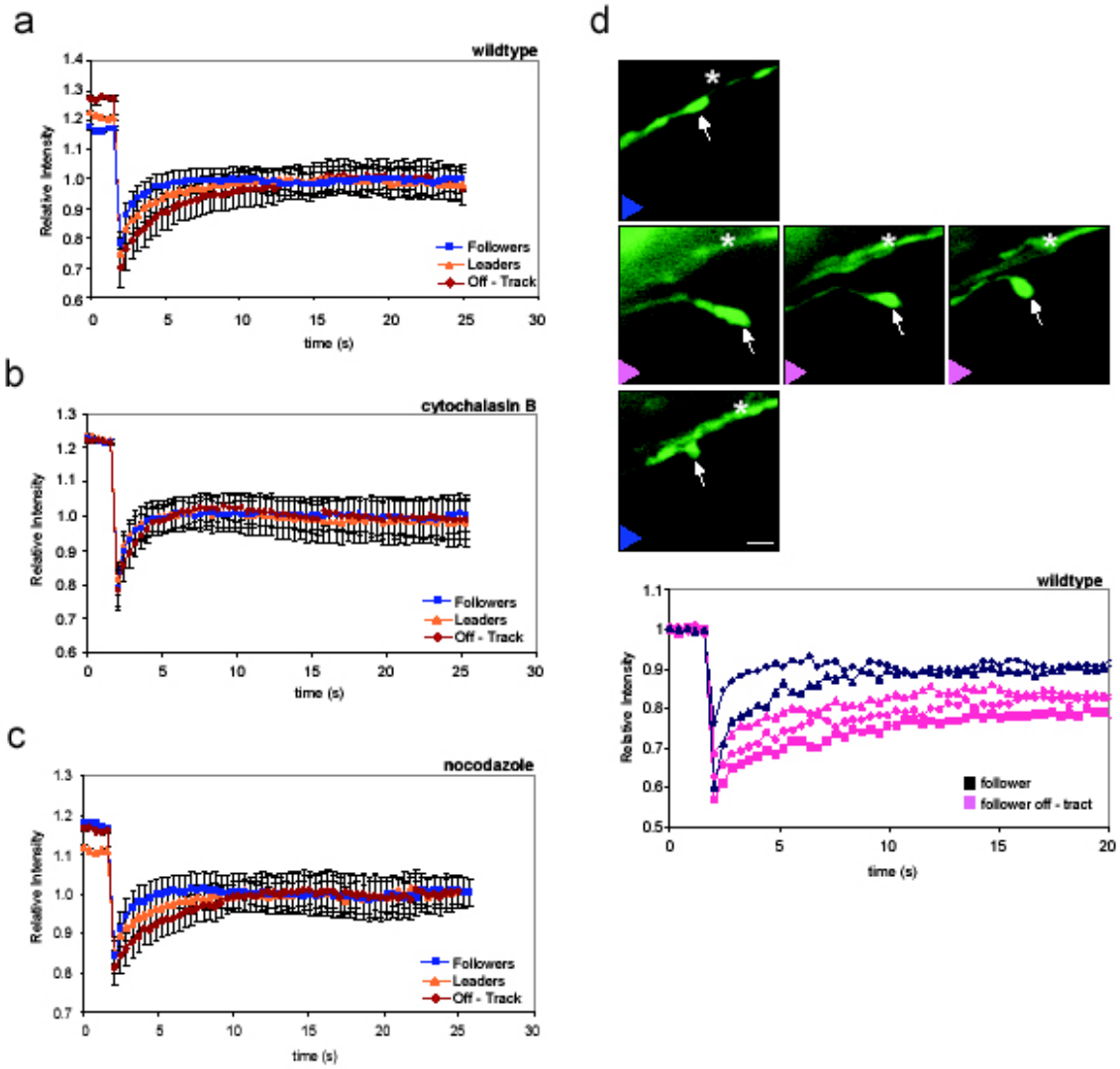

Figure 5-2 Measurement of diffusion in growth cones.

(a) Average fluorescence recovery traces in follower, leader and follower off tract wildtype growth cones. All traces have been normalized to the final recovery level post-bleach to illustrate the differences in diffusion kinetics. **(b-c)** Effects of cytochalasin B (b) and nocodazole (c) on GFP diffusion in growth cones as assayed by FRAP analysis. **(d)** Dynamic differences in GFP diffusion visualized in a single follower growth cone (arrow) as it either associates with other POC axons (star) or grows away from them. Fluorescence recovery traces corresponding to these events are plotted below. Blue traces correspond to growth cone in contact with the POC axons, pink traces when the growth cone traveled away from the POC.

a significant effect on fluorescence recovery times nor diffusion values (Figure 5-2d, Table 5-1). The efficacy of all pharmacological agents was further verified in 3T3 cells with FRAP analysis and timelapse imaging (data not shown). Taken together, these data suggest that the microtuble network does not appear to play a major role in modulating local diffusion rates in growth cones in vivo.

5.6 Conclusions

Navigating growth cones are in constant flux. Guidance receptors are constantly presented at the surface, recycled and new proteins delivered into the growth cone as well as locally synthesized[18]. These processes, along with local ion fluxes and signaling cascades are all influenced by the organization and rearrangement of the cytoskeleton. Our results demonstrate local diffusion rate differences between actively exploring leader growth cones and follower growth cones. These differences appear to be linked to the actin network. Recently, specific guidance cues have been shown to directly affect the actin and microtubule cytoskeleton (reviewed in [19]). An interesting possibility is that in addition to its role in mobility, the actin network in growth cones sets up transient boundaries that effectively limit diffusion on short time scales. This in turn could serve as a mechanism for amplifying local guidance signals and helping growth cones navigate.

Table 5-1 GFP diffusion rates in different neuronal compartments and growth cones

	Wildtype			CytochalasinB			Nocodazole		
	N	Diffusion (μm^2/sec)	S.D.	N	Diffusion (μm^2/sec)	S.D.	N	Diffusion (μm^2/sec)	S.D.
Leader G.C.	20	0.278^{H}	0.113	7	$0.674^{=}$	0.186	7	0.323	0.105
Follower G.C.	22	0.55^{H}	0.273	3	0.671	0.229	4	0.543	0.198
Off-tract G.C.	9	0.144^{H}	0.052	6	$0.37^{=}$	0.169	7	0.21	0.111
Axon	23	0.708^{H}	0.155	9	$0.874^{=}$	0.207	1	$0.902^{=}$	0.209
Cell Body	29	0.957^{H}	0.216		0.939	0.175		1.12	0.184

Diffusion coefficients for GFP in various compartments of the developing zebrafish neurons are listed above. For examining the effects of actin and microtubule networks zebrafish were injected either with cytochalasin B or nocodazole, and the diffusion coefficients for GFP were measured by region. The p values were generated by comparing across wildtype compartments for differences in diffusion ($p<0.001^{=}$, ANOVA followed by Tukey-Kramer Multiple Comparison Test). The effect of cytochalasin B or nocodazole on diffusion for each compartment was compared with wildtype using Student's T-test with $p<0.001$ noted^{H}

Table 5-2 Two-photon FRAP measurements of GFP and YFP diffusion in the cell bodies of young neurons

	N	Diffusion (μm^2/sec)	S.D.
Cell Body GFP	15	0.918	0.158
Cell Body YFP	15	0.926	0.171

Diffusion constants for GFP and YFP co-expressing zebrafish vrc neurons. GFP and YFP were simultaneously bleached. The average recovery traces are shown in Figure5-1d. The diffusion constants obtained for GFP versus YFP are not significantly different ($p>0.89$, Student's T-test).

5.7 Experimental methods

Fish maintenance

Raising and spawning of adult zebrafish were performed as outlined in the Zebrafish book and in accordance with the animal care guidelines of the California Institute of Technology.

Embryo preparation and imaging details

Embryo preparation and pharmacological treatments

Embryos at 20-22 hours post fertilization (hpf) were anesthetized with tricane in sedative amounts (0.01%) and embedded in a drop of 1-1.2% ultralow melt agarose on a cover slip-bottom petri dish in 30% danieau/0.01%tricane/0.15 mM Phenylthiourea (PTU). Pharmacological inhibitors of cytoskeleton components were injected into the neural tube of zebrafish embryos between 18-24 (hpf) and embryos were allowed to recover for 10-20min at 28°C. Nocodazole (Sigma) was used at a concentration of 20-40μM and cytochalasin B (Sigma) was used at 4μg/mL. Embryos were subsequently remounted in an inverted position to allow imaging of commissural axons. Injected embryos were imaged for a maximum of 30min.

Imaging details

All imaging was performed using an Inverted 510Meta Zeiss Confocal Scanning Microscope with a Plan-Neuofluar 40X/N.A1.3 objective. Temperature was maintained at 28-29°C throughout the imaging experiment. GFP positive cells were excited with a

30mW Argon laser using the 488 nm excitation line with a 505LP chroma filter and a pinhole setting of 1.2-1.5 airy units.

FRAP measurements and analysis

100 images (512x 512) were acquired in a continuous timelapse mode at the maximal scanning rate. Five images were acquired before the bleach to obtain a fluorescence baseline. In all in-vivo photobleaching experiments, a circular region, 1μm in radius, was defined and photobleached at full laser power (100% power, 100% transmission, 5-7 pulses) and fluorescence recovery was monitored by scanning the whole field of interest at low laser power after the bleach (100% power, 1-2% transmission) and the fluorescence intensity recovery traces recorded. Typically less than 3% of total fluorescence was lost during the entire recovery phase. The bleaching characteristics of the laser beam were determined by bleaching a spot in an immobile specimen of fluorescein using the same laser and objective settings. From this data, the beam profile and $1/e^2$ beam radius were determined.

Diffusion coefficients for GFP were determined by classical FRAP analysis, as previously described[10,12,20]. The fluorescence recovers according to the following equation:

$$\frac{F(t)}{F_p} = \sum_{n=0}^{\infty}\left[\left(\frac{(-K^n}{n!}\right)\left(\frac{1}{1+ n(1+2t/\tau_D)}\right)\right] \qquad (1)$$

where F(t) is the fluorescence intensity at time t after the bleach pulse, F_p is the fluorescence intensity immediately prior to bleach, τ_d is the characteristic diffusion time, and K is a parameter related to the degree of bleaching:

$$\frac{F_o}{F_p} = \frac{(1 - e^{-K})}{K} \quad (2)$$

where F_o is the fluorescence intensity immediately after the bleach. The K parameter was determined for each trace. The FRAP recovery curves were then used to determine the half time of recovery ($\tau_{1/2}$). $\tau_{1/2}$ is related to the characteristic diffusion time τ_d by the following relation:

$$\tau_{1/2} = \gamma\tau_d \quad (3)$$

where γ is a function of the beam shape and the extent of bleaching. Typically, for diffusive processes, when K<1.5, γ = 1.1. The diffusion constant can then be found from the following relation:

$$D = w^2/4\tau_d \quad (4)$$

where w is the $1/e^2$ beam radius as determined previously.

Diffusion coefficients for GFP were categorized by the structure of the neuron measured (cell body, process, leader growth cone, or follower growth cone).

Two-photon FRAP measurements and analysis

Diffusion coefficients for GFP and YFP were determined by two-photon FRAP analysis, as previously described[21]. Two-photon FRAP measurements were performed using a Zeiss LSM510 META confocal microscope with a Coherent Chameleon two-photon Ti:sapphire laser. Both GFP and YFP were simultaneously bleached using 900-nm light with a 40X 1.3 NA Apochromat objective. Cell body compartment was chosen based on the YFP expression being strongest in this region allowing both proteins to be excited The bleaching characteristics of the laser beam were determined by bleaching a spot in an

immobile specimen of fluorescein using the same laser and objective settings as for the two-photon in vivo imaging. From this data, the $1/e^2$ axial (w_z) and radial (w_r) beam dimensions were determined.

For all in vivo two-photon photobleaching experiments, a circular region, 1.4 μm in radius, was defined and photobleached at full laser power (100% power, 100% transmission, 7-9 pulses) and fluorescence recovery was monitored by scanning the whole field of interest at low laser power after the bleach (100% power, 10% transmission). In these FRAP experiments, typically less than 5% of total fluorescence was lost during the entire recovery phase. The fluorescence intensity recovery traces were recorded; the fluorescence recovers according to the following equation:

$$\frac{F(t)}{F_p} = \sum_{n=0}^{\infty}\left[\left(\frac{2^{3/2}(-\beta)^n}{n!}\right)\left(\frac{1}{2+2n(1+2t/\tau_D)}\right)\left(\frac{1}{(2+2n+(4nt/R\tau_D))^{1/2}}\right)\right] \qquad (5)$$

where F(t), F_p, and τ_d are as before, R is the square of the ratio of the radial to axial beam dimensions ($R \equiv w_z^2/w_r^2$), and β is a parameter related to the degree of bleaching:

$$\frac{F_o}{F_p} = \sum_{n=0}^{\infty}\frac{(-\beta)^n}{n!}\frac{1}{(1+n)^{3/2}} \qquad (6)$$

where F_o is the fluorescence intensity immediately after the bleach. The β parameter was determined for each trace. From fits of the collected data to these equations, the diffusion constant can then be found from the following relation (for two-photon FRAP):

$$D = w_r^2/8\tau_d \qquad (7)$$

where w_r is the $1/e^2$ radial beam dimension as determined previously.

Data analysis

The D coefficients for each category were compared for significance using GraphPad InStat 3.0 Software. In cases where control diffusion rate was compared to more than one perturbation, the p value was recalculated to adjust for multiple comparisons. Values of $P<0.001$ were considered significant.

5.8 References

1. Dent, E. W. & Gertler, F. Cytoskeletal dynamics and transport in growth cone motility and axon guidance. *Neuron* **40**, 209-227 (2003).
2. Meng, A., Tang, H., Ong, B., Farrell, J. & Lin, S. Promoter analysis in living zebrafish embryos identifies a cis-acting motif required for neuronal expression of GATA-2. *The Proceedings of the National Academy of Science* **94**, 6267-6272 (1997).
3. Bak, M. & Fraser, S. E. Axon fasciculation and differences in midline kinetics between pioneer and follower axons within commissural fascicles. *Development* **130**, 4999-5008 (2003).
4. Lippincott-Schwartz, J., Snapp, E. & Kenworthy, A. Studying protein dynamics in living cells. *Nature Reviews in Molecular Cell Biology* **2**, 444-456 (2001).
5. Cheutin, T. et al. Maintenance of stable heterochromatin domains by dynamic HP1 binding. *Science* **299**, 721-725 (2003).
6. Festenstein, R. et al. Modulation of heterochromatin protein 1 dynamics in primary mammalian cells. *Science* **299**, 719-721 (2003).
7. Phair, R. D. & Misteli, T. High mobility of proteins in the mammalian cell nucleus. *Nature* **404**, 604-609 (2000).
8. Nehls, S. et al. Dynamics, and retention of misfolded proteins in native ER membranes. *Nature Cell BIology* **2**, 288-295 (2000).
9. Coscoy, S. et al. Molecular analysis of microscopic ezrin dynamics by two-photon FRAP. *Proc. Nat. Acad. Sci. USA* **99**, 12813-12818 (2002).

10. Klonis, N. et al. Fluorescence photobleaching analysis for the study of cellular dynamics. *European Biophysical Journal* **31**, 36-51 (2002).

11. White, J. & Stelzer, E. Photobleaching GFP reveals protein dynamics inside live cells. *Trends in Cell Biology* **9**, 61-65 (1999).

12. Axelrod, D., Koppel, D. E., Schlessinger, J., Elson, E. & Webb, W. W. Mobility measurement by analysis of fluorescence photobleaching recovery kinetics. Biophys. J. 16, 1055-1069. *Biophysical Journal* **16**, 1055-1069 (1976).

13. Popov, S. & Poo, M. Diffusional transport of macromolecules in developing nerve processes. *The Journal of Neuroscience* **12**, 77-85 (1992).

14. Flanagan, M. D. & Lin, S. Cytochalasins block actin filament elongation by binding to high affinity sites associated with F-actin. *Journal of Biological Chemistry* **255**, 835-838 (1980).

15. Brown, S. S. & Spudich, J. A. Mechanism of action of cytochalasin: evidance that it binds to actin filaments. *Journal of Cell Biology* **88**, 487-491 (1980).

16. Forscher, P. & Smith, S. Actions of cytochalasins on the organization of actin filaments and microtubules in a neuronal growth cone. *The Journal of Cell Biology* **107**, 1505-1516 (1988).

17. Potma, E. et al. Reduced protein diffusion rate by cytoskeleton in vegetative and polarized Dictyostelium cells. *Biophysical Journal* **81**, 2010-2019 (2001).

18. Campbell, D. S. & Holt, C. E. Chemotropic responses of retinal growth cones mediated by rapid local protein synthesis and degradation. *Neuron* **20**, 1013-1026 (2001).

19. Gallo, G. & Letourneau, P. Regulation of growth cone actin fialments by guidance cues. *Journal of Neurobiology* **58**, 92-102 (2004).

20. Koppel, D. E., Axelrod, D., Schlessinger, J., Elson, E. L. & Webb, W. W. Dynamics of fluorescence marker concentration as a probe of mobility. *Biophysical Journal* **16**, 1315-1329 (1976).

21. Brown, E. B., Wu, E. S., Zipfel, W. & Webb, W. W. Measurement of molecular diffusion in solution by multiphoton fluorescence photobleaching recovery. *Biophysical Journal* **77**, 2837-2849 (1999).

Chapter 6 Conclusions

6.1 Thesis summary

This dissertation describes studies undertaken to understand early commissural axon behavior in the zebrafish forebrain *in vivo* using timelapse imaging. The work can be broadly divided into three separate studies:

POC axon kinetics study (Chapters 2 and 3)

We identified and established an imaging assay for studying commissural axon behavior of early differentiating neurons in the brain *in vivo*. Characterization of early axon behaviors revealed important insights into axon-axon interactions that occur in early axon fascicles and axon behavior at the midline.

Role of DCC and netrin in POC tract formation (Chapter 4)

We next combined molecular analysis of gene function with timelapse imaging to examine the role of DCC and netrin in POC tract formation. Our assay allowed us to study the effect of netrin on POC growth cones directly, which before has only been done in culture. These studies showed that netrin is a repulsive cue for POC axons working to prevent POC axons from growing in the dorso-anterior dierection. Further instead of acting specifically at the midline as might be expected from studies on spinal commissural axons, DCC signaling works along the entire commissural axon tract.

Free diffusion measurements inside POC growth cones (Chapter 5)

We developed a new experimental approach based on one and two-photon fluorescence recovery after photobleaching (FRAP) and timelapse imaging to permit measurements of diffusion in early neurons and growth cones *in vivo* which has not been done before. These measurements will be needed to understand growth cone guidance signaling and how diffusion of signaling components might affect growth cone guidance. We found intriguing differences in free diffusion rate between actively pioneering growth cones and follower growth cones. The data suggest that differences in diffusion rates might be linked to growth cone pathfinding.

6.2 Putting this work in context with other studies in the field

Studies of growth cones in culture have yielded a wealth of information about growth cone behavior. We now have a more intuitive understanding of the role of different guidance cues[1-5], mechanisms involved in growth cone turning[6-11] and the cytoskeletal machinery that powers growth cone navigation[12-15]. The challenge remains to determine how these events are integrated together within the developing nervous system where axon growth is orchestrated by a complex landscape of cellular and molecular players. Such analysis not only requires the use of dynamic imaging to track the behavior of growth cones over time, but also that the studies be performed *in vivo*[16].

Timelapse observations of growth cones can yield a wealth of information as illustrated by a number of studies of growth cone and axon terminal morphologies[17-18,33,47,48]. Mason and Wang analysis of retinal axon growth revealed an interesting growth

behavior. Namely, that axons grow in a discontinuous manner, alternating between extending and pausing[17,18]. Their studies also showed that growth cone shape was dependent on behavior; rapidly moving growth cones being streamlined with few filopodia while those that paused more frequently having complex shapes and greater number of filopodia[17,18]. This suggested that growth cone filopodia are likely the sampling antennas used to probe the local environment in order to orient the growth cone[18-20]. However, while the retinal axon pathway has been most utilized for studying axon guidance, examining axon growth in mouse preparations continues to be challenging because of their opaqueness and because the embryos are still developing inside their mother.

Zebrafish embryos easily lend themselves to timelapse imaging and offer a simple and accessible nervous system. Recent developments in imaging technology [21], cell labeling methods [22] and available stable trangenic lines[23-29], as well as the ability to perturb specific gene function [30,31], allow direct examination of axon growth in its natural context. Thus, for studies of axon growth and pathfinding *in vivo*, zebrafish are emerging as the model of choice.

Studies in zebrafish have provided new knowledge about axon pathfinding. Dynes and Ngai used timelapse analysis to observe axon navigation *in vivo* to determine how olfactory sensory neurons find their glomerular targets[32]. Dynamic imaging revealed that olfactory axons extend directly to their glomeruli instead of growing in a random fashion[32]. This study highlights one of the great advantages of dynamic observation which is that the behavior of the object can give us specific clues to the underlying mechanisms that cause or influence it. In the case of the olfactory neurons their highly

directed growth suggested the presence of specific pathfinding cues that guide these axons toward their glomeruli[32].

Another nice example of the power of dynamic imaging was the study by Hutson and Chien where they examined the molecular basis of axon pathfinding at the optic chiasm using wildtype and *astray* (a Robo2 defective receptor mutant) zebrafish embryos[33]. While it was previously known that Slit can function as a repulsive cue for certain axons [3,4], this study revealed that lack of functional Robo2 resulted in the inability of growth cone errors to be corrected at the optic chiasm [33]. The role of Robo2 in error-correction would have been difficult to observe in culture.

One specific characteristic of the retinal system for studying axon growth and guidance is that axonal connections are set up after the initial axon tracts wire up. Thus the retinal axons navigate through brain tissue where other axon pathways are already in place. For example in fish, the retinal axons begin to project to the optic chiasm at 36hpf, while the major early axon tracts of the brain, including the POC, are interconnected at 24hpf[34-36]. In fact, optic axons from the eye form discrete fascicles adjacent to the axons of the POC[37]. Similarly, the olfactory neurons make their projections towards the glomeruli at 38hpf[32]. This later developmental time window is likely to correspond to an increase in the number and complexity of molecularly distinct cell domains through which axons must navigate. In contrast by looking at the initial axons that are part of the earlier neuronal scaffold we can look and compare the behavior of “naïve” axons and later axons that grow along them.

Our study of early axon and growth cone behaviors during the establishment of the postoptic commissure (POC) allowed us to examine the behavior of ‘such early

commissural axons and later axons growing along them and how they behave at the midline. This work revealed important behavioral differences between leader and follower axons and showed evidence for dynamic axon interactions that in turn shape the behaviors of axons during POC commissure formation. While the behavior of commissural axons has been extensively studied in the spinal cord[3,38], our study was the first dynamic examination of the behavior of commissural axons in the brain[39]. These data revealed that contrary to what might be expected, not all commissural axons pause at the midline unlike the spinal commissural axons investigated by Bovalenta and Dodd[40]. Timelapse imaging of early POC axons revealed dynamic interaction among the POC axons. Only the first axon arriving at the midline slowed its growth while later axons were able to grow across midline at faster growth rates. Elimination of the first axon resulted in the follower axon adopting the behavior of the leader at the midline. We also found that pathfinding behavior was correlated with growth cone morphology, with leader growth cones being more complex than follower growth cones, similar to Mason and Wang [17] and consistent with the differences between growth cones reported earlier in both vertebrates and invertebrates [19,20].

The characterization of these behaviors established a powerful in vivo dynamic assay for later elucidation of molecular cues involved in guiding POC axons, similar to the approach used by Hutson and Chien[33]. Here we focused on the role of netrin, a well-established midline guidance cue for spinal commissural axons and its receptor deleted in colorectal cancer (DCC), and their role in POC formation. Combining loss- and gain-of-function experiments and timelapse imaging of POC axons, we have been able to show that instead of acting as a midline attractor as expected from their role in spinal cord,

netrin signaling via DCC serves as a repellent cue keeping POC axons in a single fascicle, pointing to netrin as an important boundary delineating guidance molecule in the zebrafish forebrain[41].

While local protein synthesis has been demonstrated in growth cones in culture and has been shown to be required for growth cone turning[6] little is known about the kinetics of local diffusion of proteins *in vivo* as growth cones navigate. Our studies of diffusion in early vrc neurons and POC axon growth cones using single and two-photon FRAP offer the first insight into this process and reveal that local diffusion is an important parameter during axon navigation. Leaders have slower diffusion rates compared to follower growth cones and the diffusion characteristics change as growth cones of follower axons establish and lose contact with the main POC tract. Furthermore, actin cytoskeleton appears to play a direct role in local diffusion rates in growth cones. More quantitative studies of the diffusion of specific molecular species in the future will aid our understanding of how a given cue or set of cues translate into growth cone guidance.

6.3 Outlook for future studies

The GFP expressing POC axons offer a suitable system to follow and understand the biology of axon growth and pathfinding *in vivo* at many levels.

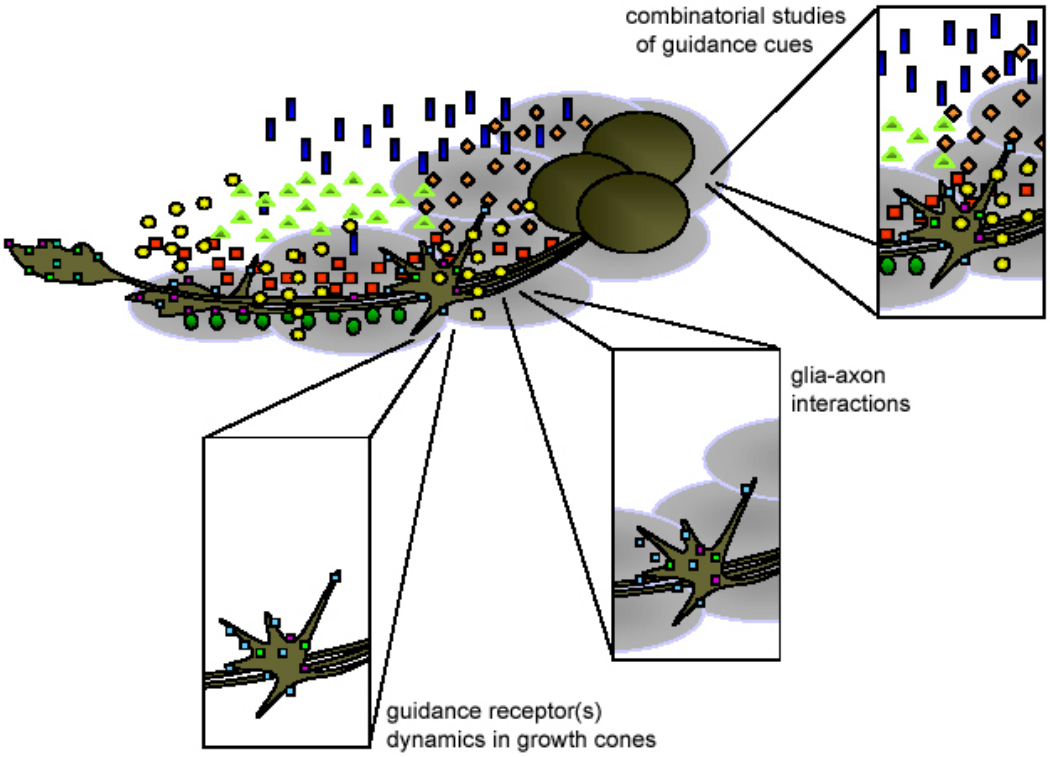

Figure 6-1 The POC commissural system and possible future directions of study

Timelapse analysis of the early POC axon tract development can be made at a number of different levels each giving information about processes that are important to axon growth and guidance.

Many of the processes that occur over days in other vertebrates such as mice or chick, take place in a matter of hours in zebrafish, thus they can be directly observed. The studies described here can be further extended in a number of fun directions that meet the challenges of axon growth and pathfinding field at the present moment. Possible

experiments in four specific areas are described in which this system, and the techniques we have developed offer significant advantages (Figure 6-1).

I. Dissection of the roles of various guidance cues using combinatorial studies

The field of axon guidance signaling has made great progress in identifying components of axon guidance signaling cascades but the challenge now is to assemble the different puzzle pieces into a complete picture of how these cues interact together. Our study of netrin and DCC function for POC axons and that of Robo2 by Hutson and Chien can be expanded combinatorially using additional MOs, cell transplants and transient expression to assess the roles of additional molecules in the same process. For example, in the POC axon assay we can imagine having some axons lack DCC receptor and others that lack both the DCC and the Robo receptor. By examining POC axon behaviors and measuring their growth kinetics, we can determine the spatial and temporal action of these genes and assay whether they also affect each other.

II. Examining the cell biology and role of glia-axon interactions for patterning early axon tracts in the CNS

Surrounding glial cells likely influence axon guidance. For example, axons of the lateral line in zebrafish which innervate the lateral primordium appear to be 'towed' by their target cells [42]. Glial cells that ensheath axons have been linked to axon fasciculation[43]. One possibility is that the local glial cells play an active role in POC axon fasciculation. Alternatively or in addition, the single POC tract we

normally see might be shaped by two separate and/or interacting forces: the surrounding inhibitory cues that force axons to grow together as suggested by our netrin studies and axons themselves as a preferred substrate as revealed by our studies of POC axon kinetics.

During POC tract formation the majority of neuroepethelial cells are still undifferentiated. However POC axons appear to be very specific about their migration route. As we have domenstrated, the errors made by POC axons are confined to specific points along the POC tract, suggesting that perhaps these areas correspond to cells involved in providing guidance cues. Detailed timelapse analysis of interactions between the filopodia of POC growth cones and the underlying neuroepethelial cells would be necessary to begin to address the role(s) that these cells play in POC formation.

III. Tracking the kinetics of specific guidance molecules and their interacting partners in growth cones during active pathfinding

For continual guidance, growth cones must be in constant molecular flux, making, and presenting new receptors in order to sense environmental guidance cues. While much has been learned about receptor function from biochemical studies on cultured cell lines, little is known about the dynamics of guidance receptors in a growth cone in contrast to a developing synapse. With recent advances in quantitative imaging techniques[44,45], we can potentially track individual guidance receptors in growth cones *in vivo* as growth cones pathfind[44,45]. Measuring the kinetics of receptor insertion, activation and deactivation while observing growth

cones navigating would allow us to understand the molecular mechanisms that result in stabilization of a given filopodia and axon growth in a given direction. This is entirely possible with current imaging methods and has been recently used to examine dendrite growth and stabilization of synaptic contacts in zebrafish[46].

IV. Analyzing growth cone behavior across different spatio-temporal domains

The growth cone is a very motile structure and the underlying biology of growth cone guidance occurs at multiple timescales. For example, local signaling events such as Ca++ transients and signaling cascades are likely to occur on the scale of micro- to milli-seconds, filopodia are rapidly added and retracted on the order of seconds, and the axon grows forward on the scale of minutes to hours. Using confocal imaging techniques to image POC axons and their growth cones, we can examine a good portion of events happening at each of these timescales separately. However, in the future it would be interesting to develop microscopy and image analysis techniques that allow imaging to be integrated in all these timescales to understand in real time how a given guidance cue translates into growth cone movement in a living organism.

6.4 References

1. Guan, K. & Rao, Y. Signaling mechanisms mediating neuronal responses to guidance cues. *Nature Reviews in Neuroscience* **4**, 941-956 (2003).
2. Kalil, K., Szebenyi, G. & Dent, E. w. Common mechanisms underlying growth cone guidance and axon branching. *Journal of Neurobiology* **44**, 145-58 (2000).
3. Kaprielian, Z., Runko, E. & Imondi, R. Axon guidance at the midline choice point. *Developmental Dynamics* **221**, 154-181 (2001).
4. Tessier-Lavigne, M. & Goodman, C. The molecular biology of axon guidance. *Science* **274**, 11231133 (1996).
5. Yoshikawa, S. & Thomas, J. Secreted cell signaling molecules in axon guidance. *Current Opinion in Neurobiology* **14**, 45-50 (2004).
6. Campbell, D. S. & Holt, C. E. Chemotropic responses of retinal growth cones mediated by rapid local protein synthesis and degradation. *Neuron* **20**, 1013-1026 (2001).
7. Ming, G. et al. Adaptation in the chemotactic guidance of nerve growth cones. *Nature* **417**, 411-418 (2002).
8. Nishiyama, M. et al. Cyclic AMP.GMP-dependent modulation of CA2+ channels sets the polarity of nerve growth-cone turning. *Nature* **423**, 990-995 (2003).
9. Ming, G. Cyclic-AMP-dependent growth cone guidance by netrin-1. *Neuron* **19**, 1225-1235 (1997).
10. Song, H. & Poo, M. The cell biology of neuronal novigation. *Nature Cell BIology* **3**, E81-E88 (2001).

11. Song, H. & Poo, M. Signal transduction underlying growth cone guidance by diffusible factors. *Current Opinion in Neurobiology* **9**, 355-363 (1999).

12. Dent, E. W. & Gertler, F. Cytoskeletal dynamics and transport in growth cone motility and axon guidance. *Neuron* **40**, 209-227 (2003).

13. Gallo, G. & Letourneau, P. Regulation of growth cone actin filaments by guidance cues. *Journal of Neurobiology* **58**, 92-102 (2004).

14. Gordon-Weeks, P. Microtubules and growth cone function. *Journal of Neurobiology* **58**, 70-83 (2004).

15. Zhou, F. & Cohan, C. How actin filaments and microtubules steer growth cones to their targets. *Journal of Neurobiology* **58**, 84-91 (2004).

16. Niell, C. M. & Smith, S. Live optical imaging of nervous system development. *Annual Reviews in Physiology* **66**, 771-98 (2004).

17. Mason, C. & Wang, C. Growth cone form is behavior-specific and consequently position-specific along the retinal axon pathway. *The Journal of Neuroscience* **17**, 1086-1100 (1997).

18. Mason, C. & Erskine, L. Growth cone form, behavior, and interactions in vivo: retinal axon pathfinding as a model. *Journal of Neurobiology* **44**, 260-270 (2000).

19. McConnell, S., Ghosh, A. & Shatz, C. Subplate neurons pioneer the first axon pathway from the cerebral cortex. *Science* **245**, 978-981 (1989).

20. Bovolenta, P. & Mason, C. Growth cone morphology varies with position in the developing mouse visual pathway from retina to first targets. *The Journal of Neuroscience* **7**, 1447-1460 (1987).

21. Megason, S. G. & Fraser, S. E. Digitizing life at the level of the cell:high performance laser-scanning microscopy and image analysis for in toto imaging of development. *Mechanisms of Development* **120**, 1407-1420 (2003).

22. Koester, R. W. & Fraser, S. E. Tracing transgene expression in living zebrafish embryos. *Developmental Biology* **233**, 329-346 (2001).

23. Goldman, D., Hankin, M., Dai, X. & Ding, J. Trangenic zebrafish for studying nervous sytem development and regeneration. *Transgenic Research* **10**, 21-33 (2001).

24. Higashijima, S., Hotta, Y. & Okamoto, H. Visualization of cranial motor neurons in live transgenic zebrafish expressing green fluorescent protein under the control of the Islet-1 promoter/enhancer. *The Journal of Neuroscience* **20**, 206-218 (2000).

25. Hoalloran, M. C. et al. Laser-induced gene expression in specific cells of trangenic zebrafish. *Development* **127**, 1953-1960 (2000).

26. Park, H-C. et al. Analysis of upstream elements in the HuC promoter leads to the establishment of transgenic zebrafish with fluorescent neurons. *Developmental Biology* **227**, 279-293 (2000).

27. Udvadia, A. J. & Linney, E. Windows into development: historic, current, and future perspectives on transgenic zebrafish. *Developmental Biology* **256**, 1-17 (2003).

28. Yoshida, T. & Mishina, M. Neuron-specific gene manipulations in transparent zebrafish embryos. *Methods in Cell Science* **25**, 15-23 (2003).

29. Meng, A., Tang, H., Ong, B., Farrell, J. & Lin, S. Promoter analysis in living zebrafish embryos identifies a cis-acting motif required for neuronal expression of GATA-2. *The Proceedings of the National Academy of Science* **94**, 6267-6272 (1997).

30. Nasevicius, A. & Ekker, S. Effective targeter gene 'kockdown' in zebrafish. *Nature Genetics* **26**, 216-220 (2000).

31. Draper, B., Marcos, P. A. & Kimmel, C. B. Inhibition of zebrafish fgf8 pre-mRNA splicing with morpholino oligos: a quantifiable method for gene knockdown. *Genesis* **30**, 154-156 (2001).

32. Dynes, J. & Ngai, J. Pathfinding of olfactory neuron axons to stereotypes glomerular targets revealed by dynamic imaging in living zebrafish embryos. *Neuron* **20**, 1081-1091 (1998).

33. Hutson, L. & Chien, C.-B. Pathfinding and error correction by retinal axons: the role of astray/robo2. *Neuron* **33**, 205-221 (2002).

34. Chitnis, A. & Kuwada, J. Axonogenesis in the brain of zebrafish embryo. *The Journal of Neuroscience* **10**, 1892-1905 (1990).

35. Ross, L., Parrett, T. & Easter, S. Axonogenesis and morphogenesis in the embryonic zebrafish brain. *The Journal of Neuroscience* **12**, 467-482 (1992).

36. Wilson, S., Brennan, C., McDonald, R., Brand, M. & Holder, N. Analysis of axon tract formation in the zebrafish brain:the role of terrirories of gene expression and their boundaries. *Cell Tissue Research* **290**, 198-196 (1997).

37. McDonald, R. et al. The Pax protein Noi is required for commissural axon pathway formation in the restral forebrain.. *Development* **124**, 2397-2408 (1997).

38. Colamarino, S. & Tessier-Lavigne, M. The role of the floor plate in axon guidance. *Annual Reviews in Neuroscience* **18**, 497-529 (1995).

39. Bak, M. & Fraser, S. E. Axon fasciculation and differences in midline kinetics between pioneer and follower axons within commissural fascicles. *Development* **130**, 4999-5008 (2003).

40. Bovolenta, P. & Dodd, J. Guidance of commissural growth cones at the floor plate in embryonic rat spinal cord. *Development* **109**, 435-447 (1990).

41. Bak-Maier, M. & Fraser, S. E. Netrin and its receptor Deleted in Colorectal Cancer (DCC) pattern early forebrain commissural axons. *Manuscript submitted to Nature Neuroscience* (2004).

42. Gilmour, D. T., Knout, H., Maischein, H.-M. & Nuesslein-Volhard, C. Towing of sensory axons by their migrating target cells in vivo. *Nature Neuroscience* **7**, 491-492 (2004).

43. Gilmour, D. T., Maischein, H.-M. & Nuesslein-Volhard, C. Migration and function of a glial subtype in the vertebrate peripheral nervous system. *Neuron* **34**, 577-588 (2002).

44. Lippincott-Schwartz, J. et al. Monitoring the dynamics and mobility of membrane proteins tagged with green fluorescent protein. *Methods in Cell Biology* **58**, 261-281 (1999).

45. Lippincott-Schwartz, J., Snapp, E. & Kenworthy, A. Studying protein dynamics in living cells. *Nature Reviews in Molecular Cell Biology* **2**, 444-456 (2001).

46. Niell, C. M., Meyer, M. P. & Smith, S. In vivo imaging of synapse formation on a growing dendritic arbor. *Nature Neuroscience* **7**, 254-260 (2004).

47. Cohen-Cory, S and Fraser, S.E. Effects of brain-derived neurotrophic factor on optic axon branching and remodeling in vivo *Nature* **378,** 192-196 (1995).

48. Harris, W.A, Holt, C.E and Bonhoeffer, F. Retinal axons with and without their somata, growing to and arborizing in the tectum of Xenopus embryos: a time-lapse video study of single fibres in vivo. Development 101, 123-133 (1987).